5-15-2009

Mineralogy and Geochemistry of the Dumper Dew Pegmatite, Oxford County, Maine

Jonathan Kyle South
University of New Orleans

Mineralogy and Geochemistry of the Dumper Dew Pegmatite, Oxford County, Maine

A Thesis

Submitted to the Graduate Faculty of the
University of New Orleans
in partial fulfillment of the
requirements for the degree of

Master of Science
in
Earth and Environmental Science

by

Jonathan Kyle South

Bachelor of Science in Geology, University of Alabama, 2006

May 2009

Acknowledgements

To acknowledge all the indebtedness I feel to those who have supported and stimulated my studies in the field of geology would impose on the reader. Let me therefore mention only those who have been directly concerned with this thesis.

Thesis advisors: Dr. William B. Simmons, Department of Earth and Environmental Sciences at the University of New Orleans, for his analytical suggestions; Alexander U. Falster, Department of Earth and Environmental Sciences at the University of New Orleans, for his suggestions and valuable time invested with the instrumentation aspects of this study; and Dr. Karen Webber, Department of Earth and Environmental Sciences at the University of New Orleans, for her invaluable critique of this manuscript.

Many thanks to Ray Sprague for his hard work, donation of explosives, and granting me the opportunity to scientifically study the pegmatites in his lease holdings.

Thanks to my field assistants: Josh Sullivan who endured torrential downpours and mosquito swarms with me in May of 2007; Tony Wielkiewicz for his valuable time and hard work in October of 2007; and Erica Plaisance for her help with sample collection and photography.

Table of Contents

List of Figures

List of Tables

Abstract

The Dumper Dew is a newly discovered pegmatite located on the east-facing slope of Uncle Tom Mountain in Oxford County, Maine. It is a geochemically evolved LCT-type pegmatite petrogenetically linked to the middle Paleozoic Sebago batholith. Shallow emplacement of the Dumper Dew is evidenced by abundant miarolitic cavities found in the pegmatite. The sheet-like structure of the pegmatite coupled with its intrusion in low-metamorphic grade country rock suggests rapid crystallization. Northern portions of the wall zone and intermediate zones have undergone hydrothermal alteration by the migration of late-stage fluids. The pegmatite hosts a diverse assemblage of rare-element mineral phases due to its high degree of geochemical fractionation. Trends of geochemical fractionation of individual mineral phases such as K-feldspar, muscovite, garnet, apatite, beryl, spodumene, triphylite-lithiophilite, tourmaline, cassiterite, and columbite-tantalite were attained via instrumentation assay. These trends illustrate an enhanced degree of magmatic differentiation relative to other pegmatites in the area.

Keywords: mineralogy, geochemistry, LCT pegmatite, rare element, geochemical fractionation, Sebago batholith, Oxford pegmatite field

Introduction

Objectives

The primary objective of this study was to gauge the economic feasibility of mining the newly discovered Dumper Dew pegmatite for rare and exotic minerals. This was accomplished by comparing it, mineralogically and geochemically, to the currently mined Emmons pegmatite. Additional parameters of this study were to establish or rule out any paragenetic links between the Dumper Dew, the Emmons and the Tiger Bill pegmatites. This study implemented both long-standing and advanced exploration techniques. Long-standing exploration techniques were implemented in order to institute any petrogenic links of the Dumper Dew to nearby pegmatites, locate distinct zonation in, and identify the presence of rare element mineralization in the Dumper Dew pegmatite. The aim of advanced exploration was to study the recently discovered dike in detail such as, the extent of fractionation and economic potential. Advanced exploration was implemented via electron microprobe analysis, directly coupled plasma spectroscopy, scanning electron microscopy, X-ray diffractometry and optical petrography.

Previous Work

The Dumper Dew is spatially located in close proximity to the Emmons and Tiger Bill pegmatites. Prior to this study there had been no preceding work aimed at the Dumper Dew, as it is a fairly recent prospect. Initial exploration of the Emmons pegmatite, was conducted by Willie Emmons around 1900. Commercial mining commenced in 1932 by the Oxford Mining and Milling Company for feldspar (Perham, 1987). The most recent mining began at the Emmons in 1990 by Ray Sprague of Andover, Massachusetts. Since this time, a vast list of mineral species has been compiled as a result of the mining operations. Falster *et al*. (2007) attests to the Emmons overall mineralogy and Simmons *et al*. (2003) comprehensively depicted the occurrence of fluorapatite from the quarry. Additionally, Hanson *et al*. (1998) described compositional variations in wodginite crystals from the Emmons core zone. The Tiger Bill pegmatite is named after "Tiger" Bill Yates who is recognized as its discoverer (Personal Communication: R. Sprague, 2008). The Penley Corporation of West Paris, Maine mined the Tiger Bill from 1948 until 1951, again sometime in 1952, and from 1955 to 1957 (Perham, 1987). To date, there have been no published mineralogical or geochemical studies of the Tiger Bill.

Geology

General Geology

The geology of New England is extremely complex, having experienced numerous orogenic and anorogenic events. The region has felt the effects of plates rifting into pieces by divergence and new ocean basins being born, followed by motion reversal, convergence back together, plate collision, and mountain building. The plate-driven processes in the region produced the Grenville orogeny during the Precambrian. Subsequent plate-driven processes produced the Penobscottian, Blountian, Taconic, Caledonian, Acadian and Alleghenian compressional events in the Appalachians.

The Grenville orogeny deformed, metamorphosed, and intruded rocks of the Laurentian craton in the eastern United States and Canada during the Precambrian between 1.3 and 1.0 billion years ago (Williams *et al*., 1999). During this time, Baltica began rifting from the Laurentian craton and resulted in the opening of the Iapetus Ocean. Passive margins developed on the east coast of Laurentia and the west coast of Baltica facing the Iapetus Ocean.

The first orogenic event important in the creation of the Appalachians was the Penobscottian (Mid- to Late Cambrian). The Penobscottian was quickly followed by the Blountian orogeny. Both tectonic events are difficult to recognize and separate from the subsequent Taconic orogeny (Drake *et al*., 1989).

Beginning in the Middle Ordovician, the passive margins of Laurentia and Baltica began to their converge, resulting in the subduction of the Iapetus plate beneath the east coast of Laurentia and thus initiating a narrowing of the Iapetus Ocean. The resulting Taconic orogeny, named after the present-day Taconic Mountains of eastern New York, central Massachusetts and Vermont, is thought to be the first major compressional episode caused by one stage of the closing of the Iapetus Ocean (Rankin *et al*., 1989).

During the Silurian, Laurentia and Baltica collided to form the larger continent of Laurasia. This collision, which closed the northern Iapetus Ocean, is marked by the Caledonian orogeny that established a mountain chain stretching from present-day eastern North America through Greenland, western Scandinavia, Scotland and Ireland (McKerrow *et al*., 2000).

During the Devonian, as the southern Iapetus Ocean narrowed between Laurasia and Gondwana, mountain building continued along the eastern margin of Laurasia with the Acadian orogeny. The Acadian orogeny affected an area from present-day New York to Newfoundland. The orogeny was most intense in the Merrimac area in southern New England and in Maine and extended northward to the Central Volcanic Belt of Newfoundland (Osberg *et al*., 1989).

During the Early Carboniferous, Gondwana collided with Laurasia, thus closing the southern Iapetus Ocean, forming part of Pangaea and generating the Alleghenian orogeny. Because Gondwana rotated clockwise relative to Laurasia, deformation generally progressed in a northeast-to-southwest direction along the Hercynian, Appalachian and Ouachita mobile belts of the two continents (Hatcher *et al*., 1989). By the end of the Carboniferous, Laurasia and Gondwana were sutured together and Pangaea had been formed. This was the last major orogenic event to affect the present-day east coast of North America. The Alleghenian orogeny was followed by rifting and extension that led to the opening of the Atlantic Ocean in the Mesozoic.

Local Geology

The Dumper Dew, the Emmons, and the Tiger Bill are peraluminous, granitic pegmatites located near the town of Greenwood, Oxford County, southwestern Maine. All three are petrogenetically associated with the Oxford pegmatite field. The Oxford field, in western Maine, is situated around the Songo pluton and the Sebago batholith (Figure 1). Pegmatites of the Oxford field are petrogenetically linked to the Sebago batholith of east-central New Hampshire and southwestern Maine (Simmons *et al*., 2003), which is the largest exposed granitic pluton in New England (Tomascak *et al*., 1996). A gravity data survey of the area (Hodge *et al*., 1982) proposed

that the batholith dips shallowly toward the northeast and varies from 1 to 2 kilometers thick. Aleinikoff *et al*. (1985) suggested the batholith is "kidney-shaped", and at its widest point measures ~80 kilometers in length along a west-northwest-east-southeast direction and measures ~35 kilometers at its maximum width. Tomascak *et al*. (1984) proposed the Sebago batholith crystallized at about 293 ±1 Ma via U-Pb monazite analysis. An intrusive age for the Sebago batholith was determined by the U-Pb zircon method as 325 ±3 MA (Aleinikoff *et al*., 1985). The Sebago batholith intruded Ordovician- to Devonian-aged, middle- to upper-amphibolite grade metasedimentary rocks of the Kearsarge-Central Maine sequence (Tomascak *et al*., 1996) within the Kearsarge-Central Maine Synclinorium (Osberg *et al*., 1985).

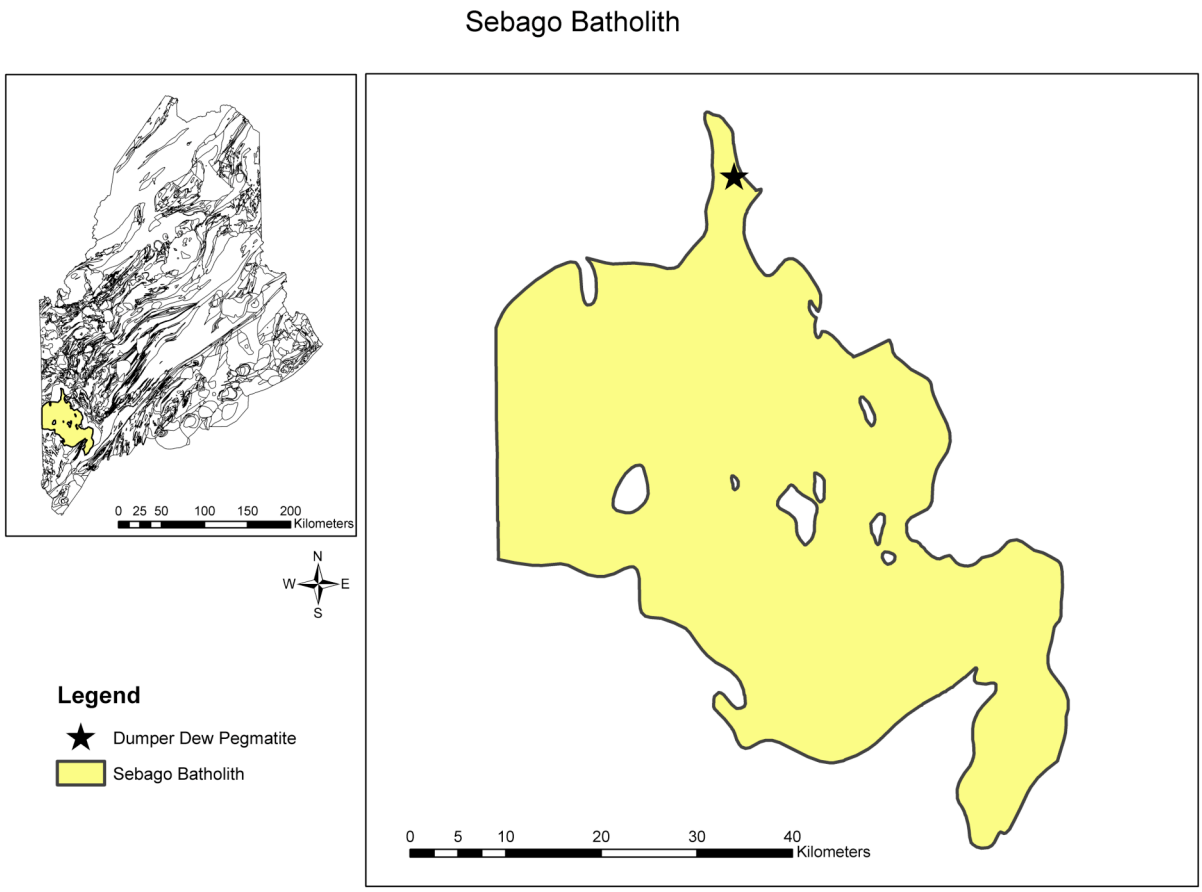

Figure 1. Geologic Map of Maine showing the locations of the Sebago batholith and Dumper Dew pegmatite. Yellow area – Sebago batholith.

Oxford Pegmatite Field

Pegmatites of southwestern Maine are associated with either the Oxford or Brunswick pegmatite fields (Figure 2). Pegmatites of the Brunswick field have been characterized as both NYF and LCT types and are further subdivided into the beryl-columbite and rare-earth subtypes (Simmons *et al*., 2003). Pegmatites of the Oxford field are characterized as LCT type and are subdivided into beryl-columbite, beryl-columbite-phosphate, petalite and spodumene subtypes (Simmons *et al*., 2003). Oxford field pegmatites are associated with Acadian-orogenic plutons spawned in the Middle Paleozoic (Dyar et al., 1999). The parent bodies of Oxford field pegmatites are thought to be the Sebago batholith in the south and some lesser plutons in the north, such as the Rumford, Phillips and Mooselookmeguntic (Wise, 1995). Pegmatites from the Oxford field are thought to have been produced through a lone magmatic episode (Wise and Francis, 1992). Simmons et al. (1995 and 1996) however, suggests an anatectic origin for some of these pegmatites.

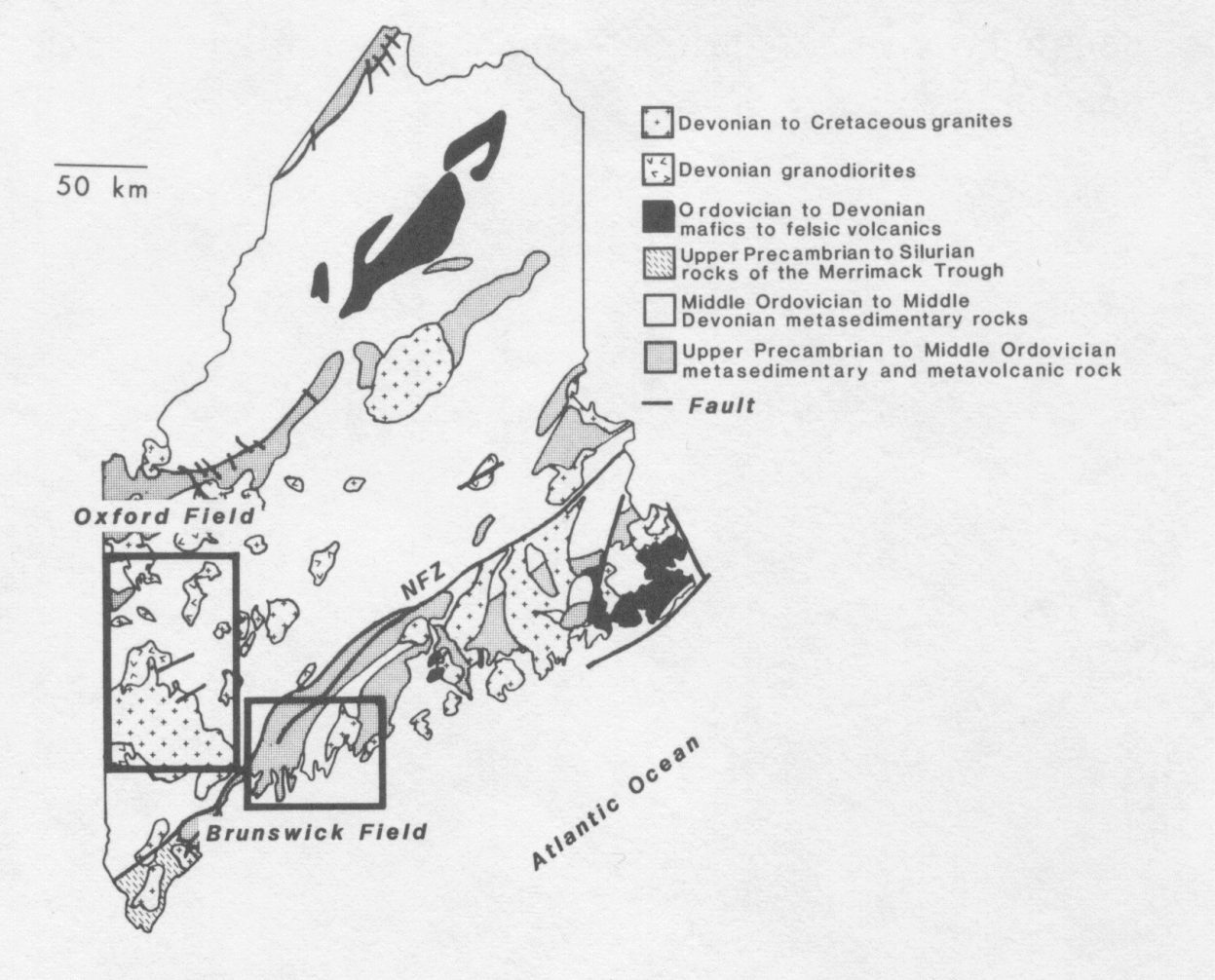

Figure 2. Generalized geologic map of Maine (Osberg et al., 1985; Wise and Francis, 1992) showing the location of the Oxford and Brunswick pegmatite fields. The large pluton in the Oxford Field is the Sebago batholith. The smaller one just to the north of the Sebago is the Songo pluton.

Dumper Dew Pegmatite

The Dumper Dew is a peraluminous, highly evolved, complex, LCT-type pegmatite located near the town of Greenwood, Oxford County, in southwestern Maine (Figure 3). Exposed portions of the pegmatite lie on the east-facing slope of Uncle Tom Mountain. The intrusion has limited outcrop exposure due to a lack of mining coupled with a sediment and vegetative cover. Both the pegmatite and host rocks are capped with a covering of surficial sediments deposited during and subsequent to the most recent glaciations. Host rock-pegmatite margins and boundaries between pegmatite zones are poorly defined due to oxidation and weathering.

The Dumper Dew crops out intermittently over a distance of approximately 140 m from the uppermost leucocratic-pegmatitic outcrop to the lowermost outcrop of intermediate zone. The width of the pegmatite measures 80 m from the most elevated wall zone outcrop to the furthermost down slope outcrop of outer intermediate zone. The pegmatite strikes northwest - southeast, dips toward the south, and is hosted in biotite schist. The pegmatite was shallowly emplaced as evidence by the many pockets encountered in the replacement unit and inner intermediate zone. Due to the asymmetric, sheet-like shape of the dike and low metamorphic grade of the country rock, the intrusion probably cooled relatively quickly. The pegmatite, overall, varies in texture from coarse- to very-coarse grained, is asymmetrically zoned and hosts a diverse assemblage of minerals. Internal

zonation consists of a wall zone, outer intermediate zone, inner intermediate zone and a replacement unit. The core or a core margin zone was not observed during my study as these zones are covered with overburden and are not exposed.

Pegmatite Zones

Wall Zone

Wall zone mineralogy consists of medium-grained plagioclase and K-feldspar; abundant anhedral quartz as well as euhedral quartz crystals in small cavities; white muscovite stacks that measure 4 cm across; accessory 5mm-sized almandine garnet; small specks of green apatite in albite; and minor quantities of schorl crystals which measure 3 mm in diameter. The wall zone is asymmetric and varies in thickness from 1 m to 30 m. The wall zone is restricted to, or more developed at the hanging-wall portion of the pegmatite. This might suggest the probability that Dumper Dew is a composite pegmatite formed by the coalescence of more than one pegmatitic lens. In the northernmost pegmatite outcrop, a 5m-long quartz lens separates the base of the wall zone from the top of the outer intermediate zone. In some portions of the pegmatite, the wall zone is absent and the host rocks are in contact with the outer intermediate zone.

Outer Intermediate Zone

There is one pegmatite outcrop where both the wall zone and outer intermediate zone are mutually visible and can be differentiated from one another; in this case the aforementioned quartz lens separates the two zones. Mineralogically, the outer intermediate zone is made up of coarser-grained plagioclase and K-feldspar than is found in the wall zone; predominantly massive but some euhedral quartz in small pockets; fine- and very-coarse grained, pseudohexagonal crystals of muscovite; accessory beryl up to 4 cm in length; schorl crystals as large as 4 cm measured perpendicular to the c-axis; bright red, millimeter-sized almandine garnet; small crystals of ferrocolumbite in albite; fracture fillings of and < 1 cm-sized green apatite crystals; and rarely biotite flakes along contact boundaries with the host rock where the wall zone is absent. The largest measured section of outer intermediate zone spans a length of ~50 m. This section was measured from the most down-slope portion of outer intermediate zone to an upslope outcrop where it contacts the wall zone. The Dumper Dew has an asymmetric outer intermediate zone and extends down the east side of the pegmatite where it hoods more interior zones. One portion of the outer intermediate zone has been partly replaced by the albite-rich replacement unit in the northernmost exposure of pegmatite.

Inner Intermediate Zone

The inner intermediate zone is the most mineralogically diverse zone and is differentiated from other zones by the presence of lithium mineralization. It is comprised of large quantities of albite; both coarse crystalline and blocky K-feldspar; both colorless and smoky varieties of massive and euhedral quartz; up to 6 cm thick books of white, silver and copper muscovite; phosphates such as montebrasite, lithiophilite and subsequent heterosite; large spodumene crystals associated with quartz and albite; cesium-rich beryl crystals; different varieties of montmorillonite from miarolitic cavities; small grains of moderately-evolved manganocolumbite; large nodules of cassiterite in an albite matrix; cookeite which encrusts and coats several other phases; schorl crystals present in a wide range of sizes; herderite encrusting books of muscovite; some pink but mostly, dark-red almandine garnet; and both purple and green varieties of apatite. Exposures of this zone are limited and therefore a scale is hard to ascertain. An exposure is located 20 m south of the replacement unit where it then sporadically outcrops, trends south and is encountered finally as the southernmost exposure of the Dumper Dew. If we assume a continuous inner intermediate zone, it spans a length of 100 m as measured from the most northerly exposure to the southernmost section. It should be noted, however, that this interior zone may be a series of disconnected lenses or it may telescope in the southern portions with adjacent zones.

Core Zone

A core zone is not presently exposed at the Dumper Dew. It presumably lies below the lithium-abundant, inner intermediate zone. The core is thought to consist predominantly of quartz due to the presence of a relatively pure, crystallized quartz lens separating the wall and outer intermediate zone. The size of the core is thought to be substantial due to the surface area and apparent thickness of the intermediate zones. Three different theories exist for the core structure: A single core unit may be present, a coalescence of multiple cores may occur in the subsurface, or as is the case with some pegmatites, the core may be segregated into discontinuous individual lenses. Both size and shape of the core depends on irregularities and bulges in the overall shape of the pegmatite body.

Replacement Unit

The exposure of the replacement unit is confined to the northernmost limits of the pegmatite body where it replaces the outer intermediate and wall zones. The replacement body is approximately 1.5 m thick and 5 m wide in its exposure. Highly-albitized portions of the replacement unit contain miarolitic cavities where a variety of minerals are present as well-formed crystals. The replacement unit is composed primarily of bladed and massive albite, but also includes thick books of muscovite and massive quartz in the form of crystals and lenses. Minor minerals include garnet,

schorl, apatite, zircon, cassiterite and manganotantalite. Well-formed, chemically zoned, purple and blue apatite crystals are situated in many of the miarolitic cavities of the albite. Garnet crystals may reach considerable sizes with compositions ranging from almandine to spessartine. No beryl crystals were found in the replacement unit but there were however, several beryl casts scattered throughout the quartz lenses. Large cassiterite nodules and also extremely evolved manganotantalite crystals are dispersed intermittently in highly-albitized portions.

Pegmatite Classification

Cerny (1991) proposed a classification scheme that categorizes pegmatites into one of four classes based on depth of emplacement and metamorphic grade: Abyssal, Muscovite, Rare-Element and Miarolitic. In the Rare-Element Class, a distinction is made between pegmatites related to anorogenic processes from those related to orogenic events. Anorogenic pegmatites are more enriched in niobium, yttrium, and fluorine and are categorized as NYF type. Pegmatites associated with orogenic events are more enriched in lithium, cesium, and tantalum and are termed LCT type. Rare-Element Class, LCT-type pegmatites can be further subdivided into types and subtypes according to their geochemical signature and their mineralogy. The Dumper Dew's mineralogy places it in Cerny's 1991 classification as a Rare-Element Class, LCT type, spodumene subtype.

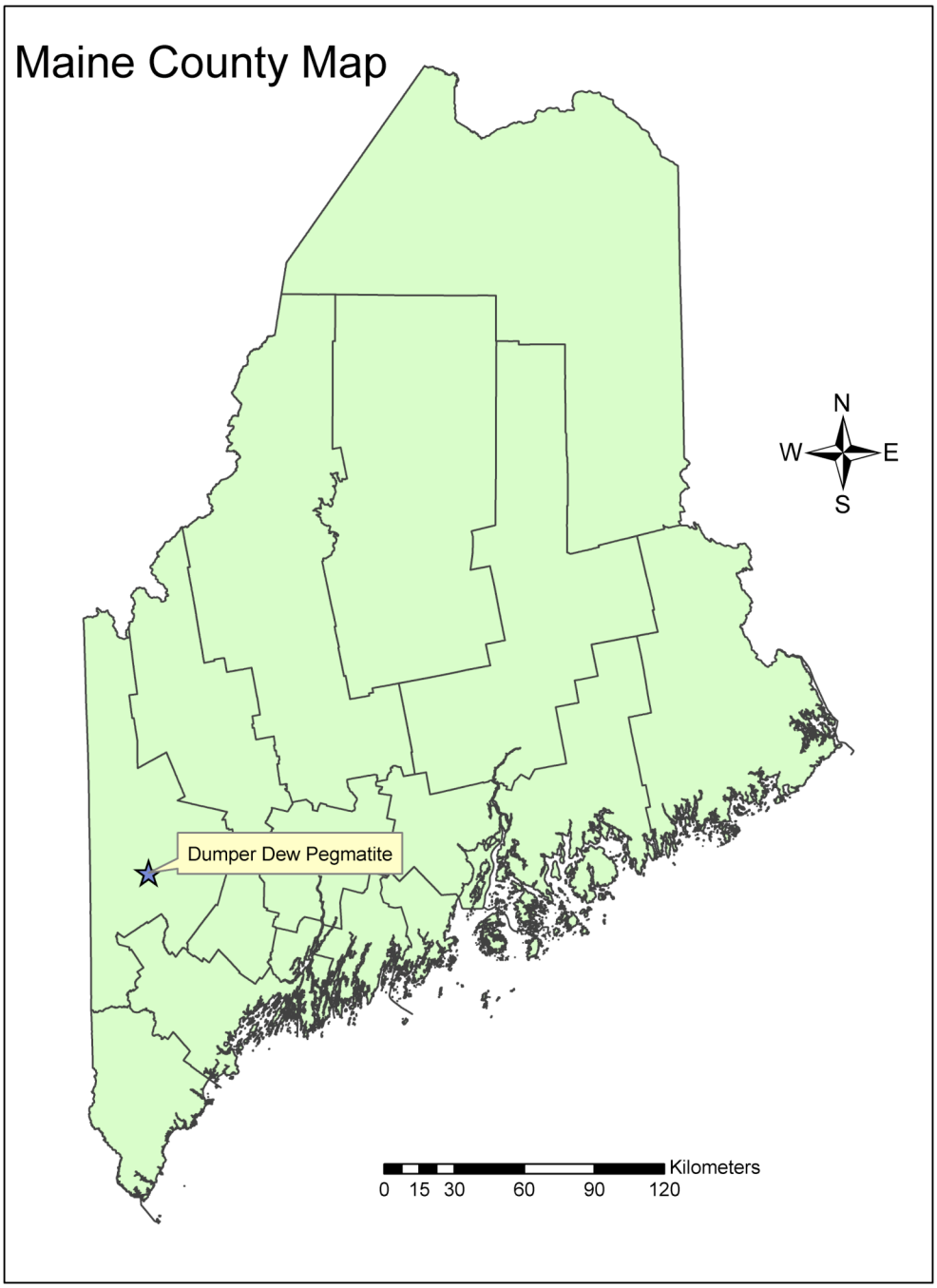

Figure 3. Location of the Dumper Dew pegmatite.

Host Rock Geochemistry

The Dumper Dew pegmatite was emplaced into a host rock of low-metamorphic grade, biotite schist. Pegmatitic fluids altered the chemical composition of the host rock, dispersing B, Li, Rb, and Tl into the surrounding schist (elemental abundances of each element are given in Appendix B, Tables B.18-22). Anomalies from trace element analyses indicate the host rock was enriched in these elements to varying degrees as a function of distance from the host rock-pegmatite contact. Samples of host rock were collected for analysis up to 20m away from the host-pegmatite boundary. As expected, samples collected < 1m from the host-pegmatite margin contain the greatest abundances Li and Rb due to low elemental mobility and a lack of Rb- and Li-mineralization. The B content is higher in samples taken the greatest distance (up to 20m) from the host-pegmatite periphery than those collected closer to the contact (<1m). This is probably due to most of the available B being integrated into the crystallization of exo- and endocontact schorl. Tl shows up as consistent proportions in a majority of analyzed host rock samples. Geospatially, Tl contents of the host rock show no discernable trends with respect to the host-pegmatite contact. The uniform occurrence of Tl in host rock samples may be attributed to the high mobility of the element.

Mineralogy

Major Minerals

Quartz (SiO_2)

Quartz is common throughout the Dumper Dew pegmatite. No chemical analyses were done on this mineral. The color ranges from colorless to white, light to dark gray and brown. Euhedral crystals are commonly found in cavities associated with albite-rich zones. The largest exposure of quartz is a lenticular-shaped mass which is exposed for a length of 5 m and eventually dips into the subsurface at an angle of 41° (Figure 4). Graphic intergrowths of quartz and feldspar were found as unconsolidated material at the base of the pegmatite. The specific zone(s) from which the two graphic-textured samples crystallized cannot be determined, as these samples were not *in situ*.

Figure 4. Lenticular-shaped quartz vein with large, blocky potassium feldspar.

Plagioclase Feldspar $NaAlSi_3O_8$

Plagioclase feldspar, species albite, is the most common mineral found in the Dumper Dew pegmatite. From the microprobe analyses in Table 1, there is hardly any deviation from the $NaAlSi_3O_8$ formula. Only minor amounts of Ca and K are present in the albite as the samples plot on a feldspar ternary diagram (Figure 5) as almost pure sodium end members. The anorthite (An) content of albite ranges from An_0 to An_1 throughout all units at the Dumper Dew. The core margin and wall zone were the only two units from which plagioclase was sampled at the Tiger Bill pegmatite. In both Tiger Bill units, anorthite compositions (An_0-An_1) were consistent with anorthite fractions calculated from Dumper Dew samples.

Albite is found throughout all zones of the pegmatite and is exsolving from potassium feldspar in most exposed units. Albite occurs as both euhedral and anhedral grains that range in color from creamy to pale white. Tabular and blade-like crystals of albite exist in and around miarolitic cavities in the innermost zones of the pegmatite. Sericitization is occurring uniformly across albite grains in thin section (Figure 6).

	Replacement Unit	Inner Intermediate	Outer Intermediate	Wall Zone	Tiger Bill Core Margin
	010-3-6-1	*002-2-5-1*	*001-1-2-1*	*008-3-8-2*	*TB-4-1-3*
Oxides (wt.%)					
SiO_2	67.667	67.643	68.056	67.555	67.655
Al_2O_3	19.588	19.650	19.796	19.633	19.589
CaO	0.024	0.032	0.018	0.110	0.057
Na_2O	11.043	11.004	11.093	11.001	10.805
K_2O	0.356	0.234	0.378	0.220	0.210
Total	98.678	98.563	99.341	98.519	98.316
Ions on the basis of 8 O					
Si	2.992	2.992	2.989	2.990	2.997
Al	1.021	1.024	1.025	1.024	1.023
Ca	0.001	0.002	0.001	0.005	0.003
Na	0.947	0.944	0.945	0.944	0.928
K	0.020	0.013	0.021	0.012	0.012
Sum	0.968	0.958	0.967	0.962	0.943

Table 1. Representative compositions by electron microprobe of albite samples taken from various zones of the Dumper Dew and the core margin of the Tiger Bill pegmatite. Additional microprobe analyses are located in Appendix A.

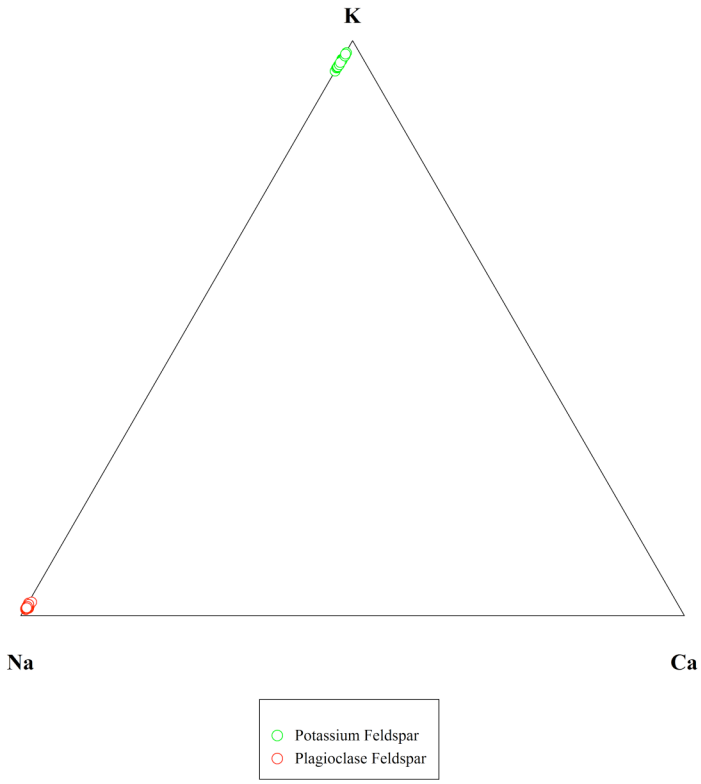

Figure 5. Ternary diagram showing end-member compositions for plagioclase and potassium feldspars from the Dumper Dew and Tiger Bill pegmatites.

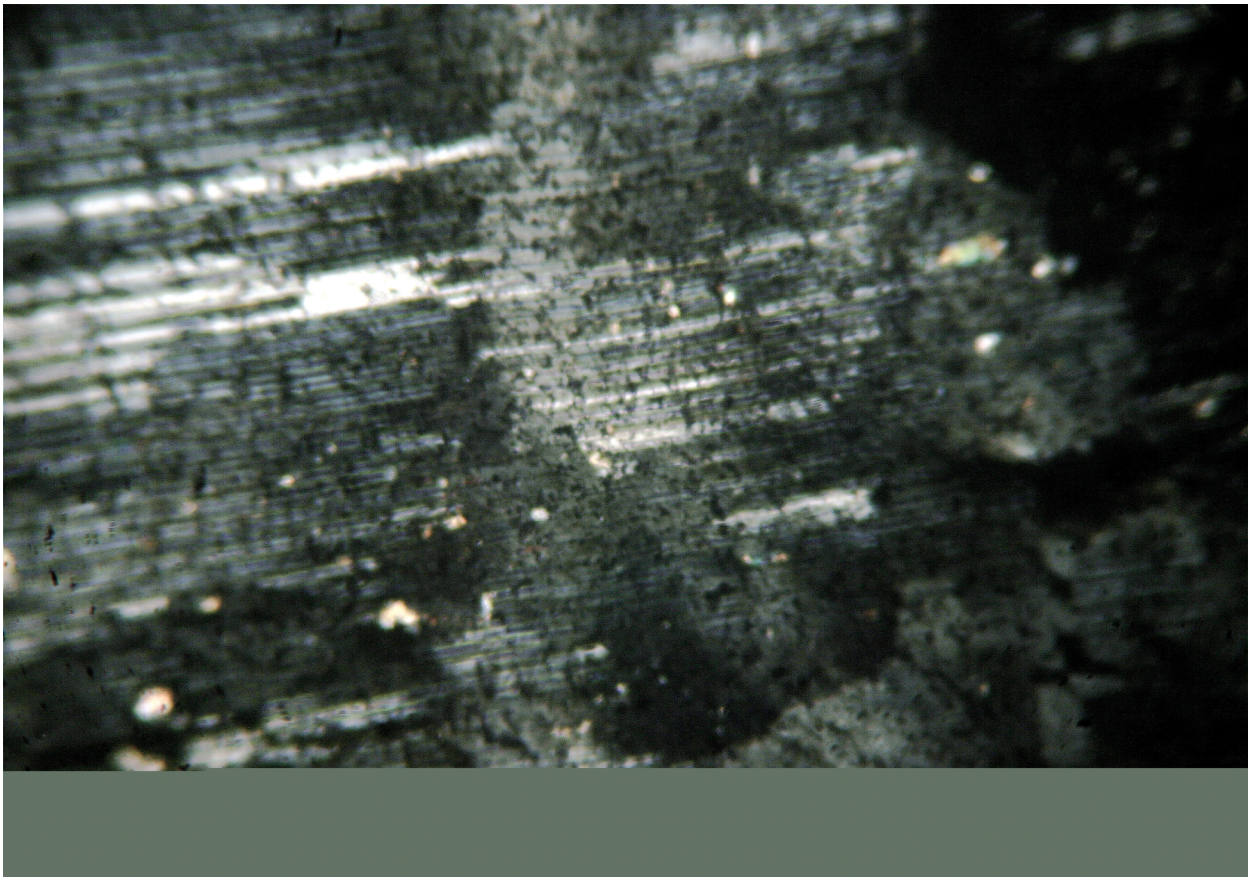

Figure 6. Photomicrograph showing sericitization of plagioclase in the Dumper Dew pegmatite. Magnification is 100x.

Potassium Feldspar $KAlSi_3O_8$

Potassium feldspar, or K-feldspar as it will be referred to hereafter, is a relatively abundant mineral at the Dumper Dew pegmatite. Color varies from very faint to deep pink. The lighter colored K-feldspar is probably due to exposed, surface weathering and is not a result of variation in chemical composition. A noticeable textural contrast exists, where medium-grained (<10cm) K-feldspar can be found in the wall zone and blocky (>50cm), coarser-grained K-feldspar can be found in the intermediate zones.

DCP analysis (Table 2) shows that the highest concentrations of Rb (>4000 ppm) in the K-feldspars are present in the inner intermediate zone at the Dumper Dew. Via the same analysis, the core-margin zone K-feldspar of the Tiger Bill pegmatite tops out at 2,204 ppm Rb. Representative microprobe analyses of muscovite are given in Table 3. Ions were calculated from microprobe analyses on the basis of 8 O apfu. K/Rb versus Cs was plotted here (Figure 8) to show the degree of fractionation of the Dumper Dew and to illustrate the degree of substitution of K by Rb in the crystal structure. Figure 7 shows the proximity of K-feldspars and plagioclase feldspars to nearly pure end-member compositions.

Both exsolution lamellae and some alteration evidence of K-feldspar can be observed in hand specimen and thin section. Large hand samples of blocky K-feldspar from the inner-intermediate zone show replacement via

albitization. Sericitization is a common alteration observed in thin section mounts of K-feldspar grains.

Elemental Abundances	Tiger Bill Core Margin *TB V*	Wall Zone *WP-008 TS*	Inner Intermediate *07-001*	Outer Intermediate *07-002 XIV*	Replacement Zone *07-010 I*
ppm B	160	179	nd	125	nd
ppm Li	nd	nd	nd	91	nd
ppm Rb	2204	2310	3717	3753	4088
ppm Tl	5	nd	nd	22	nd
ppm K	120165	123025	142034	122544	133860
K/Rb	55	53	38	33	33
K/Tl	25444	--		5571	--
K wt%	12.016	12.303	14.203	12.254	13.386
K_2O wt%	14.475	14.820	17.109	14.762	16.125

Table 2. Representative compositions by DCP analysis of potassium feldspar samples from various zones of the Dumper Dew and the core margin of the Tiger Bill pegmatite. Additional analyses are located in Appendix B.

	Inner Intermediate	Outer Intermediate	Wall Zone
	002-1-9-1	*001-1-1-1*	*008-3-3-1*
Oxides (wt.%)			
P_2O_5	0.012	0.012	0.016
SiO_2	64.512	64.311	64.517
TiO_2	0.009	0.005	0.008
Al_2O_3	18.622	18.994	18.522
FeO	0.000	0.008	0.006
CaO	0.021	0.005	0.033
Na_2O	0.440	0.566	0.267
K_2O	15.654	15.444	15.755
Rb_2O	0.377	0.344	0.643
Cs_2O	0.021	0.078	0.209
Total	99.668	99.767	99.976
Ions on the basis of 8 O			
P	0.000	0.000	0.001
Si	2.991	2.978	2.993
Ti	0.000	0.000	0.000
Sum	2.992	2.978	2.994
Al	1.018	1.037	1.013
Fe	0.000	0.000	0.000
Ca	0.001	0.000	0.002
Na	0.040	0.051	0.024
K	0.926	0.912	0.933
Rb	0.011	0.010	0.019
Cs	0.000	0.002	0.004
Sum	0.978	0.975	0.982

Table 3. Representative compositions by electron microprobe of potassium feldspar samples taken from the Dumper Dew pegmatite. Additional analyses are located in Appendix A.

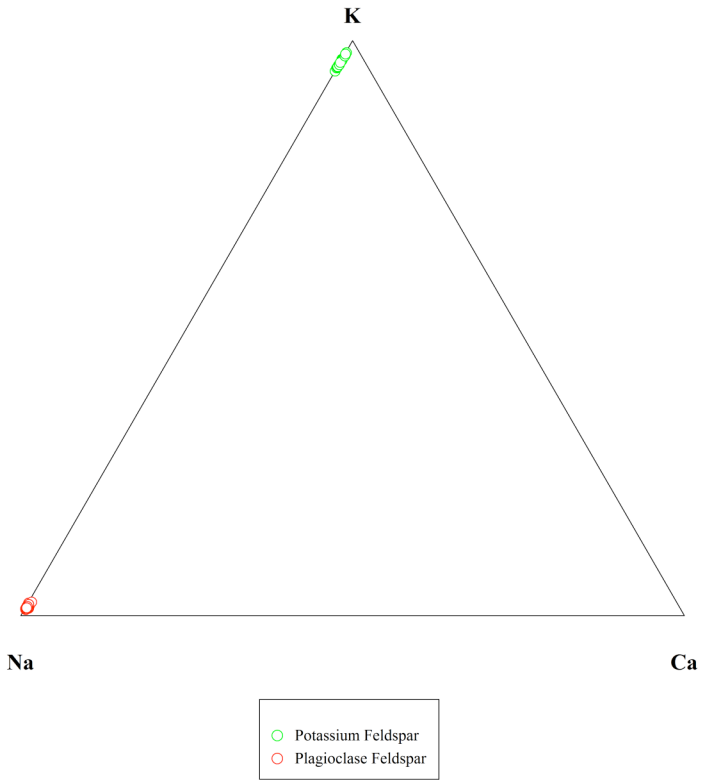

Figure 7. Ternary diagram showing end-member compositions for plagioclase and potassium feldspars from the Dumper Dew and Tiger Bill pegmatites.

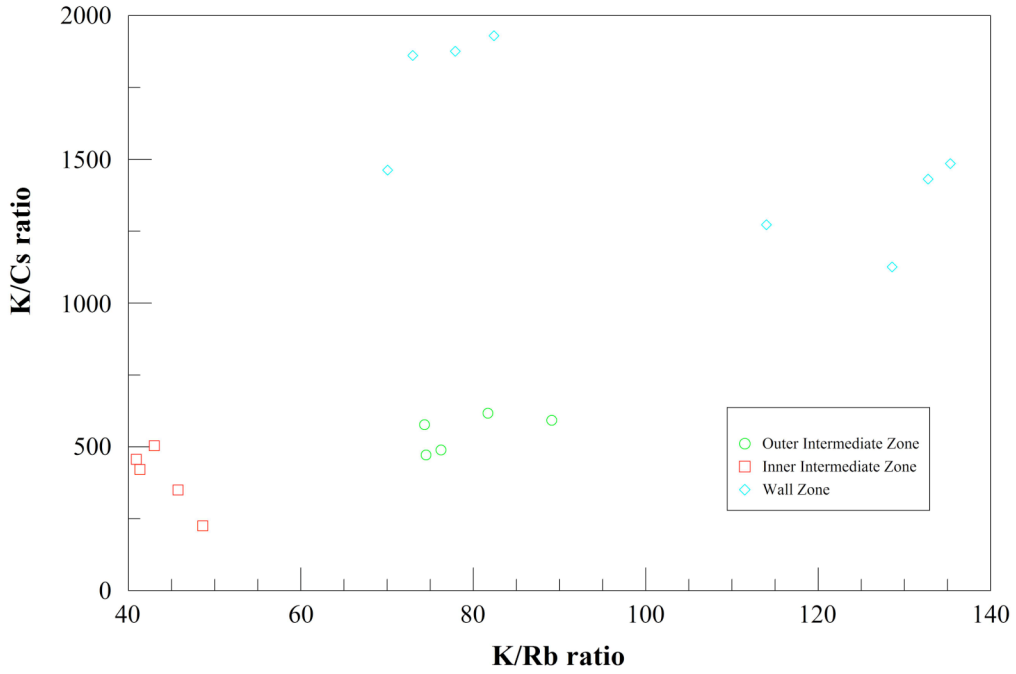

Figure 8. Plot of K/Cs versus K/Rb in potassium feldspar samples from the Dumper Dew pegmatite.

Muscovite $KAl_2(Si_3Al)O_{10}(OH,F)_2$

Muscovite is the most abundant mica in the Dumper Dew pegmatite. The muscovite from intermediate zones is of book variety with pseudohexagonal outlines. Muscovite in the wall zone most commonly occurs as micaceous flakes and tablets with irregular outlines. The muscovite ranges in color from silver to brown and measure up to 5 cm thick. Zonation is commonly seen in muscovite sheets especially from the inner zones of the pegmatite.

Both a primary and secondary generation of muscovite is visible in thin section. The primary muscovite is present as relatively large, euhedral grains. Secondary muscovite is present as sericite predominately along grain boundaries of the feldspars (Figure 9).

Representative microprobe analyses of muscovite are given in Table 4. Ions were calculated from microprobe analyses on the basis of 12 O apfu. K totals are consistently low in all probe analyses where Na, Rb, Cs and Ca may substitute for K in the interlayer site. Cs versus K/Rb is plotted in Figure 10 and illustrates the high degree of fractionation in the Dumper Dew pegmatite. Rb, Cs and Tl (Tables 4 and 5) are more abundant in and therefore, substitute for K more often in intermediate zones. Li content, via DCP analysis (Table 5), ranges from 584 to 4248 ppm. Concentrations of Li are expectedly higher toward inner zones of the pegmatite. B, ranging from 21 to 309 ppm, was detected in muscovite from the wall and intermediate

zones of the pegmatite. Tl was detected in negligible quantities from the intermediate zone and replacement unit and therefore not useful for plotting.

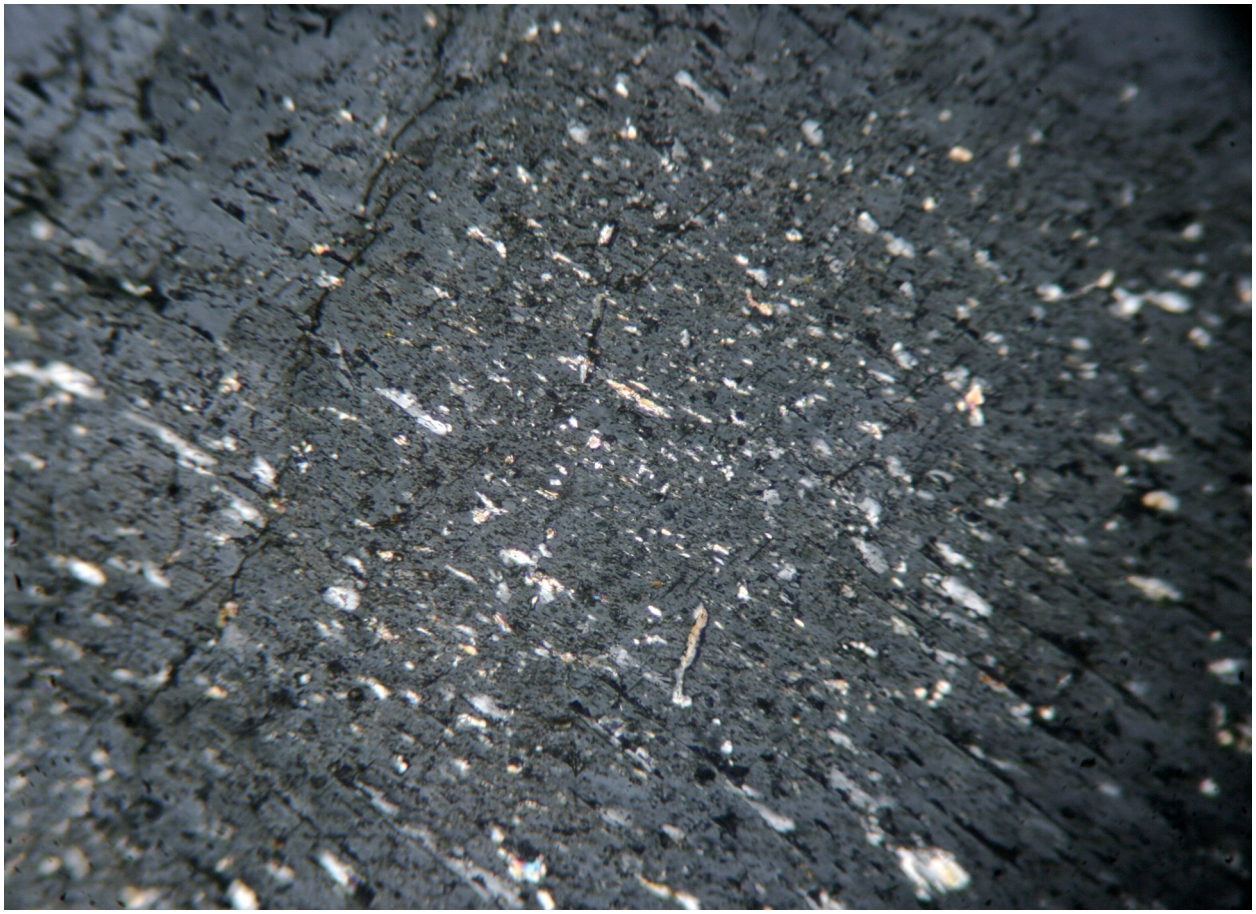

Figure 9. Photomicrograph of sericite replacing feldspar. Magnified 100x.

	Replacement Zone	Inner Intermediate	Outer Intermediate	Wall	Tiger Bill
	010-3-7-3	*002-1-13-4*	*001-1-3-2*	*008-3-4-1*	*TB-3-13-1*
Oxide (wt.%)					
SiO_2	45.633	45.387	45.442	45.700	45.487
TiO_2	0.020	0.082	0.078	0.055	0.077
Al_2O_3	36.620	36.434	35.634	36.508	35.888
FeO	2.444	2.994	2.655	2.655	2.676
MnO	0.000	0.034	0.000	0.009	0.015
MgO	0.000	0.097	0.095	0.022	0.765
CaO	0.031	0.032	0.030	0.036	0.000
Na_2O	0.256	0.132	0.333	0.217	0.228
K_2O	9.458	9.374	9.877	9.477	10.121
Rb_2O	0.633	0.632	0.645	0.344	0.031
Cs_2O	0.044	0.067	0.107	0.022	0.000
H_2O	3.292	3.491	3.586	3.470	3.858
F	2.776	2.295	2.005	2.366	1.454
Subtotal	101.207	101.051	100.487	100.881	100.600
-O=F					
Total	100.038	100.085	99.642	99.885	99.988
Ions on the basis of 12 (O,OH,F)					
Si	2.970	2.972	3.004	2.984	2.998
Ti	0.001	0.004	0.004	0.003	0.004
Sum	2.971	2.976	3.008	2.987	3.002
Al	2.809	2.812	2.776	2.810	2.788
Fe	0.133	0.164	0.147	0.145	0.147
Mn	0.000	0.002	0.000	0.000	0.001
Mg	0.000	0.009	0.009	0.002	0.075
Ca	0.002	0.008	0.002	0.003	0.002
Na	0.032	0.017	0.043	0.027	0.029
K	0.785	0.783	0.833	0.790	0.851
Rb	0.026	0.027	0.027	0.014	0.001
Cs	0.001	0.002	0.003	0.001	0.000
Sum	0.981	1.006	1.064	0.982	1.105
OH	1.429	1.525	1.581	1.511	1.697
F	0.571	0.475	0.419	0.489	0.303

Table 4. Representative compositions by electron microprobe of muscovite samples taken from various zones of the Dumper Dew and the core margin of the Tiger Bill pegmatite. Additional analyses are located in Appendix A.

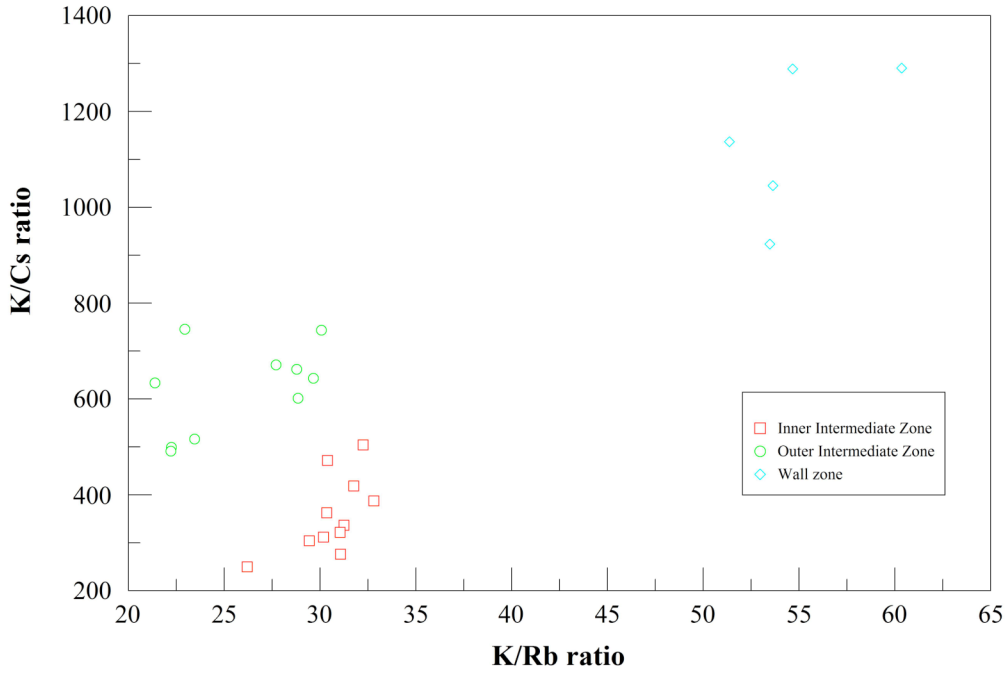

Figure 10. Plot of K/Cs versus K/Rb in muscovite samples from the Dumper Dew pegmatite.

Elemental Abundances	Tiger Bill *TB I*	Wall Zone *07-008 TSI*	Outer Intermediate *07-001 I*	Inner Intermediate *07-002 XIII*	Replacement Zone *07-010 II*
ppm B	122	nd	nd	309	303
ppm Li	1709	1234	584	4248	3500
ppm Rb	2521	1677	1063	4860	5250
ppm Tl	12	nd	nd	8	14
ppm K	82816	75638	78557	77622	92050
K/Rb	33	45	74	16	18
K/Tl	7060	--	--	9652	6658
K wt%	8.282	7.564	7.856	7.762	9.205
K_2O wt%	9.976	9.111	9.463	9.350	11.088

Table 5. Representative compositions by DCP analysis of muscovite samples from various zones of the Dumper Dew and the core margin of the Tiger Bill pegmatite. Additional analyses are located in Appendix B.

Minor Minerals

Garnet $A_3B_2(SiO_4)_3$

Garnet is a relatively abundant accessory mineral that can be found in all zones of the Dumper Dew. Crystals are euhedral and maximum diameters can exceed 5 cm. A change in color and luster were noted and can probably be attributed to a change in elemental abundances. Wall zone garnets have a deep red color and resinous luster while replacement zone crystals are brighter red and have a vitreous luster. Formulas were calculated from the oxide analyses on the basis of 12 O apfu. Representative microprobe analyses of garnet samples are given in Table 6.

Garnet has a number of solid solution series between the end members (e.g., almandine-spessartine, pyrope-grossular). Garnet compositions in the Dumper Dew and Tiger Bill pegmatites are almandine and spessartine where A= Fe or Mn, respectively (Figure 11). Garnet at the Dumper Dew and Tiger Bill is almandine, except for spessartine in the replacement zone of the Dumper Dew. Figure 12 shows that Dumper Dew garnets are the most Mn-rich and Mg-poor, and thus more fractionated. There are only minor amounts of Mg (pyrope), Ca (grossular) and Fe^{3+} (andradite) incorporated as the X-site cation in the garnet structure. The most common species of garnet analyzed from either pegmatite is Mn-rich almandine that ranges into spessartine. Garnet compositions in the Dumper Dew show a decrease in Fe content and an increase in Mn content within

more evolved portions of the pegmatite. There is a decreasing Fe/Mn ratio with increasing fractionation seen in the Dumper Dew pegmatite; garnet with Fe > Mn occurs in the wall zone, garnet with Mn almost equal to Fe occurs in the inner intermediate zone, and spessartine garnet (~23.5 wt.% MnO) occurs in the replacement unit (Figure 13). Garnet which is closest to the spessartine composition are located along with the Mn-rich green apatite of the replacement unit.

	Tiger Bill Core Margin	Replacement Zone	Wall Zone	Inner Intermediate Zone
	TB-3-14-1	010-3-11-1	008-3-2-2	002-1-15-3
Oxides (wt.%)				
SiO_2	36.433	36.456	36.455	36.543
TiO_2	0.012	0.008	0.000	0.004
Al_2O_3	20.566	20.589	20.530	20.559
Fe_2O_3	0.412	0.506	0.137	0.130
FeO	23.726	20.420	21.665	22.683
MnO	19.879	23.411	20.433	19.312
MgO	0.098	0.000	0.000	0.134
CaO	0.677	0.967	0.933	0.790
Total	101.803	102.357	100.153	100.155
Ions on the basis of 12 O				
Si	2.969	2.959	3.001	3.004
Ti	0.001	0.000	0.000	0.000
Sum	2.970	2.960	3.001	3.005
Al	1.975	1.970	1.992	1.992
Fe^{3+}	0.025	0.031	0.008	0.008
Sum	2.000	2.001	2.000	2.000
Fe^{2+}	1.617	1.386	1.491	1.560
Mn	1.372	1.610	1.425	1.345
Mg	0.012	0.000	0.000	0.016
Ca	0.059	0.084	0.082	0.070
Sum	3.060	3.080	2.998	2.990

Table 6. Representative compositions by electron microprobe of garnet from various zones of the Dumper Dew and the core margin of the Tiger Bill pegmatite. Additional microprobe analyses are located in Appendix A.

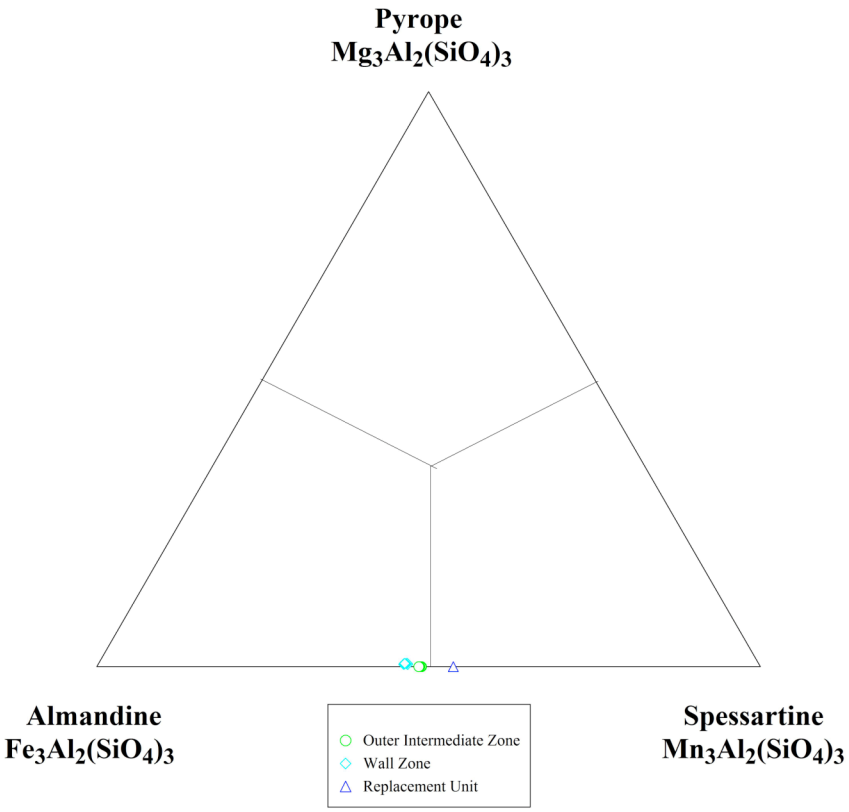

Figure 11. Almandine – Pyrope - Spessartine Ternary Diagram for Dumper Dew garnet.

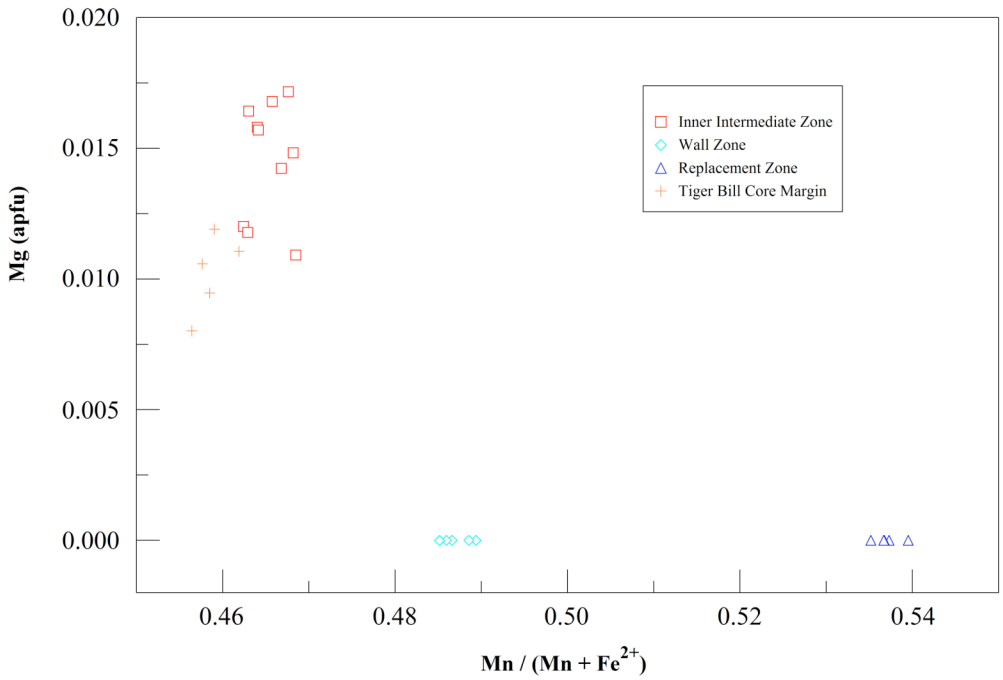

Figure 12. Mg (apfu) versus Mn/(Mn+Fe^{2+}) for garnet compositions in the Dumper Dew and Tiger Bill pegmatites (apfu stand for atoms per formula unit; i.e., the subscripted numbers in a mineral's formula).

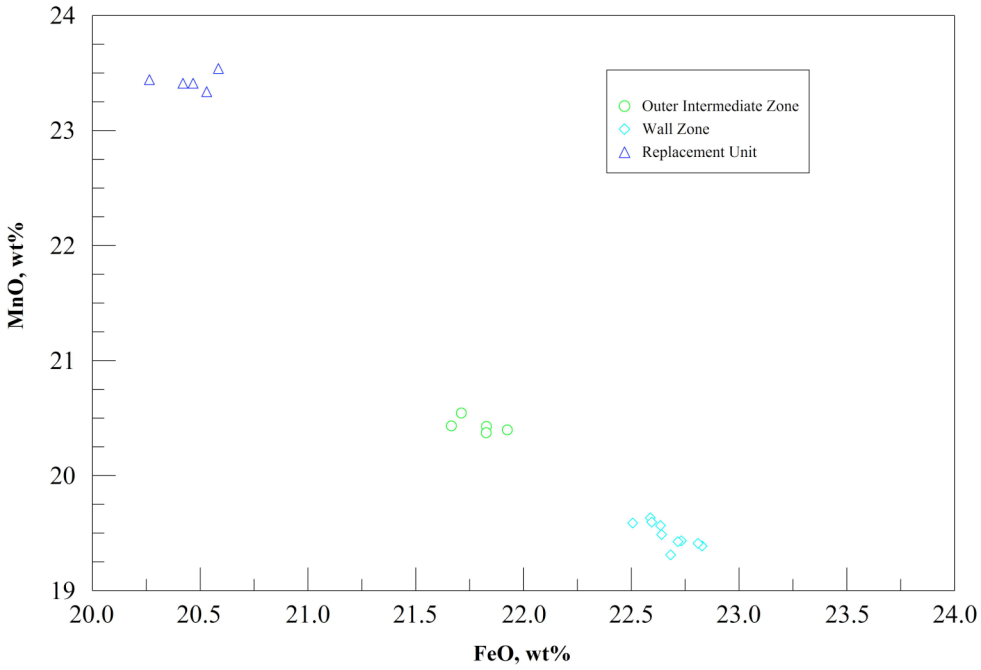

Figure 13. Weight percent MnO versus weight percent FeO for garnet compositions in the Dumper Dew pegmatite.

Apatite $Ca_5(PO_4)_3(OH,F,Cl)$

Two types of apatite are recognized from the Dumper Dew pegmatite: (1) zoned, purple and blue, up to 2 cm, euhedral grains located in the inner intermediate zone and replacement unit, almost exclusively associated with "vuggy albite" and muscovite; (2) green, less than 5 mm across, subhedral crystals dispersed in the inner intermediate and wall zones usually associated with albite, muscovite and quartz.

Electron microprobe analyses (Table 7) indicate substantial F > OH content in both types of apatite where F was analyzed and the OH content was recalculated. This categorizes both varieties as "fluorapatite." The presence of blue or green fluorapatite in a granite, pegmatite, or aplite indicates crystallization form a P-F-rich melt (Selway, et al., 2005). Type (1) varies between 53.943 and 55.222-wt % CaO and from 0.456 to 1.432-wt % MnO. Type (2) contains elevated Mn with up to 6.310 wt % MnO. A somewhat smaller amount of CaO (49.555 to 50.565-wt %) in type (2) apatite compensates for the additional Mn ions. The color of fluorapatite from the Dumper Dew changes to green when MnO rises over 5% (Figure 15). Mn-poor fluorapatite of type (1) crystallized as a result of the preferential partitioning of Mn into garnet (spessartine) or oxide minerals (manganotantalite) in the replacement unit.

Sr ranges from 0.000 to 0.434 wt-% SrO in both varieties of fluorapatite from the Dumper Dew. Sr apfu *versus* Ca apfu are plotted in

Figure 16. Overall, type (2) apatite has a greater abundance of Sr than type (1). There is no discernable trend in apatite color with respect to Sr content. Sr enters into the albite structure at the earliest onset of crystallization and is later remobilized and incorporated into the apatite structure due to the migration of late-stage fluids (Charoy *et al*., 2003).

Based on microprobe analyses. Fe and Mg are present as negligible amounts in fluorapatite. When Fe apfu are plotted against Ca apfu (Figure 17), it appears that more Fe is incorporated into the structure of type (2) apatite compared to that of type (1).

Apatite from the Dumper Dew pegmatite typically exhibits a greenish-yellow cathodoluminescence (CL; Figure 14). The intensity of CL in apatite is directly proportional to Mn/Fe ratios. While Mn acts as a strong CL activator in apatite from granites, Fe is known as a quencher of luminescence (Kempe and Götze, 2002).

	Purple Inner Intermediate	Purple Inner Intermediate	Purple Replacement Zone	Purple Replacement Zone	Green Inner Intermediate
Oxides (wt.%)					
P_2O_5	42.221	42.159	42.224	42.232	41.745
SiO_2	0.053	0.065	0.045	0.025	0.154
Al_2O_3	0.022	0.000	0.009	0.000	0.023
SrO	0.021	0.000	0.000	0.322	0.094
FeO	0.092	0.122	0.055	0.064	0.300
MnO	1.194	1.223	0.599	0.569	6.097
MgO	0.000	0.000	0.011	0.000	0.000
CaO	54.322	54.223	55.222	54.766	49.679
F	3.559	3.587	3.114	3.220	3.256
Subtotal	101.484	101.379	101.279	101.198	101.348
-O=F	1.499	1.510	1.311	1.356	1.371
Total	99.985	99.869	99.968	99.842	99.977
Ions on the basis of 13 (O,OH,F)					
P	2.996	2.995	2.996	2.998	2.987
Si	0.004	0.005	0.004	0.002	0.013
Sum	3.000	3.000	3.000	3.000	3.000
Al	0.002	0.000	0.001	0.000	0.002
Sr	0.001	0.000	0.000	0.016	0.005
Fe	0.006	0.009	0.004	0.004	0.021
Mn	0.085	0.087	0.043	0.040	0.436
Mg	0.000	0.000	0.001	0.000	0.000
Ca	4.878	4.874	4.959	4.920	4.499
Sum	4.972	4.970	5.008	4.981	4.963
F	0.943	0.952	0.825	0.854	0.870

Table 7. Representative compositions by electron microprobe of green and purple apatite samples taken from the Dumper Dew pegmatite. Additional analyses are located in Appendix A.

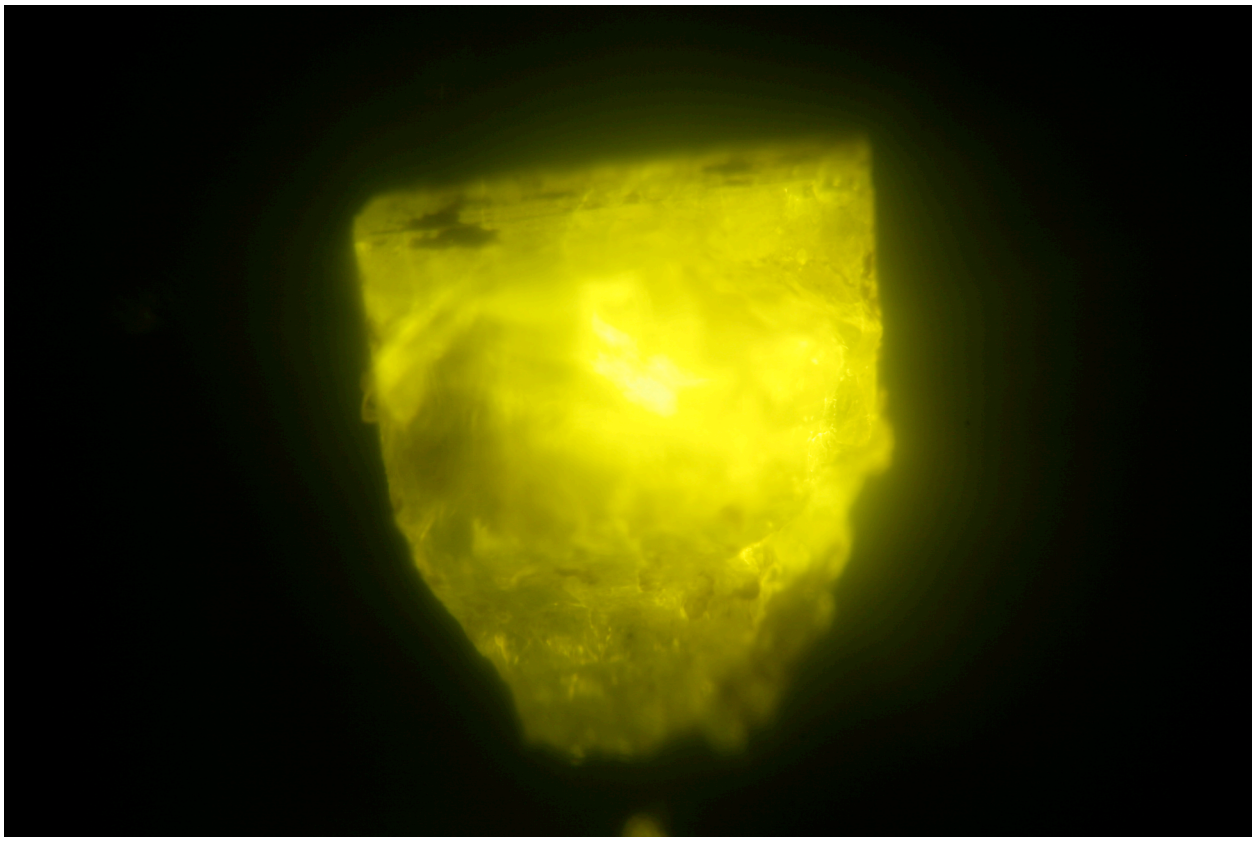

Figure 14. Zoned fluorapatite crystal exhibiting yellow cathodoluminescence.

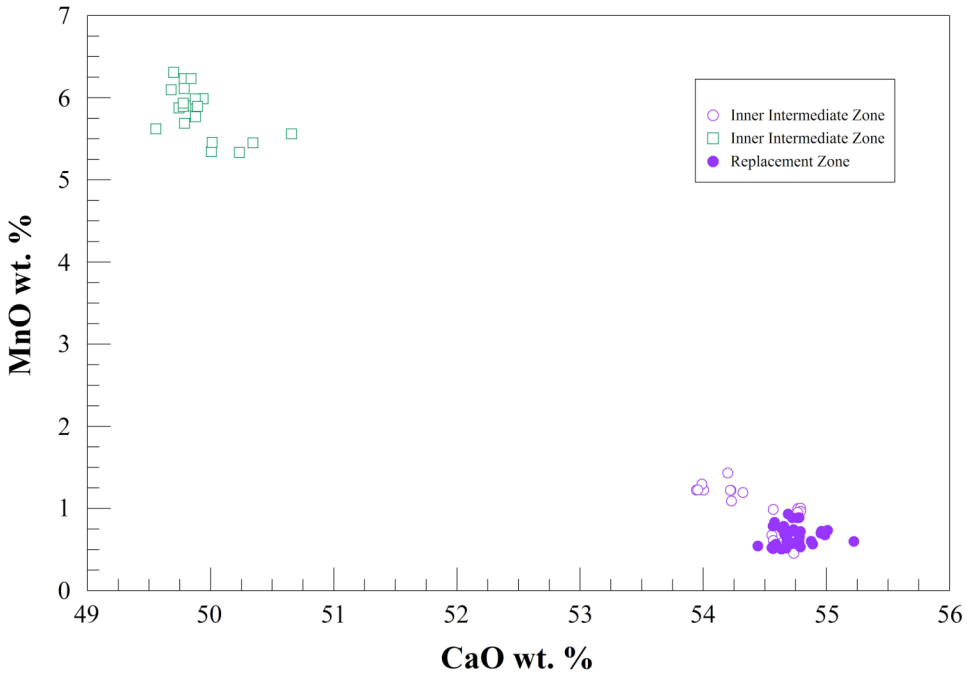

Figure 15. Plot of wt. % CaO versus wt. % MnO in purple and green apatite samples from the Dumper Dew pegmatite. Green apatite are plotted as green squares, purple apatite from the replacement zone are plotted as closed circles and purple apatite from the inner intermediate zone are plotted as open circles.

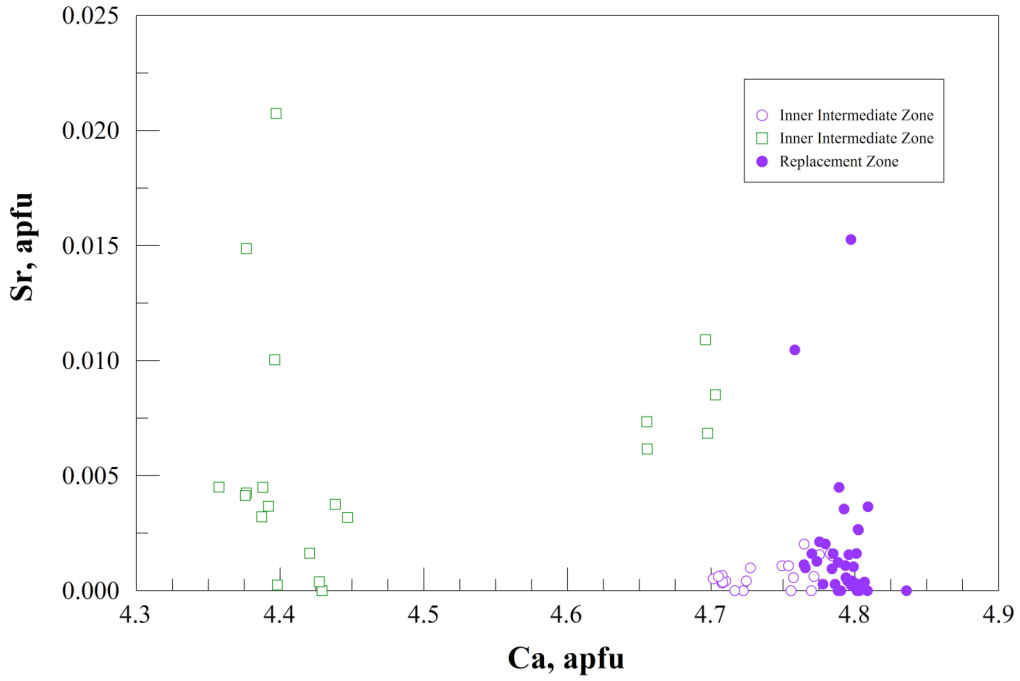

Figure 16. Plot of Ca apfu versus Sr apfu in purple and green apatite samples from the Dumper Dew pegmatite. Green apatite are plotted as green squares, purple apatite from the replacement zone are plotted as closed circles and purple apatite from the inner intermediate zone are plotted as open circles.

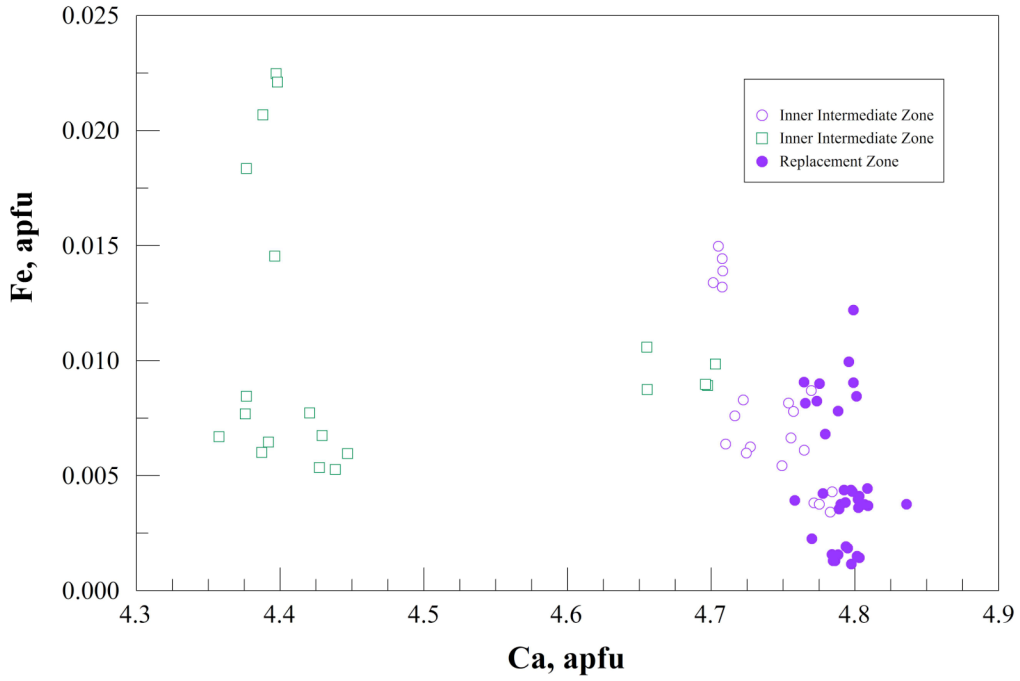

Figure 17. Plot of Ca apfu versus Fe apfu in purple and green apatite samples from the Dumper Dew pegmatite. Green apatite are plotted as green squares, purple apatite from the replacement zone are plotted as closed circles and purple apatite from the inner intermediate zone are plotted as open circles.

Tourmaline $XY_3Z_6(BO_3)_3(Si_6O_{18})(OH)_3(OH,F)$

To date, the only tourmaline species found in and around the Dumper Dew pegmatite is black schorl (Figure 18). Some schorl crystals are prismatic and measure up to 4 cm in diameter, but some schorl is also present as secondary, late fracture fillings. Schorl has been found in the exocontact, the wall zone and both the inner and outer intermediate zones of the Dumper Dew. Due to poor outcrop exposure, orientation of schorl crystals with respect to pegmatite zonation could not be determined.

All schorl samples from the Dumper Dew and Tiger Bill pegmatites plot in the alkali tourmaline field (Figure 19). Representative microprobe analyses of schorl are given in Table 8. Ions were calculated from microprobe analyses on the basis of 31 O apfu. B_2O_3 wt. % was calculated by assuming 3.000 boron ions per formula. Li_2O wt. % was calculated by filling the remaining Y-site vacancy with Li ions until a sum of 3.000 was achieved. Weight percent H_2O was calculated by filling the remaining vacancy of the hydroxyl site with OH^- ions.

X-site cations determined by microprobe analysis are primarily Na ions with some Ca and K ions also present. Na abundance fluctuates between 2.592 and 2.280 wt. % NaO in all analyzed grains. A plot of vacancy *versus* Na displays an expected trend where schorl from the inner intermediate zone is lower in Na content than schorl from outer zones (Figure 20). Another trend the plot shows is an increase in X-site vacancy occurs with

pegmatite fractionation. K enrichment ranges from 0.041 to 0.011 wt. % K_2O in all zones and no chemical trends from these analyses were observed. Microprobe analyses yielded a mean value of 0.048 wt. % CaO in all analyzed schorl.

The Y site cations in shorl are most commonly Fe and Mg, less commonly Mn, Ti, Li and Al. Jolliff *et al*. (1986) suggest a decrease in the Y site abundance of Fe and Mg may be a good indication of increased fractionation. Figure 21 illustrates the degree of Li and Al substitution in the Y site *versus* Fe and Mg. The plot confirms that substitution of Li and Al in the Y site is more prevalent with increased fractionation. The schorl data show that exocontact samples, as expected, are the most primitive tourmaline compositions analyzed. Lithium content (calculated from microprobe data) is more abundant in the interior portions of the Dumper Dew and Tiger Bill pegmatites compared to that of exocontact schorl. Calculated abundances reached 0.388 Li apfu whereas the exocontact schorl did not exceed 0.192 Li apfu. Al content at the Y site decreases in the inner zones of the Dumper Dew relative to earlier crystallized portions (0.591 Al apfu in exocontact schorl to 0.442 Al apfu in inner-intermediate zone samples). Schorl composition in the inner-intermediate zone ranges from 0.456 to 0.255 wt. % MnO while the Mn content of outer-intermediate zone samples range from 0.189 to 0.085 wt. % MnO. The Tiger Bill core margin zone has a measured Mn content between 0.122 and 0.132 wt. % MnO while

exocontact schorl varies in Mn content from 0.135 to 0.068 wt. % MnO. Mg decreases from 2.657 wt. % MgO in the exocontact tourmaline to 1.154 wt. % MgO in inner-intermediate zone samples. The inner-intermediate zone schorl from the Dumper Dew shows a greater abundance of Ti (0.588 to 0.344 wt. % TiO_2) than the outer intermediate zone samples (0.322 to 0.250 wt. % TiO_2). Exocontact schorl has a range of 0.385 to 0.013 wt. % TiO_2 and the core margin zone of the Tiger Bill pegmatite ranges from 0.331 to 0.260 wt. % TiO_2.

Boron abundance is consistent from exocontact to wall zone to inner-intermediate zone and ranges from 10.941 to 10.510 wt. % B_2O_3. OH^- ions are in greater abundance than F ions, and fill the hydroxyl site by a ratio of almost 3:1. F profusion is consistent throughout all studied samples and varies between 0.719 and 0.611 F apfu.

Representative DCP analyses of schorl grains from both the Dumper Dew and Tiger Bill pegmatites are given in Table 9. Lithium concentrations from DCP analyses follow the same trend as the Li concentrations calculated from microprobe analyses. Thallium abundance, via DCP analyses, show no noticeable change from the wall zone to inner regions of the pegmatite and varies from 38 to 23 ppm.

	Inner Intermediate *002-1-10-1*	Outer Intermediate *010-3-9-3*	Tiger Bill Core Margin *TB-4-2-3*	Exocontact Tourmaline *022-3-13-5*
Oxides (wt.%)				
SiO_2	36.665	35.623	36.599	35.555
TiO_2	0.565	0.256	0.290	0.021
B_2O_3 (calc.)	10.612	10.531	10.680	10.557
Al_2O_3	33.412	34.596	34.367	34.559
FeO	12.433	10.934	11.400	12.480
MnO	0.287	0.154	0.122	0.072
MgO	1.455	1.834	1.899	1.998
CaO	0.044	0.041	0.035	0.045
Li_2O (calc.)	0.581	0.572	0.595	0.337
Na_2O	2.388	2.532	2.549	2.488
K_2O	0.027	0.036	0.022	0.011
H_2O (calc.)	3.039	2.999	3.101	3.036
F	1.312	1.340	1.232	1.280
Subtotal	102.821	101.447	102.891	102.440
-O=F	0.552	0.564	0.519	0.539
Total	102.268	100.883	102.372	101.901
Ions on the basis of 31 (O, OH, F)				
Si	6.004	5.878	5.955	5.852
Al	0.000	0.122	0.045	0.148
Tet. Sum	6.004	6.000	6.000	6.000
B	3.000	3.000	3.000	3.000
Al (Z)	6.000	6.000	6.000	6.000
Al	0.449	0.607	0.546	0.556
Ti	0.070	0.032	0.035	0.003
Fe^{2+}	1.703	1.509	1.551	1.718
Mn	0.040	0.022	0.017	0.010
Mg	0.355	0.451	0.460	0.490
Li	0.383	0.379	0.389	0.223
Y sum	2.999	3.000	2.999	3.000
Ca	0.008	0.007	0.006	0.008
Na	0.758	0.810	0.804	0.794
K	0.006	0.008	0.005	0.002
Vacancy	0.228	0.175	0.185	0.196
X sum	1.000	1.000	1.000	1.000
F	0.679	0.699	0.634	0.666
OH	3.320	3.301	3.365	3.334

Table 8. Representative compositions by electron microprobe of schorl samples taken from various zones of the Dumper Dew and Tiger Bill core margin. Additional analyses are located in Appendix A.

Elemental Abundances	Tiger Bill	Outer Intermediate	Inner Intermediate	Replacement Zone	Wall Zone Above Quartz Lens
	TB III	*07-002 XV*	*07-002*	*WP-010*	*07-004a*
ppm B	14413	17046	17666	16959	23054
ppm Li	29	211	325	197	nd
ppm Rb	nd	nd	nd	nd	nd
ppm Tl	23	25	38	32	38
ppm K	796	1153	980	1082	1345
K/Tl	34	46	26	34	36
K wt%	0.080	0.115	0.098	0.108	0.134
K_2O wt%	0.096	0.139	0.118	0.130	0.162

Table 9. Representative compositions by DCP analysis of schorl samples from various zones of the Dumper Dew and Tiger Bill core margin. Additional analyses are located in Appendix B.

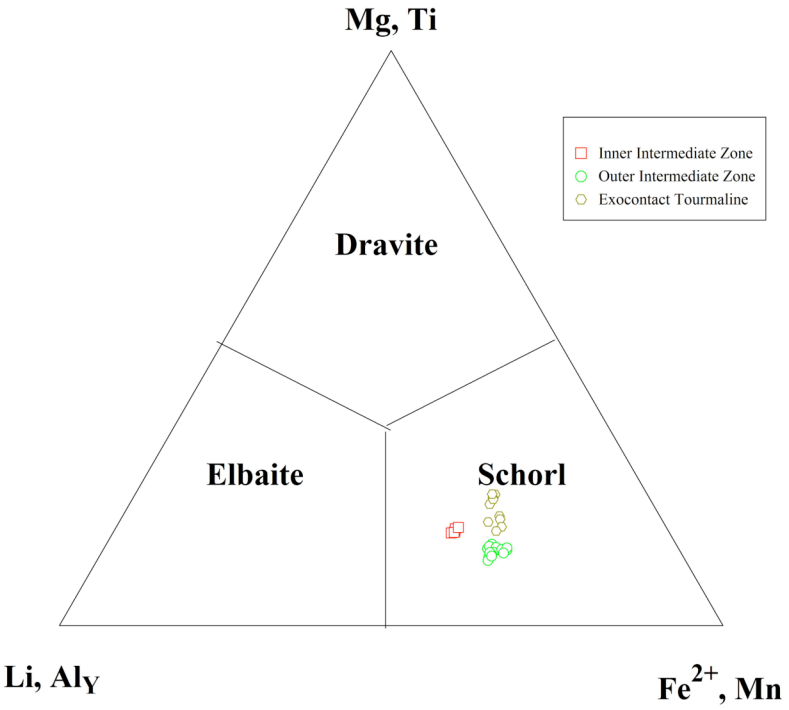

Figure 18. Ternary diagram of the main cations at the Y site in schorl samples from the Dumper Dew pegmatite.

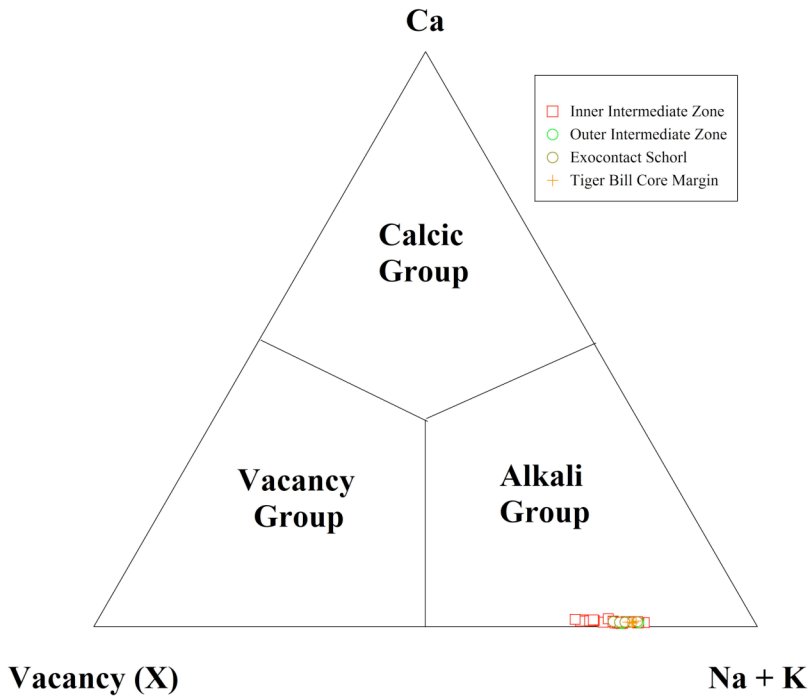

Figure 19. Ternary diagram of the main components at the X site in schorl samples from the Dumper Dew and Tiger Bill pegmatites.

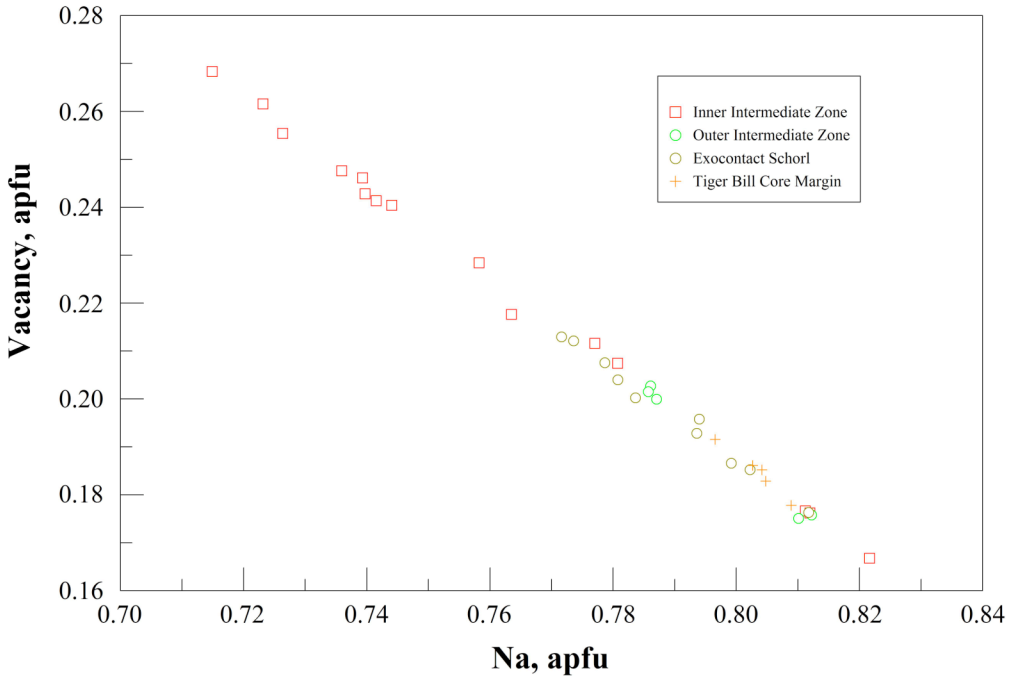

Figure 20. Plot of vacancy versus Na content at the X-site of schorl samples from the Dumper Dew and Tiger Bill pegmatites.

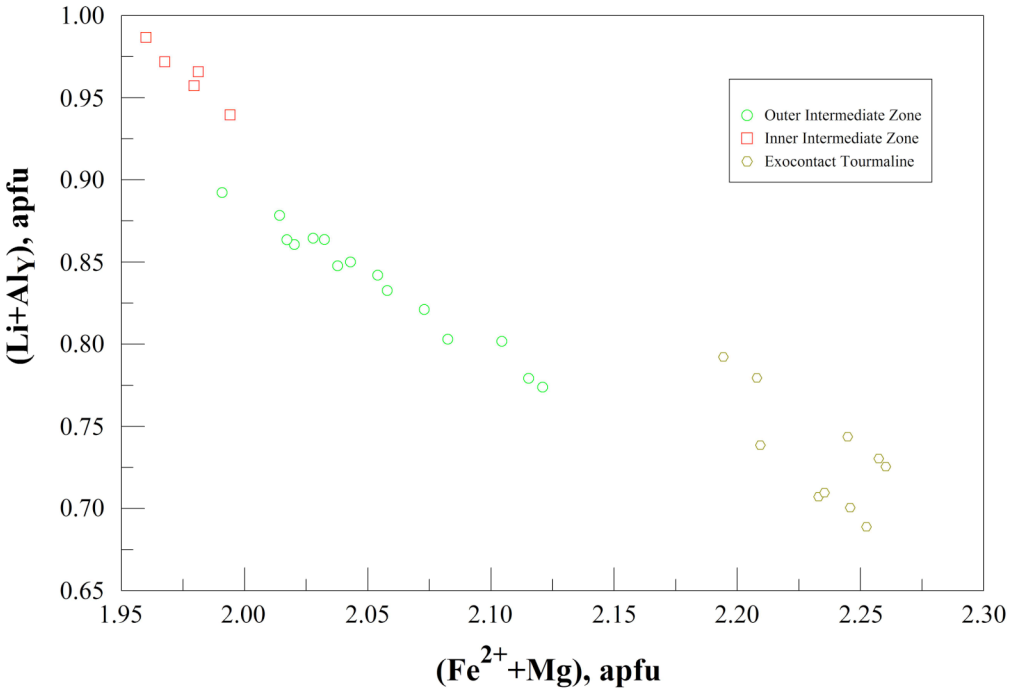

Figure 21. Plot of $Li+Al_Y$ versus $Fe^{2+}+Mg$ content at the Y-site of schorl samples from the Dumper Dew pegmatite.

Accessory Minerals

Beryl $Al_2Be_3Si_6O_{18}$

Beryl is present in minor quantities throughout both intermediate zones of the Dumper Dew pegmatite. It is commonly associated with albite, muscovite, quartz and spodumene. Crystals occur as hexagonal prisms and measure up to 4 cm in length. Colorless, green, white and golden varieties have been encountered. Beryl casts were encountered along an area of one of the intermediate zones where late-stage fluids removed previously present beryl crystals. Some beryl crystals show extreme cathodoluminescence when exposed to shortwave ultraviolet light (Figure 23). Cathodoluminescence may be attributed to one or both activator elements, such as Ti or Mn, present in the beryl samples.

In this study there were no analyses performed to quantitatively measure amounts of lithium or beryllium present in the beryl samples. The number of Be ions were assumed to be 3.000 apfu for each analysis based on the chemical formula of beryl. Representative microprobe analyses of Dumper Dew beryl are given in Table 10. Ion proportions were calculated on the basis of 18 O apfu. Low wt % totals for some analyses are probably indicative of higher H_2O content in some samples (Hawthorne and Cerny, 1977). According to previous work by Cerny (1975), the center channel of the beryl structure may be occupied by minor amounts of Na, K, Cs and Rb. These elements are present in the following quantities: Na (0.220-1.320 wt

% Na_2O), K (0.000-0.389 wt % K_2O), Cs (0.000-0.987 wt % Cs_2O) and Rb (0.000-0.243 wt % Rb_2O). Cs concentrations increased as crystallization and melt fractionation progressed inward (Figure 22). Cs fractionation is also evident as the beryl crystals are zoned with Cs-poor cores and Cs-rich rims. Although Rb concentrations follow the same trend as Cs, Rb is present in smaller quantities. In the octahedral site, minor amounts of Fe (0.000-0.654 wt % FeO), Mn (0.000-0.077 wt % MnO), and Mg (0.000-0.032 wt % MgO) have substituted for Al (Cerny and Hawthorne, 1976).

	Outer Intermediate Pink Rim	Outer Intermediate Golden Rim	Inner Intermediate Green Rim	Inner Intermediate Colorless Rim	Inner Intermediate Colorless Rim
Oxides (wt.%)					
SiO_2	66.623	64.455	64.523	64.403	66.442
Al_2O_3	18.623	18.555	18.554	18.411	18.465
FeO	0.113	0.287	0.465	0.000	0.095
Cs_2O	0.033	0.026	0.010	0.334	0.987
Rb_2O	0.020	0.020	0.000	0.084	0.230
MnO	0.077	0.018	0.009	0.009	0.021
Na_2O	0.312	0.345	0.213	0.500	1.123
K_2O	0.276	0.054	0.043	0.055	0.288
BeO	13.888	13.516	13.527	13.485	13.919
Total	99.965	97.276	97.344	97.281	101.578
Ions by 18 (O)					
Si	5.991	5.955	5.957	5.964	5.961
Al	1.974	2.021	2.019	2.009	1.952
Fe	0.008	0.022	0.036	0.000	0.007
Cs	0.001	0.008	0.000		0.034
Rb	0.001	0.001	0.000	0.005	0.013
Mn	0.006	0.001	0.001	0.001	0.002
Mg	0.000	0.000	0.000	0.000	0.000
Ca	0.000	0.000	0.000	0.000	0.000
Na	0.054	0.062	0.038	0.090	0.195
K	0.032	0.006	0.005	0.006	0.033
Sum	0.103	0.101	0.080	0.102	0.284
Be	3.000	3.000	3.000	3.000	3.000

Table 10. Representative compositions by electron microprobe of beryl from the Dumper Dew pegmatite. Additional microprobe analyses are located in Appendix A.

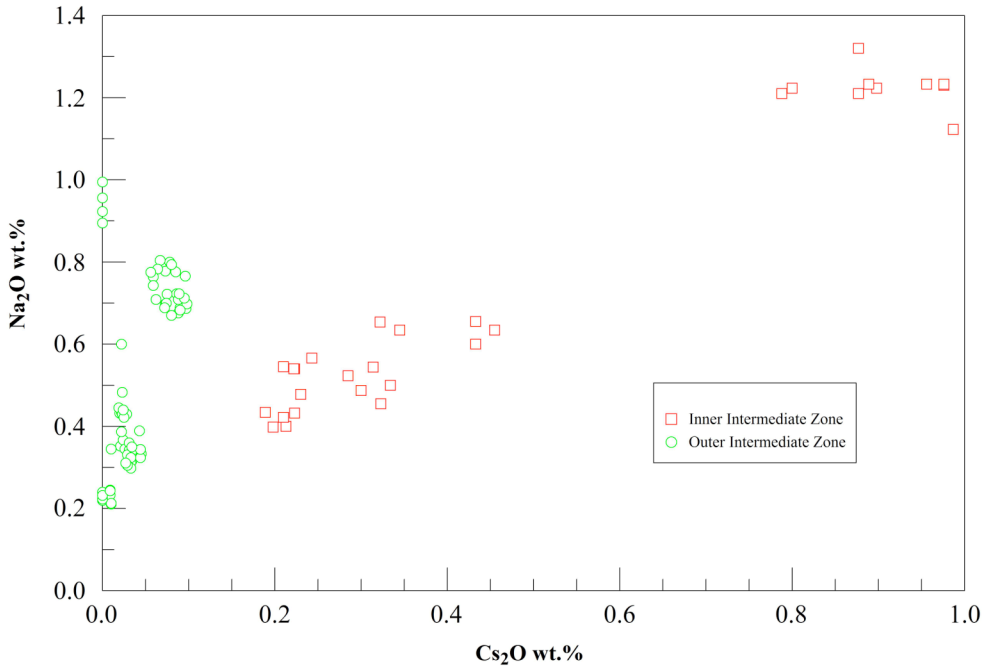

Figure 22. Cs_2O wt. % *versus* Na_2O wt. % for beryl compositions in the Dumper Dew pegmatite.

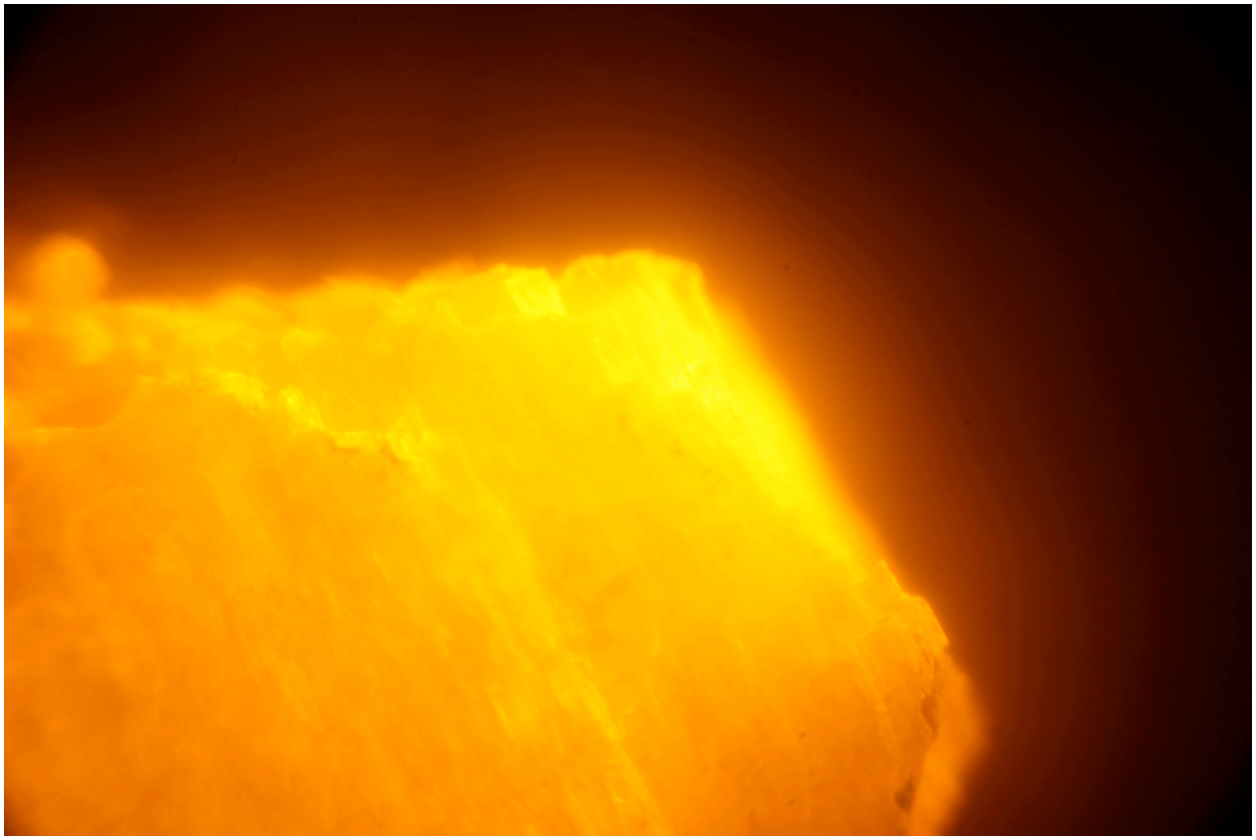

Figure 23. Beryl crystal exhibiting cathodoluminescence.

Columbite-Tantalite $(Mn,Fe)(Nb,Ta)_2O_6$

An important characteristic of rare-element pegmatites is the presence of columbite-tantalite group minerals. These minerals serve as one of the most valuable indicators of fractionation in granitic pegmatites and are not constrained within a single zone of a pegmatite. Analyses of columbite-tantalite group minerals were performed via electron microprobe and ions were calculated on the basis of 6 O apfu. Representative analyses are given in Table 11.

Columbite-tantalite group minerals from the Dumper Dew pegmatite have been noted and analyzed from the outer intermediate and inner intermediate zones and the replacement unit. No Nb-Ta oxides were identified from wall zone samples. A fractionation trend exists of primitive ferrocolumbite (Fe,Nb) in the outer intermediate zone, to manganocolumbite (Mn,Nb) in the inner intermediate zone, to evolved manganotantalite (Mn,Ta) in the replacement unit (Figure 24).

Most columbite-tantalite group minerals at the Dumper Dew are associated with the albite-rich assemblages of each zone. The crystals are metallic, subhedral and vary in color from black to dark brown. Crystal habit can range from flat and tabular to stubby and prismatic. The largest recorded dimensions of a single columbite-tantalite crystal found in the inner intermediate zone measured 3 x 5 mm. Columbite-tantalite appears red in thin section as seen from an inner-intermediate zone sample (Figure 25).

	Outer Intermediate Zone	Inner Intermediate Zone	Replacement Unit
	001-6-4-2	002-2-7	010-6-3-9
Oxides (wt.%)			
FeO	16.877	2.219	1.098
MnO	3.309	17.233	15.476
TiO_2	0.187	0.033	0.096
Ta_2O_5	14.009	18.030	69.170
Nb_2O_5	66.312	62.166	10.315
SnO_2	0.278	0.233	0.312
Total	100.972	99.914	96.467
Ions the basis of 6 (O)			
Fe	0.831	0.112	0.075
Mn	0.165	0.883	1.076
Sum	0.996	0.995	1.151
Ti	0.008	0.002	0.006
Ta	0.224	0.297	1.544
Nb	1.765	1.700	0.383
Sn	0.007	0.006	0.010
Sum	2.004	2.003	1.943

Table 11. Representative compositions by electron microprobe of columbite-tantalite group minerals from inner-intermediate, outer-intermediate and replacement zone samples of the Dumper Dew pegmatite. Additional analyses are located in Appendix A.

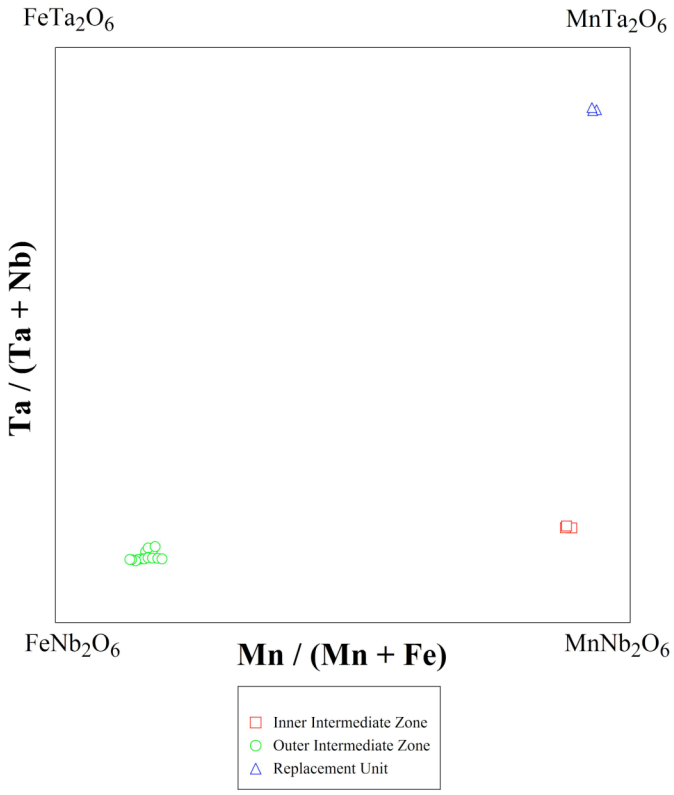

Figure 24. Ta/(Ta+Nb) vs. Mn/(Mn+Fe) for columbite-tantalite compositions plotted in the columbite-tantalite quadrilateral.

Figure 25. Photomicrograph of columbite-tantalite group mineral in thin section from the Dumper Dew. Magnification is 100x.

Cassiterite SnO_2

Cassiterite crystals occur in the inner intermediate zone and the replacement unit, where they are associated with quartz, albite and muscovite. Crystals are black, have a subhedral to anhedral habit, and an adamantine luster. The largest dimensions of a cassiterite mass measured 1.5 cm X 2 cm (Figure 26). Chemical compositions of sampled cassiterite are represented in Table 12. The analyses illustrate a dominance of Sn and Ta cations in the crystal structure. Relative proportions of Ta, Nb and Ti are plotted on a ternary diagram in Figure 27.

Figure 26. Photograph of cassiterite crystal in albite from an inner-intermediate zone sample of the Dumper Dew pegmatite. Field of view is 2 cm.

	Replacement Unit		Inner Intermediate Zone	
	010-6-2-2	*010-6-2-3*	*002-2-4*	*002-2-5*
Oxides (wt.%)				
SnO_2	99.523	99.451	99.232	99.200
Ta_2O_5	0.114	0.089	0.134	0.139
Total	99.637	99.540	99.366	99.339
Ions on the basis of 2 (O)				
Sn	0.998	0.998	0.998	0.998
Ta	0.001	0.001	0.001	0.001
X sum	0.999	0.999	0.999	0.999

Table 12. Representative compositions by electron microprobe of cassiterite samples taken from the inner intermediate and replacement zones of the Dumper Dew pegmatite. Additional analyses are available in Appendix A.

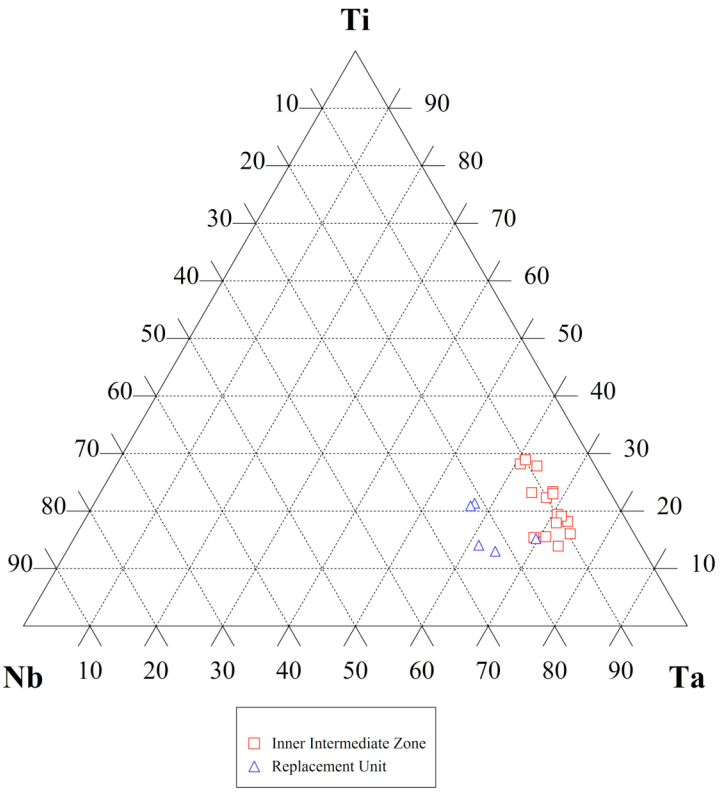

Figure 27. Ta – Nb - Ti Ternary Diagram for Dumper Dew cassiterite samples collected from the inner intermediate zone and replacement unit.

Heterosite-Purpurite $(Fe^{3+}, Mn^{3+})\ PO_4$

Microprobe data obtained from the analysis of several altered phosphate nodules illustrate a dominance of Fe over Mn (Table 13). Based on the prevalence of Fe in the samples, heterosite is the lone end member of the heterosite-purpurite series confirmed by microprobe analyses. Ion proportions were calculated from microprobe analyses on the basis of 4 O apfu.

Heterosite occurs throughout the inner intermediate zone and is found on and around clusters of quartz crystals or as thumbnail-sized nodules encased in feldspar. Specimens have a luster that ranges from submetallic to earthy with colors that range from dark bluish-purple to bright purple (Figure 28). Heterosite nodules from this zone characteristically reach well over 5 cm in diameter.

Chemical composition	Inner-Intermediate Zone Samples			
	002-1-6-2	*002-1-6-3*	*002-2-8-4*	*002-2-8-5*
Oxides (wt.%)				
Fe_2O_3	28.888	28.677	26.564	26.600
Mn_2O_3	20.777	20.887	23.655	23.587
CaO	0.997	1.213	0.098	1.098
P_2O_5	46.676	46.589	46.333	46.655
Total	97.394	97.366	96.650	97.940
Ions on the basis of 4 (O)				
Fe^{3+}	0.550	0.547	0.510	0.507
Mn^{3+}	0.400	0.403	0.459	0.455
Ca	0.027	0.033	0.003	0.030
X sum	0.977	0.983	0.971	0.991
P	1.000	1.000	1.000	1.000

Table 13. Representative compositions by electron microprobe of heterosite-purpurite samples taken from the Dumper Dew pegmatite. For microprobe analysis, all Fe and Mn were recalculated as trivalent.

Figure 28. Photograph of heterosite crystal from an inner-intermediate zone sample of the Dumper Dew pegmatite. Field of view is 1.5 cm.

Manganese and Iron Oxides

Abundant manganese- and iron-bearing phosphates and resultant oxides are found in the replacement and inner intermediate zone of the Dumper Dew pegmatite. Alteration of manganese- and iron-bearing mineral phases has caused the formation of manganese and iron oxides on the outside of residual minerals. Oxides appear as black and dark-brown masses ranging in size from a few millimeters to a few centimeters in size. Most exhibit reddish-brown staining around the rim when embedded in lighter-colored phases.

Alteration of a phosphate to an oxide can occur both in the late- and post-crystallization history of a pegmatite in either hydrothermal or near surface weathering environments (Shigley and Brown, 1985). Iron- and manganese-bearing phosphates from the inner-intermediate zone and the replacement unit have experienced varying degrees of alteration, as shown in Table 14. Alteration and the loss of phosphorous ions are probably responsible for the low weight percent oxide total in the analyses. It has not yet been determined whether these phosphates were converted to oxides through near surface oxidation or hydrothermal alteration.

	Replacement Unit Samples		Inner-Intermediate Zone Samples	
	010-3-5-1	*010-3-5-2*	*002-4-10-1*	*002-4-10-2*
Oxides (wt.%)				
FeO	83.677	82.956	3.233	4.233
MnO	6.344	6.448	80.460	79.677
CaO	0.056	0.129	0.020	0.034
Total	90.077	89.533	83.713	83.944
Ions on the basis of 3 (O)				
Fe	2.784	2.776	0.114	0.149
Mn	0.214	0.219	2.885	2.849
Ca	0.002	0.006	0.001	0.002
X sum	3.000	3.000	3.000	3.000

Table 14. Representative compositions by electron microprobe of Fe and Mn oxides from the Dumper Dew. Additional analyses are located in Appendix A.

Spodumene $LiAl(SiO_3)_2$

Spodumene occurs in the inner intermediate zone as euhedral, tabular crystals elongated along [001] and flattened on [100]. Relatively large crystals are found which measure up to 20 cm in maximum dimension. Most crystals show an earthy-luster and an alteration rind on the crystal faces. When crystals are cut perpendicular to elongation, the fresh-cut inner regions are dark gray to green in color and exhibit a vitreous luster. Spodumene samples exhibited no cathodoluminescence.

Oxide wt. % from microprobe data was used to calculate ion proportions on the basis of 5.5 O per formula unit. Low totals from microprobe analyses are attributed to alteration where Li has been stripped out and replaced by H_2O. Li concentrations were calculated from ion proportions to wt. % Li_2O using 1.000 apfu Li. Microprobe analyses yielded results which approach ideal compositions of spodumene with less than 1 total wt. % of impurities such as Mn, Ca, Na, Rb and K (Tables 15).

DCP assay show quantities of Li, Rb and K and are given in Table 16. Li concentrations ranged for 13717 to 18513 ppm, which translates to 2.95 to 3.98 wt. % respectively. Insignificant amounts of Rb (0-61 ppm) and K (1625-2013 ppm) were reported from DCP analyses.

Inner-Intermediate Zone Samples		
	002-1-5-2	*002-1-5-3*
Oxides (wt.%)		
SiO_2	63.722	63.766
Al_2O_3	27.330	27.233
MnO	0.008	0.011
CaO	0.007	0.009
Li_2O	7.918	7.911
Na_2O	0.044	0.042
K_2O	0.021	0.031
Total	99.050	99.003
Ions the basis of 5.5 O		
Si	1.993	1.995
Al	1.008	1.004
Mn	0.000	0.000
Ca	0.000	0.000
Li	0.996	0.996
Na	0.003	0.003
K	0.001	0.001
Sum	1.000	1.000

Table 15. Representative compositions by electron microprobe of spodumene samples taken from the inner intermediate zone of the Dumper Dew pegmatite.

Elemental Abundances	Inner-Intermediate Zone Samples		
	07-002 VI	*07-002 VII*	*07-002 IX*
ppm B	nd	nd	nd
ppm Li	13717	18513	16555
ppm Rb	61	nd	nd
ppm Tl	nd	nd	nd
ppm K	1625	1939	2013
K/Rb	27	na	na
K wt%	0.163	0.194	0.201
K_2O wt%	0.196	0.234	0.242

Table 16. Representative compositions by DCP analysis of spodumene samples taken from the inner intermediate zone of the Dumper Dew pegmatite. Additional analyses are located in Appendix B.

Hydroxyl-Herderite $CaBe[(F,OH)PO_4]$

Herderite forms a solid solution series with hydroxyl-herderite. Dominance of OH^- versus F (Table 17) in microprobe data confirms that the samples are indeed hydroxyl-herderite. Euhedral hydroxyl-herderite crystals were found encrusting thick books of muscovite in the inner intermediate zone (Figure 29). Crystals from the Dumper Dew are typically stubby, prismatic, and white in color with a vitreous luster. Measured dimensions of larger herderite crystals were up to 7 mm across.

	Inner-Intermediate Zone Samples				
	002-4-14-1	*002-4-14-2*	*002-4-14-3*	*002-4-14-4*	*002-4-14-5*
Oxides (wt.%)					
P_2O_5	44.211	44.093	44.006	44.133	44.111
SiO_2	0.014	0.022	0.043	0.036	0.040
Al_2O_3	0.022	0.043	0.037	0.050	0.034
CaO	33.998	34.095	34.064	33.985	34.120
BeO (calc.)	15.178	15.069	15.044	15.155	15.084
F	0.320	0.340	0.345	0.376	0.332
H_2O (calc.)	5.182	5.164	5.155	5.157	5.171
Subtotal	98.790	98.683	98.548	98.734	98.753
-O=F	0.135	0.143	0.145	0.158	0.140
Total	98.655	98.540	98.403	98.576	98.613
Ions the basis of 5 (O)					
P	1.000	1.000	1.000	1.000	1.000
Si	0.000	0.001	0.001	0.001	0.001
Al	0.001	0.001	0.001	0.002	0.001
Ca	1.025	1.030	1.030	1.025	1.030
Be	0.974	0.969	0.969	0.973	0.969
Sum	2.000	2.000	2.000	2.000	2.000
F	0.027	0.029	0.029	0.032	0.028
OH	0.973	0.971	0.971	0.968	0.972
Sum	1.000	1.000	1.000	1.000	1.000

Table 17. Representative compositions by electron microprobe of hydroxyl-herderite from inner-intermediate zone samples of the Dumper Dew pegmatite.

Figure 29. Photograph of hydroxyl-herderite on muscovite from the intermediate zone of the Dumper Dew pegmatite. Field of view is 2 cm.

Cookeite $LiAl_4(Si_3Al)O_{10}(OH)_8$

Cookeite occurs as anhedral, mint-green crystals with pearly luster. A very fine-grained mass of outer-intermediate zone cookeite measured 10 cm across. Coatings and encrustations of cookeite are found on quartz, albite and spodumene. Electron microprobe analyses of cookeite were recast into ion proportions on the basis of 14 O apfu. The only analyzed samples of cookeite were collected from the inner intermediate zone and are given in Table 18. Minor amounts of Na, K and Rb may substitute for Li in the structure. Mn, Mg, Fe and Ca are also present as inconsequential amounts and substitute for Al in the octahedral site (Deer *et al*., 1963).

	Inner-Intermediate Zone Samples				
	002-3-1	*002-3-2*	*002-3-3*	*002-3-4*	*002-3-5*
Oxides (wt.%)					
SiO_2	33.455	33.342	33.466	33.451	33.511
Al_2O_3	47.449	47.333	47.512	47.512	47.387
FeO	1.007	0.956	0.996	1.013	0.955
MnO	0.008	0.009	0.006	0.009	0.007
MgO	0.088	0.108	0.079	0.085	0.094
CaO	0.678	0.623	0.733	0.652	0.634
Li_2O (calc.)	2.258	2.271	2.255	2.230	2.278
Na_2O	0.032	0.022	0.025	0.035	0.034
K_2O	0.022	0.025	0.023	0.020	0.019
Rb_2O	0.034	0.025	0.032	0.260	0.026
H_2O (calc.)	13.070	13.025	13.083	13.082	13.062
Total	98.108	97.739	98.210	98.355	98.006
Ions the basis of 14 (O)					
Si	3.070	3.070	3.068	3.067	3.077
Al	1.000	1.000	1.000	1.000	1.000
Al	4.132	4.137	4.133	4.133	4.128
Fe	0.077	0.074	0.076	0.078	0.073
Mn	0.001	0.001	0.000	0.001	0.001
Mg	0.012	0.015	0.011	0.012	0.013
Ca	0.067	0.061	0.072	0.064	0.062
Li	0.833	0.841	0.831	0.822	0.841
Na	0.006	0.004	0.004	0.006	0.006
K	0.003	0.003	0.003	0.002	0.002
Rb	0.002	0.001	0.002	0.015	0.002
OH	8.000	8.000	8.000	8.000	8.000

Table 18. Representative compositions by electron microprobe of cookeite samples taken from the inner intermediate zone of the Dumper Dew pegmatite.

Amblygonite-Montebrasite ($LiAlPO_4F$ – $LiAlPO_4OH$)

Montebrasite can be found in the inner intermediate zone of the Dumper Dew pegmatite. Crystals are subhedral and measure up to 3.5 cm across. Samples collected are milky white and entirely enclosed in quartz.

Analyses of montebrasite were performed via electron microprobe and ions were calculated on the basis of 5 O apfu (Table 19). The montebrasite ranges in F content from 5.212 to 5.773 wt. %. This falls on the montebrasite side of the compositional boundary between amblygonite and montebrasite (atomic F/OH = 1.0, at 6.47 wt. % F). According to Cerny (1972), primary amblygonite-montebrasite contains from 4 to 7 wt. % F. Alternately, a secondary phase of montebrasite consists of only 1 to 4 wt. % F. Therefore, the measured quantity of F in samples from this study lies within the range of primary-phase montebrasite assigned by Cerny (1972).

	Inner-Intermediate Zone Samples				
	002-2-16-1	*002-2-16-2*	*002-2-16-3*	*002-2-16-4*	*002-2-16-5*
Oxides (wt.%)					
P_2O_5	48.210	48.546	48.312	48.634	48.233
SiO_2	0.022	0.026	0.032	0.029	0.024
Al_2O_3	34.887	34.674	34.745	34.679	35.004
CaO	0.009	0.011	0.012	0.009	0.012
Li_2O	9.035	9.008	9.029	8.976	8.955
Na_2O	0.045	0.065	0.053	0.048	0.050
H_2O	3.013	3.121	3.024	3.241	3.230
F	5.787	5.556	5.773	5.245	5.212
Subtotal	101.008	101.007	100.980	100.861	100.720
-O=F	2.437	2.340	2.431	2.209	2.195
Total	98.571	98.668	98.549	98.653	98.525
Ions on the basis of 5 (O,OH,F)					
P	0.999	0.999	0.999	0.999	0.999
Si	0.001	0.001	0.001	0.001	0.001
Sum	1.000	1.000	1.000	1.000	1.000
Al	1.007	0.994	1.000	0.992	1.010
Li	0.998	0.997	0.997	0.998	0.997
Ca	0.000	0.000	0.000	0.000	0.000
Na	0.002	0.003	0.003	0.002	0.002
Sum	1.000	1.000	1.000	1.000	1.000
OH	0.552	0.573	0.554	0.597	0.597
F	0.448	0.427	0.446	0.403	0.403
Sum	1.000	1.000	1.000	1.000	1.000

Table 19. Representative compositions by electron microprobe of montebrasite samples taken from the inner intermediate zone of the Dumper Dew pegmatite.

Biotite $K(Fe,Mg)_3AlSi_3O_{10}(OH)_2$

Biotite is restricted to the outer portions of zones in contact with the host rock. The biotite is found as black, micaceous flakes, in irregular shapes with maximum dimensions of less than 5 cm.

Microprobe analyses of biotite were calculated on the basis of 12 oxygen ions per structural formula and are presented in Table 20. The biotite composition is closest to the Fe-rich end member known as annite. There are minor amounts of Na and Ca substituting for K in the interlayer site. There are also substantial amounts of F substituting for OH in the hydroxyl sites.

Pleochroic halos are visible in thin section grains of biotite (Figure 30) and are an indication of the inclusion of radioactive elements. Some grain boundaries of biotite appear colorless in thin section and indicate alteration from biotite to chlorite. Additionally, there are several grains of biotite present in thin section with needles of rutile inclusions.

	Outer-Intermediate Zone Samples				
	001-6-1-1	*001-6-1-2*	*001-6-1-3*	*001-6-1-4*	*001-6-1-5*
Oxides (wt.%)					
SiO_2	34.675	34.774	34.673	34.655	34.673
TiO_2	1.212	1.233	1.430	1.432	1.633
Al_2O_3	18.645	18.777	18.687	18.713	18.734
FeO	25.887	25.930	25.934	25.984	25.984
MnO	0.566	0.600	0.576	0.623	0.587
MgO	5.445	5.655	5.486	5.745	5.632
CaO	0.007	0.000	0.000	0.006	0.006
Na_2O	0.322	0.455	0.511	0.489	0.093
K2O	8.978	9.003	8.875	8.773	8.798
H2O	2.657	2.657	2.674	2.616	2.653
F	2.673	2.734	2.673	2.834	2.734
Subtotal	98.410	99.161	98.845	99.254	98.874
-O=F	1.126	1.151	1.126	1.193	1.151
Total	97.284	98.010	97.719	98.061	97.723
Ions on the basis of 12 (O,OH,F)					
Si	2.638	2.626	2.626	2.613	2.621
Ti	0.069	0.070	0.081	0.081	0.093
Sum	2.707	2.696	2.708	2.695	2.714
Al	1.672	1.671	1.668	1.663	1.669
Fe	1.647	1.638	1.643	1.639	1.643
Mn	0.036	0.038	0.037	0.040	0.038
Mg	0.618	0.637	0.620	0.646	0.635
Ca	0.001	0.000	0.000	0.000	0.000
Na	0.047	0.067	0.075	0.071	0.014
K	0.871	0.867	0.858	0.844	0.848
Sum	3.220	3.246	3.232	3.240	3.177
OH	1.357	1.347	1.360	1.324	1.346
F	0.643	0.653	0.640	0.676	0.654

Table 20. Representative compositions by electron microprobe of biotite samples taken from the Dumper Dew pegmatite.

Figure 30. Photomicrograph of pleochroic halos in biotite. Magnification is 100x.

Montmorillonite $[(Na,Ca)_{0.33}(Al,Mg)_2(Si_4O_{10})(OH)_2 \bullet nH_2O]$

X-ray diffraction (XRD) was used in the confirmation of two pink smectite samples collected from the intermediate zone. Both samples were established to be montmorillonite by XRD analysis, however two different varieties of montmorillonite were confirmed. One sample was found to have a basal spacing of 15 Å and the other, a basal spacing of 21 Å. Figure 31 and Figure 32 displays basal-spacing measurements of both analyzed minerals.

XRD analysis verified the existence of a third variety of montmorillonite. Altered schorl crystals from the replacement zone were analyzed and resulted in the verification of a third variety of montmorillonite. Initially, the schorl was thought to be altering to chlorite, which is a common alteration product of Fe-rich tourmaline. After XRD analysis, alteration from schorl to chlorite was ruled out and a third occurrence of montmorillonite was established. The third variety of montmorillonite differed from the two previously analyzed samples in color and basal spacing. The third occurrence was green in color with a basal spacing of 18 Å. Figure 33 displays basal-spacing measurements of the altered tourmaline.

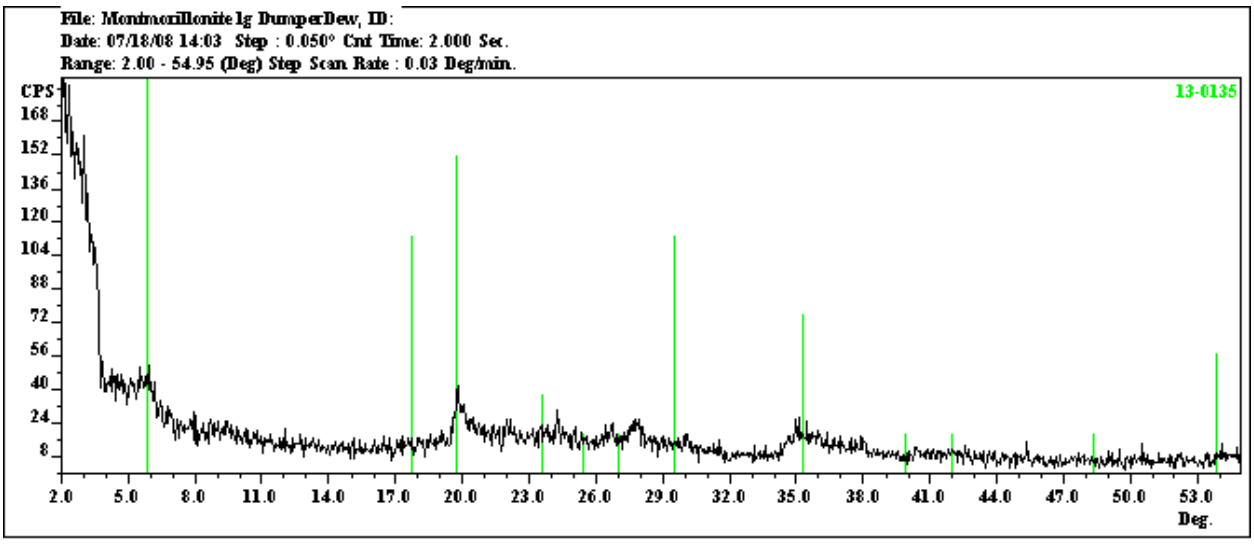

Figure 31. Basal-spacing measurement acquired via XRD of an intermediate zone montmorillonite sample with a basal spacing of 15Å.

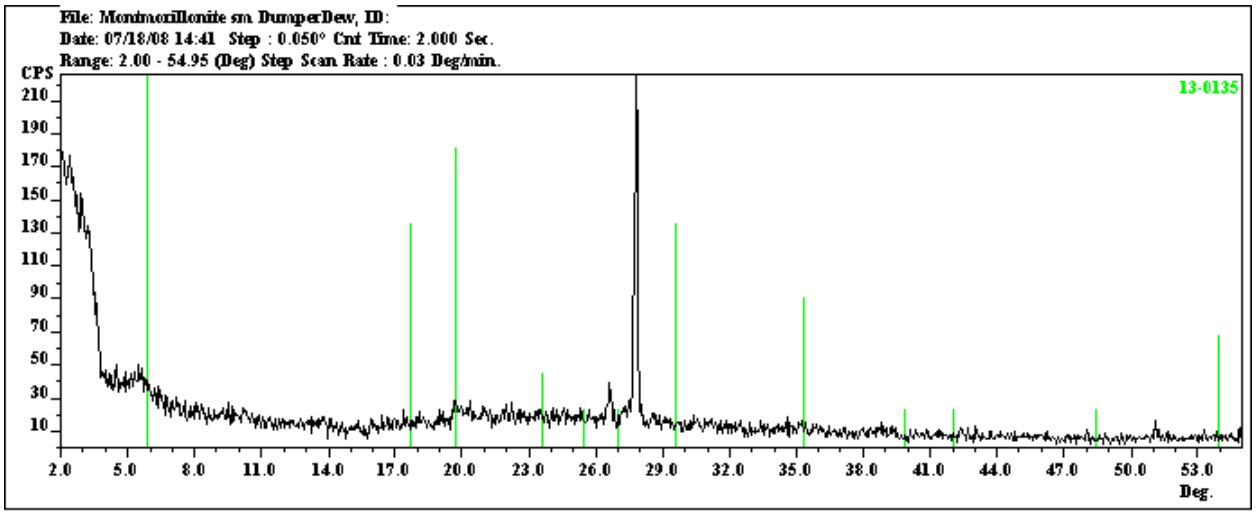

Figure 32. Basal-spacing measurement acquired via XRD of an additional intermediate zone montmorillonite sample with a basal spacing of 21Å.

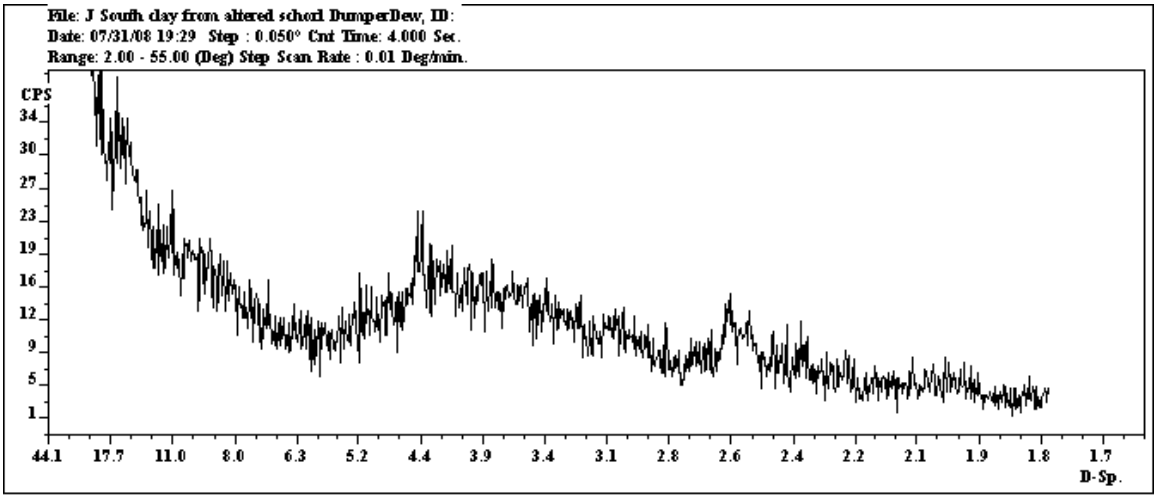

Figure 33. Basal-spacing measurement acquired via XRD of altered tourmaline from replacement unit.

Zircon $ZrSiO_4$

Zircon was confirmed by SEM identification. Samples were obtained via heavy mineral separation. No additional analyses were performed on this mineral.

Pyrite FeS_2

Pyrite was confirmed by SEM identification. Samples were obtained via heavy mineral separation. No additional analyses were performed on this mineral.

Hyalite Opal $SiO_2 \bullet nH_2O$

Hyalite occurs as a late-stage mineral covering fractures in the Dumper Dew pegmatite. The hyalite from the Dumper Dew exhibits either a brilliant green or bright orange fluorescence when exposed to ultraviolet light.

Monazite $(Ce,La,Th,Nd,Y)PO_4$

Ce-dominant monazite was confirmed via SEM analysis as microscopic grains. Samples were recovered from pocket-fill material along with euhedral quartz crystals and fine-grained muscovite. No additional analyses were performed on this mineral.

Löllingite $Fe^{2+}As_2$

Löllingite can be found as microscopic grains in the inner intermediate zone of the Dumper Dew pegmatite. The presence of l*ö*llingite was confirmed by SEM analysis (Figure 34). No additional analyses were performed on this mineral.

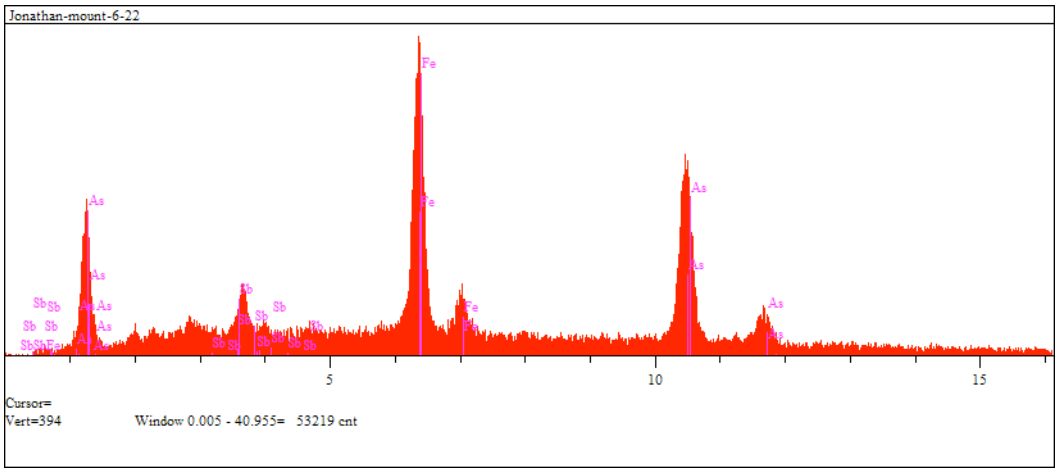

Figure 34. X-ray spectra of löllingite acquired via SEM analysis.

Geochemistry

As a pegmatitic melt crystallizes and fractionates, minerals become more enriched in rare elements. This fractionation trend is recognized by an increase of Rb and Cs in K-feldspar and muscovite; garnet becomes enriched in Mn; and apatite becomes enriched in F. Increasing fractionation also leads to crystallization of Li-Be-B-Ta-Cs-bearing minerals. For example, Li-rich mineralization includes spodumene, petalite, lepidolite, lithiophilite, elbaite and amblygonite/montebrasite; adequate concentrations of Be result in the crystallization of beryl; B profusion gives way to tourmaline; columbite-tantalite group minerals crystallize as manganotantalite from Ta enrichment; and residual melts enriched in elemental Cs will precipitate the ore mineral pollucite.

Various pegmatites show enrichment in rare earth elements to differing degrees. The Dumper Dew pegmatite exemplifies similar, major and trace element trends illustrated by other highly evolved LCT-type pegmatites. The geochemical signature of the Dumper Dew can be represented by fractionation trends of the following elements: an increase in the substitution of Rb and Cs versus K; an increase of Mn over Fe; an elevated P and F content, the fractionation of Ta as opposed to Nb; and relatively high concentrations of Li.

Rubidium

Due to the similar geochemical behaviors of K and Rb, a fractionation trend can be discerned from the elemental ratio. Decreasing K/Rb with advancing crystallization infers the depletion of K and the accumulation of Rb. The result is a noted increase in the incorporation of Rb, versus K, in common rock-forming phases such as K-feldspar and muscovite.

Feldspars are the dominant mineral phase throughout the Dumper Dew, with albite being more abundant than K-feldspar. The feldspars are highly ordered as albite and K-feldspar samples plot on a Na-K-Ca ternary as relatively pure end members. High concentrations of Rb and a low K/Rb ratio in some samples illustrate the highly evolved character of the Dumper Dew k-spars. Muscovite is the most abundant mica throughout the pegmatite. Like the K-feldspars, muscovite samples exemplify an increase in fractionation of Rb from the wall zone inward.

Cesium

The main minerals to incorporate Cs into their structures are K-feldspar, beryl, pollucite, and some micas. The precipitation of Cs mineralization is restricted to later stages of pegmatite crystallization due to elemental incompatibility. Cs has a larger ionic radius than K and is substituted into potassic minerals less frequently than Rb. For this reason, Cs was more concentrated in the residual melt and became incorporated

more frequently into muscovite and K-feldspar in later crystallized zones. Fractionation of Cs is consistent in both K-feldspar and muscovite samples. K-feldspar shows an increase in Cs concentration from the outer zones, inward. Muscovite samples from both intermediate zones display a greater Cs abundance than analyzed wall zone samples.

In highly evolved pegmatites, Cs is incorporated into the structural channels of beryl crystals. Beryl crystals from interior zones of the Dumper Dew show an increased fractionation trend with respect to Cs. Inner-intermediate zone beryl is notably more cesium-rich than outer zone samples, whereas some outer zone samples contain no detectable amounts of Cs.

Lithium

Li enrichment in the pegmatitic melt was sufficient enough to precipitate spodumene and Li-phosphates. Triphylite-lithiophilite was the first lithium mineral to crystallize and can be found in both the outer and inner intermediate zones. Spodumene formed only in the late-crystallizing, interior portions of the dike due to the low ionic radius and charge of the Li ion. Amblygonite-montebrasite formed in the spodumene-rich inner intermediate zone in the absence of Fe and Mn.

Elevated Li content in the pegmatite also lead to the incorporation of Li into the structure of early rock-forming phases. Li contents in muscovite

samples increase toward the pegmatite interior and show a similar fractionation trend as Rb and Cs. Additionally, a marked increase of Li was noted in schorl crystals from the interior pegmatite zones when compared to outer zone samples.

Phosphorous and Fluorine

The pegmatite is enriched in P and F as evidenced by the presence of purple and green fluorapatite. Fluorapatite from the wall and outer intermediate zones crystallized as Mn-rich varieties whereas apatite from the replacement unit crystallized as Mn-poor fluorapatite. This is due to the preferential partitioning of Mn into garnet and the oxide minerals in the replacement unit.

Iron and Manganese

Fe^{2+} and Mn^{2+} cations are similar in many respects but the Mn^{2+} cation is slightly larger in size. This size discrepancy results in a greater concentration of Mn in residual melts and thus is a useful fractionation indicator in pegmatites.

Fractionation of Fe to Mn from the wall zone toward more interior zones is apparent within the garnet samples. Fe-rich almandine is the most common garnet composition in the pegmatite but some samples from the replacement unit are Mn-rich spessartine. The Fe and Mn content of schorl

samples from the Dumper Dew show an inverse relationship with respect to Li. As Fe and Mn contents decrease toward interior zones, Li abundances increase near inner zones. Columbite-tantalite mineralization shows a fractionation trend from less fractionated ferrocolumbite in the outer intermediate zone, to manganocolumbite in the inner intermediate zone, to highly evolved manganotantalite in the replacement unit.

Pegmatite Comparison

The Dumper Dew and Emmons pegmatites are both of LCT affinity and are located in the Oxford pegmatite field, which is petrogenetically linked to the Sebago batholith. Both pegmatites are mineralogically similar owing to their mutual derivation from a rare-element enriched parent magma (Tables 21 & 22). Using Cerny's 1991 classification, both pegmatites are of the complex, rare element type but differ in subtype categorization. The Emmons pegmatite more closely resembles the amblygonite subtype, while the Dumper Dew is best classified as a spodumene subtype. The major difference between the Emmons and Dumper Dew arises from the degree of fractionation experienced by their respective pegmatitic melts. Evolutionary differences between the two pegmatites are illustrated and inferred from the geochemical analyses of K-feldspar, muscovite, fluorapatite, triphylite-lithiophilite, columbite-tantalite, and tourmaline.

K-feldspar

Analyses of K-feldspar are an excellent fractionation indicator. The key elements examined in this study are K, Rb and Cs. The K/Rb *versus* K/Cs plot for K-feldspar is a standard plot used to evaluate the degree of fractionation in a pegmatite, and is a measure of the degree of substitution of K by Rb and Cs in the K-feldspar crystal structure. Elevated Rb and Cs contents in the feldspar from the Emmons and Dumper Dew indicate that

both pegmatites are highly fractionated bodies (Figure 35). The most fractionated parts of the Dumper Dew that are exposed have K-feldspars with K/Rb and K/Cs ratios of 40 and 200, respectively. Assay of K-feldspar from the most highly evolved portions of the Emmons have K/Rb <20 and a K/Cs number of 23.

Micas

The color and grain size of mica changes with increasing fractionation. Muscovite may be brown, silver, sometimes pink, and coarse grained. In highly fractionated pegmatites, muscovite may have Li-enriched zonations or sometimes crystallize as lepidolite. Usually, lepidolite is purple mica in highly fractionated pegmatites. With increasing fractionation, the composition of mica will change from muscovite to Li-rich muscovite to lepidolite. The most fractionated portion of the Emmons contains lepidolite whereas, exposed portions of the Dumper Dew host Li-rich muscovite. The chemical analyses of muscovite are also an excellent fractionation indicator. Elemental abundances used in the examination of muscovite for this study are K, Rb, and Cs. As was used to evaluate fractionation in K-feldspar, a plot of K/Rb *versus* K/Cs in muscovite is used to compare the degree of fractionation of the two pegmatites (Figure 36). The K/Rb and K/Cs ratios measure the degree of substitution of Rb and Cs for K in the muscovite's crystal structure. Highly evolved zones of the Dumper Dew

exhibit K/Rb and K/Cs ratios of 21 and 250, respectively. The most highly fractionated portion of the Emmons contains muscovite with K/Rb as low as 12 and K/Cs equal to 75.

Fluorapatite

The presence of fluorapatite in a pegmatite indicates crystallization from a P-F-rich melt. As a melt fractionates, it may produce elevated Mn contents in fluorapatite, and concentrate rare elements in the pegmatite. The plot of MnO *versus* CaO illustrates the varied Mn content of fluorapatite from both the Dumper Dew and the Emmons (Figure 37). Fluorapatite in the Emmons and Dumper Dew pegmatites contain up to 6 wt. % MnO. Some of the fluorapatite crystallized as Mn-poor varieties due to the preferential partitioning of Mn into garnet or oxide minerals over fluorapatite. The replacement unit of the Dumper Dew contains fluorapatite with <1 wt. % MnO associated with spessartine and manganotantalite.

Triphylite-Lithiophilite

The presence of lithium-phosphate minerals indicates both pegmatitic melts contained elevated P and Li contents. Triphylite-lithiophilite is a good fractionation indicator because its composition changes with increasing fractionation of a melt. The trend illustrated in Figure 38 is similar to columbite-tantalite group minerals and indicates the melt fractionated with

increasing Mn over Fe content. Present chemical data of lithium phosphates from the Emmons show the melt had experienced a greater degree of fractionation than the Dumper Dew. Lithium phosphates in the Dumper Dew crystallized as Mn-rich triphylite while Emmons samples plot as lithiophilite.

Columbite-Tantalite

Columbite-Tantalite group minerals are also excellent indicators to the degree of chemical evolution a pegmatite has attained. Tantalum mineralization occurs in the most highly fractionated zones within a zoned pegmatite. As a pegmatite crystallizes the composition of columbite-tantalite minerals change due to fractionation of the melt. The fractionation trend illustrated by both the Dumper Dew and the Emmons is: ferrocolumbite to manganocolumbite to manganotantalite (Figure 39). Similar to garnet, this trend is also an indication that both pegmatitic melts fractionated with increasing Mn and Ta contents. This trend also can attest to the highly evolved nature of both pegmatites.

Tourmaline

Tourmaline is another excellent fractionation indicator because its color and composition change with increasing fractionation. Tourmaline from the Emmons and Dumper Dew plot as alkali group species on a tourmaline ternary diagram (Figure 40). The most common tourmaline species in both

pegmatites is black schorl. In addition to schorl, the Emmons also contains foitite near the wall zone and elbaite in the innermost zones (Figure 41). Unlike the Emmons, Dumper Dew has not produced any other tourmaline species other than schorl. As the Emmons melt crystallized it became depleted in Fe and enriched in Li, and the tourmaline composition changed from schorl to elbaite (Figure 42).

DUMPER DEW MINERALOGY

Silicates:	albite beryl biotite garnet microcline montmorillonite	muscovite quartz schorl spodumene zircon cookeite
Oxides:	cassiterite columbite-tantalite	hematite todorokite*
Sulfides:	pyrite löllingite	
Carbonates:	siderite rodochrosite	
Primary Phosphates:	amblygonite-montebrasite fluorapatite lithiophlite-triphylite monazite	
Secondary Phosphates:	fairfieldite* heterosite-purpurite hydroxyl herderite jahnsite*	stewartite* strunzite* vivianite*

Table 21. Table of Dumper Dew Mineralogy.
* Indicates mineral occurrence from previous work by Ray Sprague.

EMMONS MINERALOGY		
Silicates:	albite bertrandite beryl biotite cookeite elbaite foitite garnet lepidolite	microcline montmorillonite muscovite pollucite quartz schorl spodumene zircon
Oxides:	cassiterite columbite-tantalite gahnite goethite	hematite wodginite todorokite uraninite
Sulfides:	pyrite löllingite	
Carbonates:	siderite rodochrosite	
Primary Phosphates:	amblygonite-montebrasite fluorapatite triphylite-lithiophilite	
Secondary Phosphates:	autunite/meta-autunite beraunite bermanite childrenite-eosphorite crandallite diadochite dickinsonite earlshannonite fairfieldite goyazite hureaulite hydroxyl herderite jahnsite group kastningite landesite laueite leucophosphite	ludlamite mitridatite moraesite perhamite phosphosiderite phosphouranylite robertsite rockbridgeite scorodite reddingite stewartite strengite strunzite switzerite/metaswitzerite vivianite whitmoreite

Table 22. Table of Emmons Mineralogy, from Falster et al., (2007).

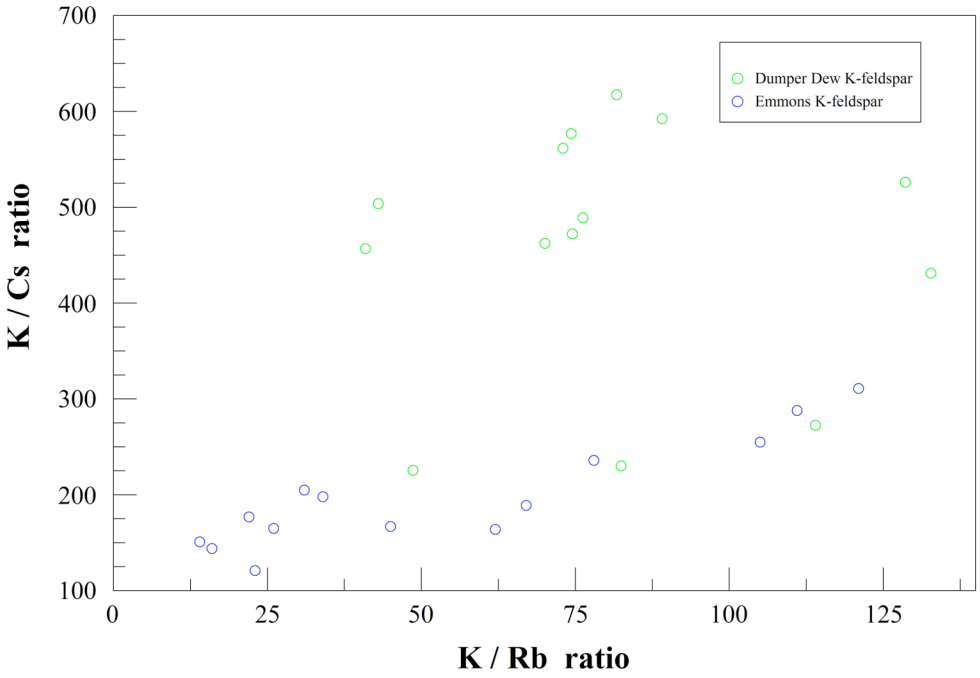

Figure 35. Plot of K/Cs versus K/Rb in potassium feldspar samples from the Dumper Dew and Emmons pegmatites. Dumper Dew samples are plotted as green circles and Emmons samples are plotted as blue circles. Emmons data was obtained as unpublished data from Falster et al.

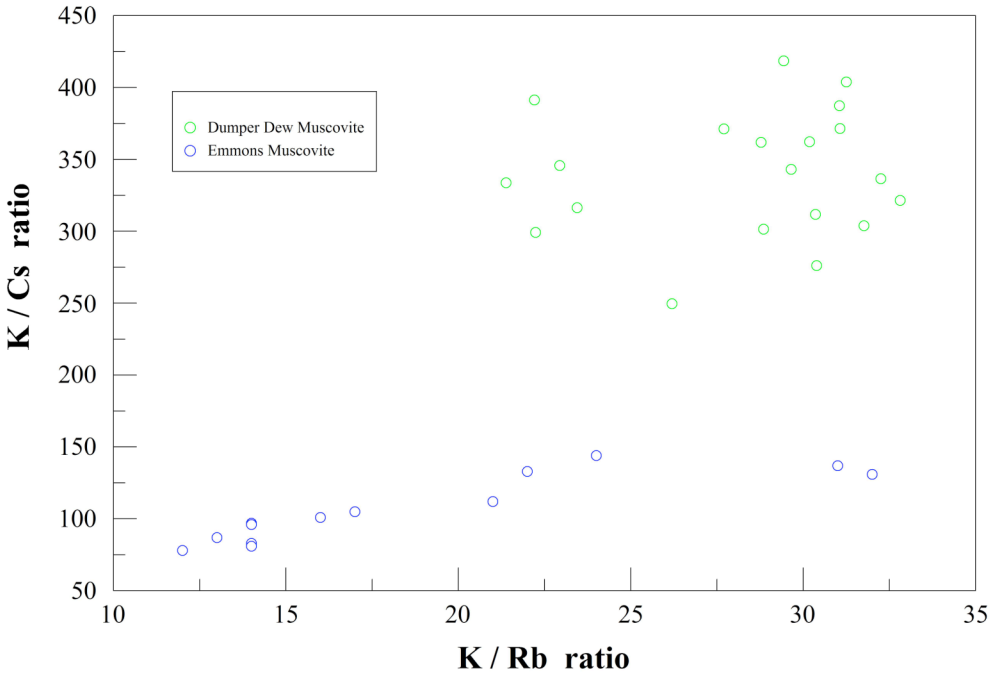

Figure 36. Plot of K/Cs versus K/Rb in muscovite samples from the Dumper Dew and Emmons pegmatites. Dumper Dew samples are plotted as green circles and Emmons samples are plotted as blue circles. Emmons data was obtained as unpublished data from Falster et al.

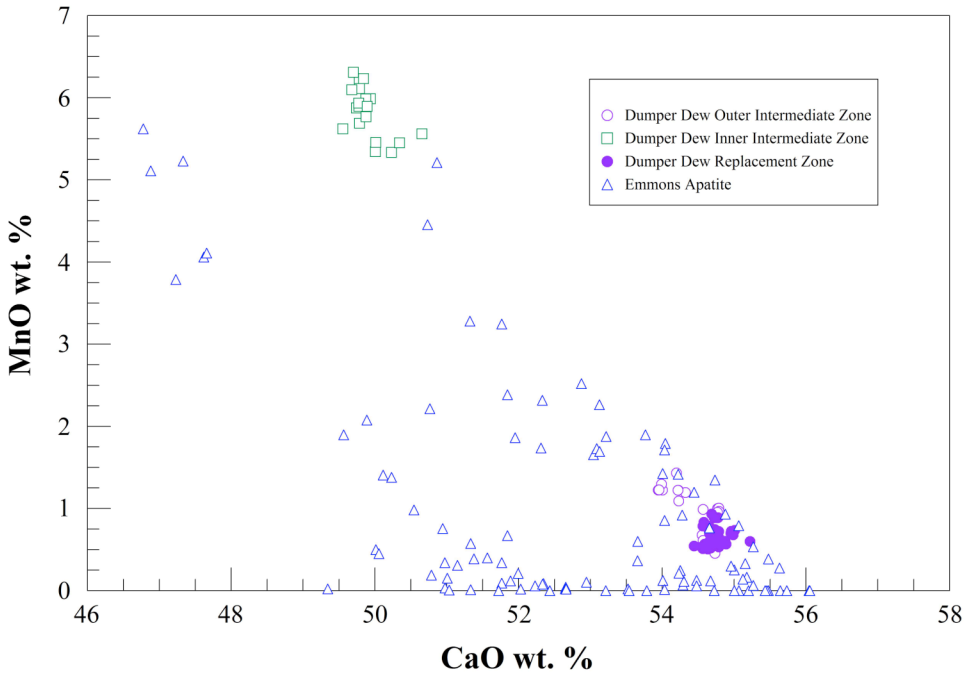

Figure 37. Plot of wt. % CaO versus wt. % MnO in apatite samples from the Emmons and Dumper Dew pegmatites. Green apatite are plotted as green squares, purple apatite from the replacement zone are plotted as closed circles, purple apatite from the inner intermediate zone are plotted as open circles and Emmons samples are plotted as blue triangles. Emmons data was obtained as unpublished data from Falster et al.

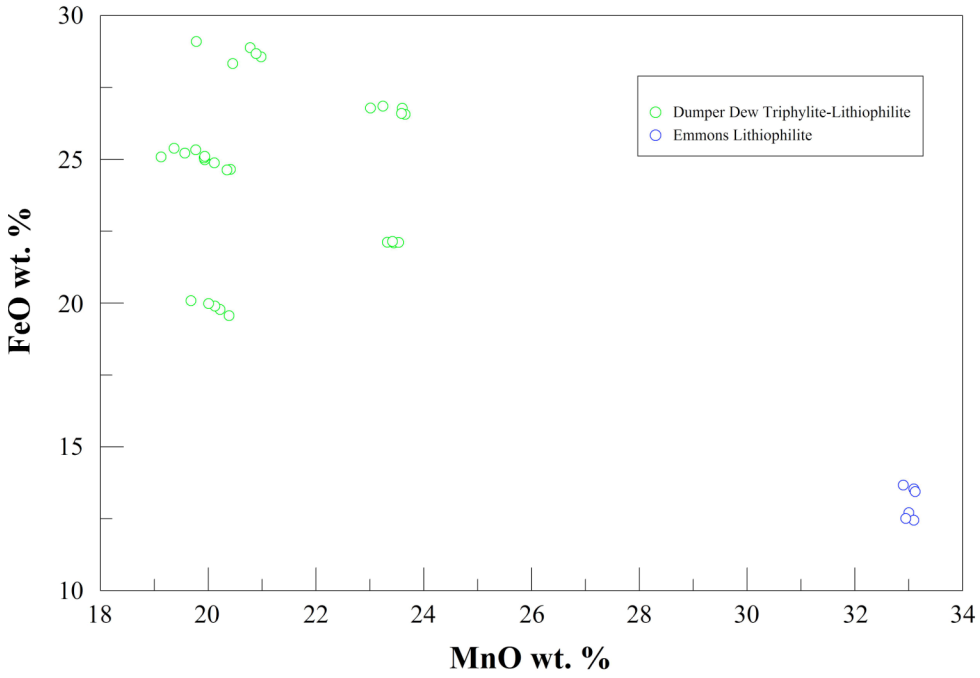

Figure 38. Plot of FeO versus MnO wt. % for triphylite-lithiophilite samples from the Dumper Dew and Emmons pegmatites. Dumper Dew samples are plotted as green circles and Emmons samples are plotted as blue circles. Emmons data was obtained as unpublished data from Falster et al.

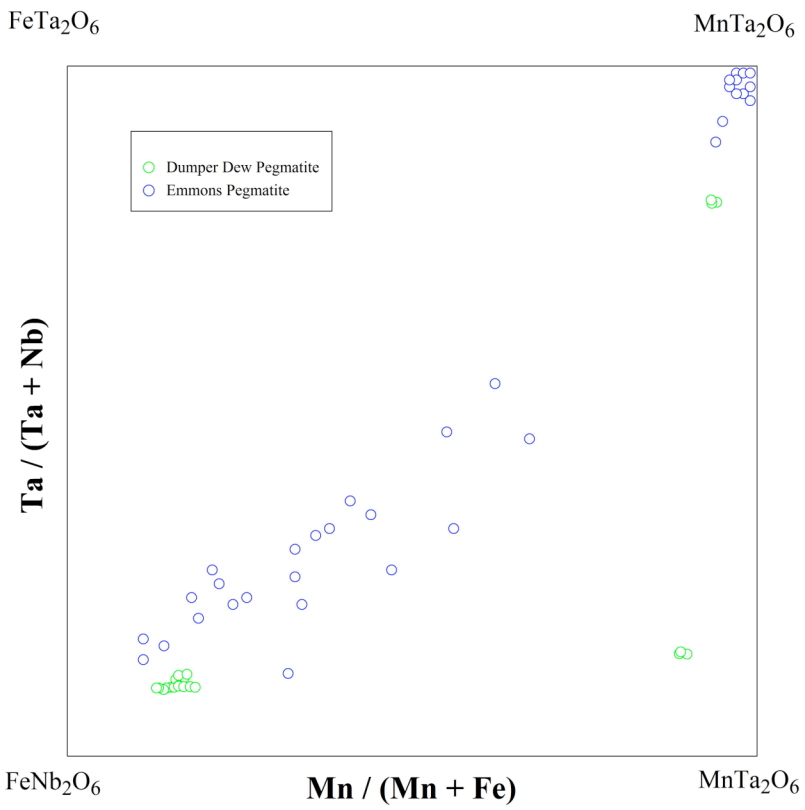

Figure 39. Ta/(Ta+Nb) versus Mn/(Mn+Fe) for columbite-tantalite compositions plotted in the columbite-tantalite quadrilateral. Dumper Dew samples are plotted as green circles and Emmons samples are plotted as blue circles. Emmons data was obtained as unpublished data from Falster et al.

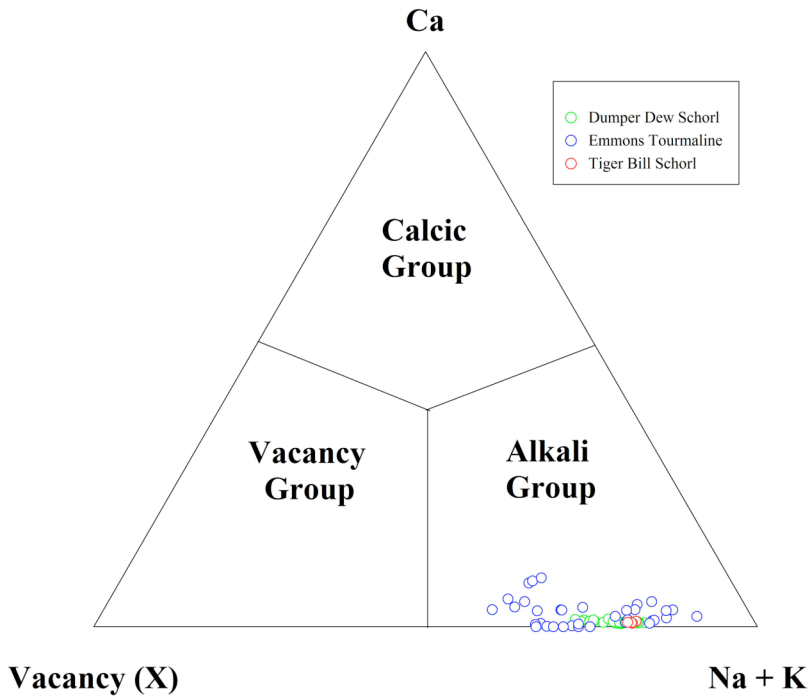

Figure 40. Ternary diagram of the main components at the X-site in tourmaline samples from the Dumper Dew, Emmons and Tiger Bill pegmatites. Emmons data was obtained as unpublished data from Falster et al.

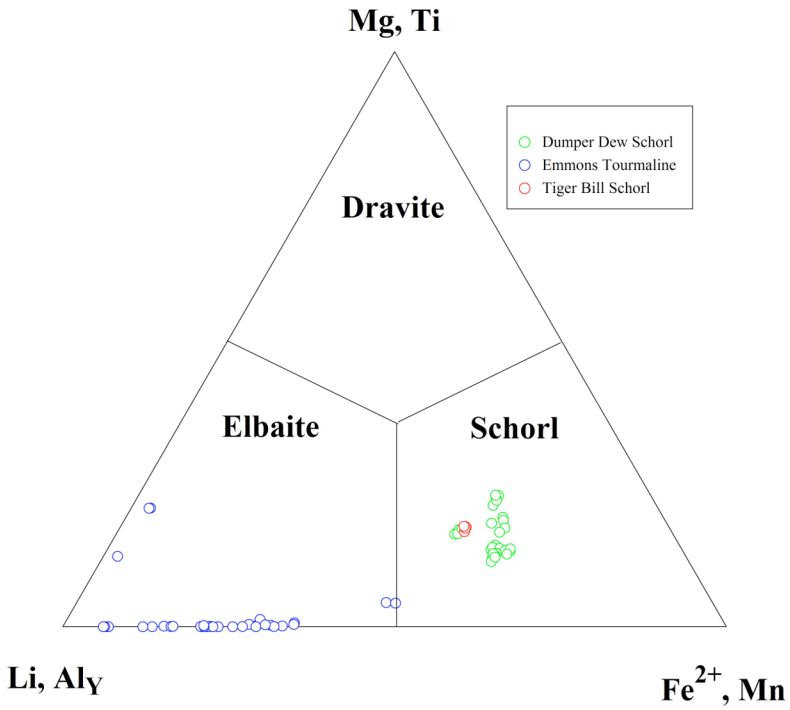

Figure 41. Ternary diagram of the main cations at the Y-site in tourmaline samples from the Dumper Dew, Emmons and Tiger Bill pegmatites. Emmons data was obtained as unpublished data from Falster et al.

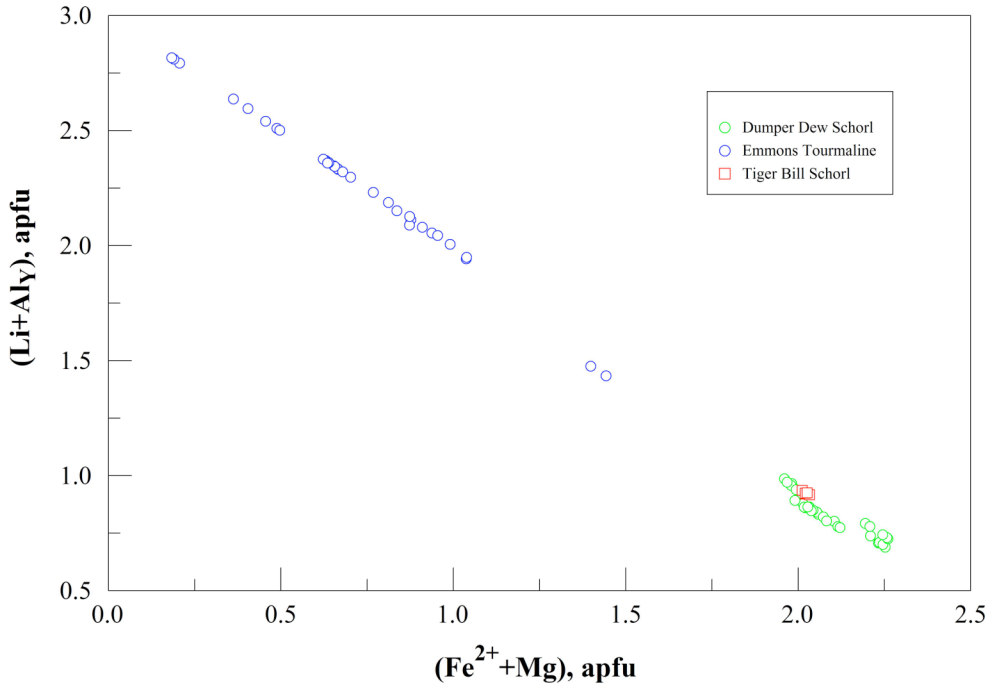

Figure 42. Plot of $Li+Al_Y$ versus $Fe^{2+}+Mg$ content at the Y-site of tourmaline samples from the Dumper Dew, Emmons and Tiger Bill pegmatites. Emmons data was obtained as unpublished data from Falster et al.

Conclusions

Geospatially, the Dumper Dew and the Emmons pegmatites are located in close proximity to one another. Their mutual parent granite is the Sebago batholith. Both pegmatites are spatially related to the northern geographic margin of the Sebago. Common geological resemblances, structural similarities, pegmatite classification, and mutual granitoid sources relate the Emmons and Dumper Dew to other pegmatites of the Oxford pegmatite field.

Based on Cerny's 1991 classification, the Dumper Dew and Emmons pegmatites are of the rare-element class and can be additionally subdivided into complex type pegmatites. Further taxonomy of the two pegmatites organizes each into a different subtype. Due to a lack of petalite, lepidolite, and amblygonite, the Dumper Dew is characterized as a spodumene subtype. Based on the occurrence of amblygonite at the Emmons, it systematically falls under the amblygonite subtype.

The Dumper Dew and Emmons share many mineralogical, geochemical and structural features. Both pegmatites are highly evolved LCT-type pegmatites; are complexly zoned; contain numerous miarolitic cavities; and consist of portions that have undergone replacement by late-stage fluids. Based on the current geochemical data greater abundances of Rb, Cs, Ta and Li are bound in Emmons mineralization.

Increased fractionation of Rb and Cs in K-feldspar and muscovite occurs in both pegmatites from the wall zone inward. K/Rb and K/Cs ratios are lower from the Dumper Dew as compared to the Emmons. The Emmons has produced the only known pollucite from the two localities. Pollucite may be present at the Dumper Dew but due to limited exposure this cannot be verified at this point.

Li mineralization is not as pronounced in the Dumper Dew as in the Emmons quarry. Both melts contained sufficient amounts of Li that lead to the crystallization of spodumene. Li content in the micas is more highly concentrated at the Emmons, as some inner zone mica crystallized as lepidolite. The Dumper Dew contains Li-rich muscovite but no lepidolite has been recovered from the prospect. If present, lepidolite would have crystallized in the more interior portions of the Dumper Dew but a lack of exposure prohibits confirmation. The Emmons has produced elbaite while the only noted tourmaline species form the Dumper Dew is schorl. If elbaite were present at the Dumper Dew, it would follow lepidolite and have crystallized within the innermost pegmatite zones.

Highly evolved Mn and Ta mineralization has been noted in the Emmons and Dumper Dew. Mn-rich phases of garnet, fluorapatite, and manganotantalite attest to the high Mn content of both pegmatites. Ta mineralization, with respect to columbite-tantalite, in the Emmons is at its fractionation apex and consists of highly evolved manganotantalite. The

Dumper Dew also crystallized highly evolved manganotantalite that rivals the Nb-Ta fractionation at the Emmons.

Key mineralogical and geochemical features are common to both the Emmons and Dumper Dew pegmatites. These attributes can be used to gauge the economic feasibility of mining the Dumper Dew prospect for rare and exotic minerals when compared to the Emmons quarry. Based on geochemical analyses of samples collected from exposures at the Dumper Dew, there is evidence for a variation in the degree of melt fractionation that culminated in the crystallization of the Dumper Dew and Emmons pegmatites. These analyses suggest the Emmons is a more highly evolved pegmatite than the Dumper Dew. Therefore, the Emmons hosts a wider variety of rare-element minerals than what has been currently found at the Dumper Dew.

However, the Dumper Dew is a highly evolved pegmatite as evidenced by the enrichment of volatiles and incompatible elements in its mineralogy. The occurrence of substantially evolved manganotantalite coupled with the evidence for late-stage hydrothermal replacement suggests that the unearthing of more interior portions of the Dumper Dew may yield additional mineral phases and more highly fractionated zones which rival those found at the Emmons.

Methods

Field Methods

Field research was performed on three separate occasions at the Dumper Dew and Tiger Bill pegmatites in Oxford County, Maine. Preliminary fieldwork began June 2 and continued through June 5, 2007. Several months later, October 4 through October 6, a second fieldwork session was conducted to more thoroughly sample the outcrops that were of particular interest. A final field research session was conducted between the days of May 29 and June 8, 2008 to collect additional samples for chemical analysis.

Whole rock samples were extracted from the pegmatite outcrop and also from surrounding country rock with the use of a rock hammer, a crack hammer and a chisel. Two of the more highly fractionated zones and thus significant pegmatite outcrops were drilled and then blasted; the purpose was to increase exposure area and also to obtain the freshest samples possible for chemical analysis. Measurements of pegmatite outcrops and country rock were taken using a measuring tape. A Brunton™ and a Silva Ranger™ compass was used for mapping purposes and to gain a better estimate of the size and orientation of the intrusion. A total of 46 outcrop markers were recorded in Universal Transverse Mercator (UTM) coordinates using an Etrex™ Global Positioning System (GPS) device, as a way of cataloging and referencing sample locales, and to represent outcrops geospatially.

Initial Field Session

During the initial fieldwork session, UTM coordinates of 27 pertinent outcrops were recorded with a GPS device. The width and height of each outcrop were recorded along with the relative compass bearings and orientations of any significant structures. Samples from all relevant outcrops were collected, tagged, packed and taken to the University of New Orleans for chemical analysis. There, whole country rock samples and also fractions of representative minerals: potassium feldspar, spodumene, cookeite, tourmaline, muscovite and biotite were extracted from the collected samples of pegmatite. The samples were then analyzed for traces of rubidium, lithium, and boron using a direct-coupled plasma spectrometer (DCP). Interpretation of acquired DCP data confirmed relatively greater trace-element abundances in some pegmatite outcrops.

Second Field Session

During the second visit to the field area, additional samples were collected and additional UTM coordinates were recorded from both the Dumper Dew and Tiger Bill pegmatites. Due to the nearly impenetrable nature of the crystalline rock, explosives were used to expose fresh surfaces for sample collection and to increase the exposure area of more highly evolved outcrops. Blast locations were selected on the basis of rubidium content, which had been determined by DCP analysis of previously collected

samples. The first blast was conducted at the inner-intermediate zone, where rubidium content was of the greatest fraction. The second blast was focused on a replacement unit, where the mineralogy was more diverse than some other previously sampled locations. Bulk samples from each blast site were collected, tagged, packed, and transported to the University of New Orleans for further analysis.

Final Field Session

During the final field research session, extraneous whole rock samples were collected and individual pegmatite zones were mapped. Both pegmatite and host rock samples were collected from individual outcrops at the Dumper Dew and Tiger Bill pegmatites. Each rock sample was tagged and referenced to a specific pegmatite zone and set of UTM coordinates. Individual pegmatite zones were measured, orientated, mapped and referenced geospatially.

Directly Coupled Plasma (DCP) Analyses

Coexisting pegmatite minerals and the surrounding host rock were analyzed from ten locations of the Dumper Dew and Tiger Bill pegmatites in order to calculate elemental abundances of boron, lithium, rubidium, thallium and potassium. Fifty samples of potassium feldspar, muscovite, biotite, schorl, spodumene, cookeite and aggregates of country rock were

chosen for study on the basis of surrounding mineral assemblages and collection locality. Each sample was pulverized using a mortar and pestle to augment dissolution in hydrofluoric acid. An accurate sample weighing was carried out with a target weight of 200 mg. Each sample weighed between 199.6 and 200.7 mg. After sample masses were measured and recorded, each powdered sample was placed in a flask and filled with 35 mL dilute HF. Elemental analyses were performed with a SPECTRONICS SPECTROSCAN V™ direct-coupled plasma spectrometer (DCP). Samples were analyzed based on parts per million (ppm) of boron, lithium, rubidium, potassium and thallium. DCP calibration was set with the following parameters: For boron, the plasma position was set at "0", a wavelength of 249.773 nm was used, the 1 ppm standard solution measured 0.894 with a 10 second count time and the range was calibrated at 0.1 to 100 ppm. For lithium, a plasma position of "+1", a wavelength of 610.362 nm, the 1-ppm standard read 0.9 with a 10 second count time and a range of 0.1 to 100 ppm was calibrated. For rubidium, the DCP was calibrated with a plasma position of "+1", a wavelength of 780.023 nm, the 1 ppm standard read 1.09 with a 10 second count time and a range of 0.1 to 100 ppm was used. For thallium, the DCP was calibrated with a plasma position of "0", a wavelength of 535.046 nm, and the 1ppm standard measured 1.11 ppm with a 10 second count time and a range of 0.001 to 10 ppm was used. For potassium, the samples were diluted 10X with distilled water with the DCP calibrated to a plasma position

of "+1", a wavelength of 769.896 nm, the 1 ppm standard measured 1.15 ppm with a 5 second count time and a range of 0.1 to 100 ppm was used.

Scanning Electron Microscopy (SEM) Analysis

An ARAY 1820™ Scanning Electron Microscope was used to gauge the diversity of mineral species present at the Dumper Dew and Tiger Bill pegmatites via the "heavy mineral separation method. Operating parameters for SEM work were as follows: 15 to 20 kV acceleration potential, tilt varied between 10 and 25°, and an 18 mm working distance was used with EDS2008 software by IXRFSYSTEMS, Inc.™.

Mineral grains with a density greater than 2.95 gm/cm^3 were separated and prepared through the following steps: Whole rock samples were selected from different zones of both pegmatites. The rock samples were crushed into smaller grains and suspended in a solution of lithium metatungstate. Mineral grains with a density less than 2.95 gm/cm^3 migrated to the top of the solution while any minerals with a density greater than 2.95 gm/cm^3 collected at the bottom of the solution. The less dense mineral grains were then separated from the fraction of higher density. "Heavier" grains were epoxied onto 1-inch glass discs and polished to a smooth surface. Finally, the sample discs were carbon coated to a thickness of 250±20 Å for SEM analysis.

X-Ray Diffraction

X-ray diffraction was performed at the University of New Orleans for the identification and confirmation of various mineral specimens. A SCINTAG (DMSNT™) XDS 2000 X-ray diffractometer was used for all XRD analyses. The diffractometer was operated at 35 kV and 15 mA. A 0.05 step scan was performed with a 2 second count time per step and a scan range of 2 to 55º 2 theta with DMS™ software.

Electron Microprobe

Mineral grains used for microprobe analysis were epoxied onto 1-inch glass discs and then polished. The discs were then carbon coated to a thickness of 250±20 Å. All analyses were performed on an ARL-SEMQ™. PROBE FOR WINDOWS™ software was used for all microprobe analyses. Each analysis was collected with a count time of 30 to 45 seconds per spot and a beam diameter of 2μm. Silicate analyses were conducted at an accelerating voltage of 15 kV and a beam current varying from 10 to 15 nA. Oxides and columbite-tantalite group minerals were conducted at an accelerating voltage of 20 kV and an intensity of 20 nA.

Standards

MAN standards were used as applicable for the major elements and included: ZnO (synthetic), V_2O_5 (synthetic), PbO (synthetic), ZrO_2 (synthetic), ThO_2 (synthetic), Al_2O_3 (synthetic) and SiO_2 (synthetic).

Feldspar analyses were conducted with the following reference standards: Si-albite, Al-An_{50}, Mg-CPX, Mn-spessartine, Ti-rutile, Fe-CPX, Ca-An_{50}, K-adularia, Na-albite, Rb-zinc phosphate, Cs-pollucite, P-fluorapatite and Sr-strontium sulfate.

Apatite analyses were conducted with the following reference standards: Si-adularia, Al-adularia, Mg-CPX, Mn-Fe & Mn phosphate, Ti-rutile, Fe-K & Fe phosphate, Ca-fluorapatite, F-fluorapatite, P-fluorapatite and Sr-strontium sulfate.

Beryl analyses were conducted with the following reference standards: Si-albite, Al-andalusite, Mg-CPX, Mn-spessartine, Ti-rutile, Fe-CPX, Ca-An_{50}, K-adularia, Na-albite, Rb-zinc phosphate and Cs-pollucite.

Oxide analyses were conducted with the following reference standards: Si-adularia, Al-adularia, Mg-periclase, Mn-spessartine, Ti-rutile, Fe-hematite and Ca-CPX.

Phosphate analyses were conducted with the following reference standards: Si-adularia, Al-adularia, Mg-CPX, Mn-Fe & Mn phosphate, Ti-rutile, Fe-K & Fe phosphate, Ca-fluorapatite, F-fluorapatite, P-fluorapatite and Sr-strontium sulfate.

Garnet analyses were conducted with the following reference standards: Si- almandine pyrope solid solution, Al- almandine pyrope solid solution, Mg- almandine pyrope solid solution, Mn-spessartine, Ti-rutile, Fe-almandine pyrope solid solution and Ca-grossular.

Herderite analyses were conducted with the following reference standards: Si-adularia, Al-adularia, Mg-CPX, Mn-Fe & Mn phosphate, Ti-rutile, Fe-K & Fe phosphate, Ca-fluorapatite, F-fluorapatite, P-fluorapatite and Sr-strontium sulfate.

Spodumene analyses were conducted with the following reference standards: Si-albite, Al-andalusite, Mg-CPX, Mn-spessartine, Ti-rutile, Fe-CPX, Ca-An_{50}, K-adularia, Na-albite, Rb-zinc phosphate and Cs-pollucite.

Columbite-tantalite group and cassiterite analyses were conducted with the following reference standards: Si-andalusite, Al-andalusite, Mg-periclase, Mn-manganotantalite, Ti-rutile, Fe-hematite, Ca-CPX, Ta-manganotantalite, Nb-$YNbO_4$ (synthetic) and Sn-SnO_2 (synthetic).

Montebrasite analyses were conducted with the following reference standards: Si-adularia, Al-adularia, Mg-CPX, Mn-Fe & Mn phosphate, Ti-rutile, Fe-K & Fe phosphate, Ca-fluorapatite, F-fluorapatite, P-fluorapatite, Sr-strontium sulfate and F-amblygonite.

Micas analyses were conducted with the following reference standards: Si-albite, Al-An_{50}, Mg-CPX, Mn-spessartine, Ti-rutile, Fe-CPX, Ca-

An_{50}, K-adularia, Na-albite, Rb-zinc phosphate, Cs-pollucite, P-fluorapatite, Sr-strontium sulfate and F-fluorphlogopite (synthetic).

Data Plotting

Electron microprobe and DCP data were plotted as elemental weight percent, oxide weight percent and ion proportions where applicable. PSI-PLOT Version 8.03 for WINDOWS™ was used to plot trends and represent spatial attributes of collected data.

References

Aleinikoff, J.N., Moench, R.H., Lyons, J.B., 1985, Carboniferous U-Pb age of the Sebago batholith, southwestern Maine: Metamorphic and tectonic implications: Geological Society of America Bulletin, v. 96, p. 990-996.

Alfonso, P., Melgarejo, J.C., Yusta, I., Velasco, F, 2003, Geochemistry of Feldspars and Muscovite in Granitic Pegmatite from the Cap De Creus Field, Catalonia, Spain: The Canadian Mineralogist, v. 41, p. 103-116.

Bhattacharjee, J., Chaudhari, M.W., 1963, Trace Element Geochemistry of Potassium Feldspars from Bhilwara Mica Belt, Rajasthan, and its Bearing on Pegmatite Evolution: Memoir: Geological Society of India, v. 7, p. 385-395.

Cameron, E.N., Jahns, R.H., McNair, A.H., Page, L.R., 1949, Internal Structure of Granitic Pegmatites: Monograph 2: Economic Geology, Urbana, Illlinoise: Economic Geology Publishing Co.

Cerna, I., Cerny, P., Ferguson, R.B., 1972, The Tanco pegmatite at Bernic Lake, Manitoba: III. Amblygonite-Montebrasite: Canadian Mineralogist, v. 11, p. 643-659.

Cerna, I., Cerny, P., Selway, J.B., Chapman, R., 2002, Paragenesis and Origin of Secondary Beryllophosphates: Beryllonite and Hydroxylherderite from the BEP Granitic Pegmatite, Southeastern Manitoba, Canada: The Canadian Mineralogist, v. 40, p. 1339-1345.

Cerny, P. 1975, Alkali Variations in Pegmatitic Beryl and their Petrogenetic Implications: Neues Jahrbuch fu¨r Mineralogie. Abhandlungen, n. 123, p. 198-212.

Cerny, P. and Hawthorne, F.C., 1976, Refractive indices versus alkali content in beryl: general limitations and applications to some pegmatite types: Canadian Mineralogist, v. 14, p. 491-497.

Cerny, P., Smith, J.V., Mason, R.A., Delaney, J.S., 1984, Geochemistry and Petrology of Feldspar Crystallization in the Vezna Pegmatite, Czechoslovakia: Canadian Mineralogist, v. 22, p. 631-651.

Cerny, P., Meintzer, R.E., Anderson, A.J., 1985, Extreme Fractionation in Rare-Element Granitic Pegmatites: Selected Examples of Data and Mechanisms: Canadian Mineralogist, v. 23, p. 381-421.

Cerny, P., Lenton, P.G., 1995, The Buck and Pegli Lithium Deposits, Southeastern Manitoba: The Problem of Updip Fractionation in Subhorizontal Pegmatite Sheets: Economic Geology, v. 90, p. 658-675.

Cerny, P., Anderson, A.J., Tomascak, P.B., Chapman, R., 2003, Geochemical and Morphological Features of Beryl from the Bikita Granitic Pegmatite, Zimbabwe, v. 41, p. 1003-1011.

Cerny, P., Chapman, R., Ferreira, K., Smeds, S., 2004, Geochemistry of Oxide Minerals of Nb, Ta, Sn, and Sb in the Varutrask Granitic Pegmatite, Sweden: The case of "Anomalous" Columbite-Tantalite Trend: American Mineralogist, v. 89, p. 505-518.

Cerny, P., Ercit, T.S., 2005, The Classification of Granitic Pegmatites Revisited: The Canadian Mineralogist, v. 43, p. 2005-2026.

Chakhmouradian, A.R., Reguir, E.P., Mitchell, R.H., 2002, Strontium-Apatite: New Occurrences, and the extent of Sr-for-Ca Substitution in Apatite-Group Minerals, v. 40, p. 121-136.

Charoy, B., Chaussidon, M., Le Carlier De Veslud, C., Duthou, J.L., 2003, Evidence of Sr mobility in and around the albite-lepidolite-topaz granite of Beauvoir (France): an in-situ ion and electron probe study of secondary Sr-rich phosphates: Contributions Mineralogy and Petrology, v. 145, p. 673-690.

Drake, A.A., Sinha, A.K., Laird, J., Guy, R.E., 1989, The Taconic Orogen: The Geology of North America, v. F-2, The Appalachian-Ouachita Orogen in the United States: Boulder, The Geologic Society of America, p. 101-178.

Dyar, M.A., Guidott, C.V., Core, D.P., Wearn, K.M., Wise, M.A., Francis, C.A., Johnson, K., Brady, J.B., Robertson, J.D., Cross, L.R., 1999, Stable Isotope and Crystal Chemistry of Tourmaline across Pegmatite-Country Rock Boundaries at Black Mountain and Mount Mica, Southwestern Maine, U.S.A.: Europeans Journal of Mineralogy, v. 11, p. 281-294.

Ercit, T.S., Groat, L.A., Gault, R.A., 2003, Granitic Pegmatites of the O'Grady Batholith, N.W.T., Canada: A case study of the evolution of the elbaite subtype of rare-element granitic pegmatite: Canadian Mineralogist, v. 41, p. 117-137.

Falster, A.U., Simmons, W.B., Webber, K.L., 2001, Unorthodox Compositional Trends in Columbite-Group Minerals from the Animikie Red Ace Pegmatite, Wisconsin, USA: Journal of Czech Geological Society, v. 46, n. 1-2, p. 69-79.

Falster, A.U., Simmons, W.B., Sprague, R., 2007, Mineralogy of the Emmons Pegmatite, Oxford County, Maine: An example of a highly evolved LCT-type pegmatite [abs.]: Rocks and Minerals, Contributed Papers in Specimen Mineralogy: Part 3, v. 82, p. 410.

Galliski, M.S., Cerny, P., 2006, Geochemistry and Structural State of Columbite-Group Mineralization in Granitic Pegmatites of the Pampean Ranges, Argentina: The Canadian Mineralogist, v. 44, p. 645-666.

Goad, B.E., Cerny, P., 1981, Peraluminous Pegmatitic Granites and their Pegmatite Aureoles in the Winnipeg River District, southeastern Manitoba: Canadian Mineralogist, v. 19, p. 177-194.

Groat, L.A., Chakoumakos, B.C., Brouwer, D.H., Hoffman, C.M., Fyfe, C.A., Morell, H., Schultz, A.J., 2003, The Amblygonite ($LiAlPO_4F$)-Montebrasite ($LiAlPO_4OH$) Solid Solution: A Combined Powder and Single-Crystal Neutron Diffraction and Solid-State ^6Li MAS, CP MAS, and REDOR NMR Study: American Mineralogist, v. 88, p. 195-210.

Groat, L.A., Mulia, T., Mauthner, M.H.F., Ercit, T.S., Raudsepp, M., Gault, R.A., Rollo, H.A., 2003, Geology and Mineralogy of the Little Nahanni Rare-Element Granitic Pegmatites, Northwest Territories: The Canadian Mineralogist, v. 41, p. 139-160.

Halden, N.M., Fryer, N.M., 1999, Geochemical characteristics of the Eden Lake Complex: evidence for anorogenic magmatism in the Trans-Hudson Orogen: Canadian Journal of Earth Science, v. 36, p. 91-103.

Hanson, S.L., Simmons, W.B., Webber, K.L., Falster, A.U., 1992, Rare-Earth-Element Mineralogy of Granitic Pegmatites in the Trout Creek Pass District, Chaffee County, Colorado: Canadian Mineralogist, v. 30, p. 676-686.

Hanson, S.L., Sprague, R., Wielkiewics, T., Falster, A.U., Simmons, W.B., 1998, Wodginite from the Emmons Pegmatite, Oxford County, Maine: Rock and Minerals, v. 73, p. 199.

Hatcher, R.D., Thomas, W.H., Geiser, P.A., Snoke, A.W., Mosher, S., Wiltschko, D.V., 1989, Alleghanian Orogen: The Geology of North America, v. F-2, The Appalachian-Ouachita Orogen in the United States: Boulder, The Geologic Society of America, p. 233-318.

Hawthorne, F.C., Cerny, P., 1977, The alkali-metal positions in Cs-Li beryl: Canadian Mineralogist, v. 145, p. 414-421.

Hodge, D.S., Abbey, D.A., Harkin, M.A., Patterson, J.L., Ring, M.J., Sweeney, J.F., 1982, Gravity studies of subsurface mass distributions of granitic rocks in Maine and New Hampshire: American Journal of Science, v. 282, p. 1289-1324.

Jolliff, B.L., Papike, J.J., Shearer, C.K., 1986, Tourmaline as a recorder of pegmatite evolution: Bob Ingersoll pegmatite, Black Hills, South Dakota: American Mineralogist, v. 71, p. 472-500.

Jolliff, B.L., Papike, J.J., Shearer, C.K., 1987, Fractionation trends in mica and tourmaline as indicators of pegmatite internal evolution: Bob Ingersoll pegmatite, Black Hills, South Dakota: Geochimica et Cosmochimica Acta, v. 51, n. 3, p. 519-534.

Kasemann, S., Erzinger, J., Franz, G., 2000, Boron recycling in the continental crust of the central Andes from Paleozoic to Mesozoic, NW Argentina: Contributions Mineralogy and Petrology, v. 140, p. 328-343.

Kontak, D.J., 2006, Nature and Origin of an LCT-Suite Pegmatite with Late-Stage Sodium Enrichment, Brazil Lake, Yarmouth county, Nova Scotia. I. Geological Setting and Petrology: The Canadian Mineralogist, v. 44, p. 563-598.

London, D., 1986, Formation of tourmaline-rich gem pockets in miarolitic pegmatites: American Mineralogist, v. 71, p. 396-405.

London, D., 1999, Stability of Tourmaline in Peraluminous Granite Systems: The Boron Cycle from Anatexis to Hydrothermal Aureoles: European Journal of Mineralogy, v. 11, p. 253-262.

McKerrow, W.S., Mac Niocaill, C., Dewey, J.F., 2000, The Caledonian Orogeny redefined: Journal of the Geological Society, London, v. 157, p. 1149-1154.

Kempe, U., Gotze, J., 2002, Cathodoluminescence (CL) behaviuor and crystal chemistry of apatite from rare-metal deposits: Mineralogical Magazine, v. 66, n. 1, p. 151-172.

Mulia, T., Williams-Jones, A.E., Martin, R.F., Wood, S.A., 1996, Compositional Variation and Structural State of Columbite-Tantalite in Rare-Element Granitic Pegmatites of the Preissac-Lacorne Batholith, Quebec, Canada: American Mineralogist, v. 81, p. 147-157.

Osberg, P.H., Hussey, A.M., Boone, G.M., 1985, Bedrock Geologic Map of Maine: Maine Geologic Survey, Scale 1:500,000.

Osberg, P.H., Tull, J.F., Robison, P., Hon, R., Butler, J.R., 1989, The Acadian Orogeny: The Geology of North America, v. F-2, The Appalachian-Ouachita Orogen in the United States: Boulder, The Geologic Society of America, p. 179-232.

Perham, J.C., 1987, Maine's Treasure Chest: Gems and Minerals of Oxford County, Quicksilver Publications, West Paris, Maine, p. 81-84.

Pough, F.H., 1993, Mineral Notes; Herderite: The Lapidary Journal, v. 47, n. 3, p. 14-16.

Que, M., Allen, A.R., 1996, Sericitization of plagioclase in the Rosses Granite Complex, Co. Donegal, Ireland: Mineralogical Magazine, v. 60, p. 927-936.

Rakovan, J.F., Hughes, J.M., 2000, Strontium in the Apatite Structure: Strontian Fluorapatite and Belovite-(Ca): The Canadian Mineralogist, v. 38, p. 839-845.

Rankin, D.W., Drake, A.A., Glover III, L., Goldsmith, R., Hall, L.M., Murray, D.P., Ratcliffe, N.M., Read, J.F., Secor, D.T., Stanley, R.S., 1989, Pre-orogenic terranes: The Geology of North America, v. F-2, The Appalachian-Ouachita Orogen in the United States: Boulder, The Geologic Society of America, p. 7-100.

Selway, J.B., Novak, M., Cerny, P., Hawthorne, F.C., 2000, The Tanco pegmatite at Bernic Lake, Manitoba. XIII. Exocontact Tourmaline: The Canadian Mineralogist, v. 38, p. 869-876.

Selway, J.B., Cerny, P., Hawthorne, F.C., Novak, M., 2000, The Tanco pegmatite at Bernic Lake, Manitoba. XIV. Internal Tourmaline: The Canadian Mineralogist, v. 38, p. 877-891.

Selway, J.B., Breaks, F.W., Tindle, A.G., 2005, A Review of rare-element (Li-Cs-Ta) pegmatite exploration techniques for the Superior Province, Canada, and large worldwide tantalum deposits: Exploration and Mining Geology, v. 14, p. 1-30.

Shigley, J.E., Brown, G.E., 1985, Occurrence and alteration of phosphate minerals at the Stewart Pegmatite, Pala District, San Diego, California: American Mineralogist, v. 70, p. 395-408.

Simmons, W.B., Foord, E.E., Falster, A.U., King, V.T., 1995, Evidence for an Anatectic Origin of Granitic Pegmatites, Western Maine, U.S.A.: G.S.A. Ann. Mtng., New Orleans, LA., Abstr. Prog., p. 478.

Simmons, W.B., Foord, E.E., Falster, A.U., 1996, Anatectic Origin of Granitic Pegmatites, Western Maine, U.S.A.: GAC-MAC Ann. Mtng., Winnipeg, Abstr. Prog., p. A87.

Simmons, W.B., Webber, K.L., Falster, A.U., Nizamoff, J.W., 2003, Pegmatology: Pegmatite Mineralogy, Petrology and Petrogenesis: Rubellite Press, New Orleans.

Simmons, W.B., Falster, A.U., Sprague, R., Wielkiewicz, T., Giller, B.S., 2003, Fluorapatite from the Emmons Pegmatite, Oxford County, Maine: Rocks and Minerals, v. 78, p. 123.

Simmons, W.B., Laurs, B.M., Falster, A.U., Koivula, F.I., Webber, K.L., 2005, Mt. Mica: A Renaissance in Maine's Gem Tourmaline Production: Gems & Gemology, p. 150-163.

Sirbescu, M.C., Nabelek, P.I., 2003, Crystallization conditions and evolution of magmatic fluids in the Harney Peak Granite and associated pegmatites, Black Hills, South Dakota-Evidence from fluid inclusions: Geochimica et Cosmochimica Acta, v. 67, n. 13, p. 2443-2465.

Stilling, A., Cerny, P., Vansone, P.J., 2006, The Tanco Pegmatite at Bernic Lake, Manitoba. XVI Zonal and Bulk Compositions and their Petrogenetic Significance: The Canadian Mineralogist, v. 44, p. 599-623.

Thomas, R., Förster, H., Heinrich, W., 2003, The behavior of boron in a peraluminous granite-pegmatite system and associated hydrothermal solutions: a melt and fluid-inclusion study: Contributions to Mineralogy and Petrology, v. 144, p. 457-472.

Tomascak, P.B., Walker, R.J., Krogstad, E.J., 1984, Geochemistry and geochronology of evolved granitic rocks in southwestern Maine: tectonic implications: U.S. Geological Survey circular, p. 150-151.

Tomascak, P.B., Krogstad, E.J., Walker, R.J., 1996, U-Pb Monazite Geochronology of Granitic Rocks from Maine: Implications for Late Paleozoic Tectonics in the Northern Appalachians: The Journal of Geology, v. 104, p. 185-195.

Tomascak, P.B., Krogstad, E.J., Walker, R.J., 1996, Nature of the crust in Maine, USA: Evidence from the Sebago batholith: Contributions to Mineralogy and Petrology, v. 125, p. 45-59.

Veksler, V., Thomas, R., 2002, An experimental study of B-, P, and F-rich synthetic granite pegmatite at 0.1 and 0.2 GPa: Contributions Mineralogy and Petrology, v. 143, p. 673-683.

Williams, H., Dehler, S.A., Grant, A.C., Oakey, G.N., 1999, Tectonics of Atlantic Canada: Geoscience Canada, v. 26, n. 2, p. 51-71.

Wise, M.A., Francis, C.A., 1992, Distribution, Classification and Geologic Setting of Granitic Pegmatites in Maine: Northeastern Geology, no. 14, 82-93.

Wise, M.A., 1995, Petrology of the Sebago Batholith and Related Pegmatites: NEIGC Guidebook, p. 229-240.

Wise, M.A., Rose, T.R., 2000, The Bennet Pegmatite, Oxford County, Maine: Maine Geological Survey: Mineralogy of Maine, v. 2, p. 323-332.

Zhang, A., Wang, R., Li, Y., Hu, H., Lu, X., Ji, J., Zhang, H, 2008, Tourmalines from the Kotokay No.3 pegmatite, Altai, NW China: spectroscopic characterization and relationships with the pegmatite evolution: European Journal of Mineralogy, v. 20, p. 143-154.

Electron Microprobe Analyses

Table A.1 Electron microprobe analyses of plagioclase feldspar from inner-intermediate zone samples of the Dumper Dew pegmatite.

	Inner-Intermediate Zone Samples				
	002-2-5-1	*002-2-5-2*	*002-2-5-3*	*002-2-5-4*	*002-2-5-5*
Oxides (wt.%)					
SiO_2	67.643	67.633	67.643	67.559	67.643
Al_2O_3	19.650	19.566	19.577	19.602	19.583
CaO	0.032	0.029	0.027	0.038	0.022
Na_2O	11.004	10.983	11.093	11.004	10.083
K_2O	0.234	0.204	0.205	0.198	0.205
Total	98.563	98.415	98.545	98.401	97.536
Ions on the basis of 8 O					
Si	2.992	2.995	2.993	2.993	3.009
Al	1.024	1.021	1.021	1.023	1.027
Ca	0.002	0.001	0.001	0.002	0.001
Na	0.944	0.943	0.952	0.945	0.870
K	0.013	0.012	0.012	0.011	0.012
Sum	0.958	0.956	0.964	0.958	0.882

Table A.2 Electron microprobe analyses of plagioclase feldspar from replacement unit samples of the Dumper Dew pegmatite.

	Replacement Unit Samples				
	010-3-6-1	*010-3-6-2*	*010-3-6-3*	*010-3-6-4*	*010-3-6-5*
Oxides (wt.%)					
SiO_2	67.667	67.589	67.622	67.544	67.625
Al_2O_3	19.588	19.544	19.517	19.458	19.533
CaO	0.024	0.021	0.043	0.055	0.032
Na_2O	11.043	11.087	11.100	11.078	10.998
K_2O	0.356	0.289	0.309	0.276	0.307
Total	98.678	98.530	98.591	98.411	98.495
Ions on the basis of 8 O					
Si	2.992	2.993	2.993	2.994	2.994
Al	1.021	1.020	1.018	1.017	1.019
Ca	0.001	0.001	0.002	0.003	0.002
Na	0.947	0.952	0.953	0.952	0.944
K	0.020	0.016	0.017	0.016	0.017
Sum	0.968	0.969	0.972	0.970	0.963

Table A.3 Electron microprobe analyses of plagioclase feldspar from wall zone samples of the Dumper Dew pegmatite.

	Wall Zone Samples				
	008-3-8-1	*008-3-8-2*	*008-3-8-3*	*008-3-8-4*	*008-3-8-5*
Oxides (wt.%)					
SiO_2	67.489	67.555	67.499	67.523	67.533
Al_2O_3	19.566	19.633	19.572	19.556	19.588
CaO	0.089	0.110	0.097	0.085	0.094
Na_2O	10.966	11.001	10.978	10.967	10.993
K_2O	0.276	0.220	0.235	0.237	0.218
Total	98.386	98.519	98.381	98.368	98.426
Ions on the basis of 8 O					
Si	2.992	2.990	2.992	2.993	2.992
Al	1.022	1.024	1.022	1.022	1.023
Ca	0.004	0.005	0.005	0.004	0.004
Na	0.942	0.944	0.943	0.942	0.944
K	0.016	0.012	0.013	0.013	0.012
Sum	0.962	0.962	0.961	0.960	0.961

Table A.4 Electron microprobe analyses of plagioclase feldspar from the wall zone above a quartz lens of the Dumper Dew pegmatite.

	Wall Zone Samples				
	003-3-1-1	*003-3-1-2*	*003-3-1-3*	*003-3-1-4*	*003-3-1-5*
Oxides (wt.%)					
SiO_2	67.642	67.644	67.645	67.569	67.654
Al_2O_3	19.565	19.547	19.555	19.523	19.455
CaO	0.038	0.034	0.029	0.034	0.044
Na_2O	11.009	10.984	10.945	11.008	10.966
K_2O	0.321	0.309	0.278	0.226	0.266
Total	98.575	98.518	98.452	98.360	98.385
Ions on the basis of 8 O					
Si	2.993	2.994	2.995	2.995	2.998
Al	1.020	1.020	1.020	1.020	1.016
Ca	0.002	0.002	0.001	0.002	0.002
Na	0.945	0.943	0.940	0.946	0.942
K	0.018	0.017	0.016	0.013	0.015
Sum	0.964	0.962	0.957	0.960	0.959

Table A.5 Electron microprobe analyses of extraneous plagioclase feldspar samples from Uncle Tom Mountain.

	Extraneous Samples Collected on Uncle Tom Mountain				
	022-3-16-1	*022-3-16-2*	*022-3-16-3*	*022-3-16-4*	*022-3-16-5*
Oxides (wt.%)					
SiO_2	67.633	67.615	67.589	67.599	67.600
Al_2O_3	19.777	19.643	19.489	19.548	19.543
CaO	0.044	0.045	0.047	0.044	0.048
Na_2O	10.934	10.988	11.120	11.137	11.215
K_2O	0.299	0.295	0.340	0.277	0.234
Total	98.687	98.586	98.585	98.605	98.640
Ions on the basis of 8 O					
Si	2.988	2.991	2.993	2.991	2.991
Al	1.030	1.024	1.017	1.020	1.019
Ca	0.002	0.002	0.002	0.002	0.002
Na	0.937	0.942	0.955	0.956	0.962
K	0.017	0.017	0.019	0.016	0.013
Sum	0.956	0.961	0.976	0.973	0.978

Table A.6 Electron microprobe analyses of plagioclase feldspar from core margin zone samples of the Tiger Bill pegmatite.

	Tiger Bill Core Margin Zone Samples				
	TB-4-1-1	*TB-4-1-2*	*TB-4-1-3*	*TB-4-1-4*	*TB-4-1-5*
Oxides (wt.%)					
SiO_2	67.654	67.599	67.655	67.612	67.499
Al_2O_3	19.576	19.622	19.589	19.600	19.562
CaO	0.044	0.055	0.057	0.045	0.065
Na_2O	10.789	10.800	10.805	10.785	10.745
K_2O	0.217	0.189	0.210	0.178	0.206
Total	98.280	98.265	98.316	98.220	98.077
Ions on the basis of 8 O					
Si	2.998	2.995	2.997	2.997	2.997
Al	1.022	1.025	1.023	1.024	1.024
Ca	0.002	0.003	0.003	0.002	0.003
Na	0.927	0.928	0.928	0.927	0.925
K	0.012	0.011	0.012	0.010	0.012
Sum	0.941	0.941	0.943	0.939	0.940

Table A.7 Electron microprobe analyses of plagioclase feldspar from outer-intermediate zone samples of the Dumper Dew pegmatite.

	Outer-Intermediate Zone Samples			
	001-1-2-1	*001-1-2-2*	*001-1-2-3*	*001-1-2-4*
Oxides (wt.%)				
SiO_2	68.056	67.966	67.963	68.009
Al_2O_3	19.796	19.712	19.709	19.767
CaO	0.018	0.088	0.078	0.094
Na_2O	11.093	11.110	11.088	11.069
K_2O	0.378	0.287	0.334	0.412
Total	99.341	99.163	99.172	99.351
Ions on the basis of 8 O				
Si	2.989	2.990	2.990	2.988
Al	1.025	1.022	1.022	1.024
Ca	0.001	0.004	0.004	0.004
Na	0.945	0.948	0.946	0.943
K	0.021	0.016	0.019	0.023
Sum	0.967	0.968	0.968	0.971

Table A.8 Electron microprobe analyses of potassium feldspar from inner-intermediate zone samples of the Dumper Dew pegmatite.

	Inner-Intermediate Zone Samples				
	002-1-9-1	*002-1-9-2*	*002-1-9-3*	*002-1-9-4*	*002-1-9-5*
Oxides (wt.%)					
P_2O_5	0.012	0.009	0.012	0.008	0.000
SiO_2	64.512	64.488	64.495	64.530	64.492
TiO_2	0.009	0.010	0.008	0.008	0.011
Al_2O_3	18.622	18.511	18.543	18.545	18.600
FeO	bdl	bdl	bdl	bdl	bdl
CaO	0.021	0.017	0.022	0.020	0.012
Na_2O	0.440	0.333	0.356	0.365	0.400
K_2O	15.654	15.467	15.547	15.556	15.643
Rb_2O	0.377	0.412	0.396	0.423	0.443
Cs_2O	0.021	0.098	0.012	0.025	0.032
Total	99.668	99.345	99.391	99.480	99.633
Ions on the basis of 8 O					
P	0.000	0.000	0.000	0.000	0.000
Si	2.991	2.998	2.996	2.996	2.992
Ti	0.000	0.000	0.000	0.000	0.000
Sum	2.992	2.998	2.997	2.997	2.993
Al	1.018	1.014	1.015	1.015	1.017
Fe	bdl	bdl	bdl	bdl	bdl
Ca	0.001	0.001	0.001	0.001	0.001
Na	0.040	0.030	0.032	0.033	0.036
K	0.926	0.917	0.921	0.921	0.926
Rb	0.011	0.012	0.012	0.013	0.013
Cs	0.000	0.002	0.000	0.000	0.001
Sum	0.978	0.962	0.967	0.968	0.976

Table A.9 Electron microprobe analyses of potassium feldspar from wall zone samples of the Dumper Dew pegmatite.

	Wall Zone Samples				
	008-3-3-1	*008-3-3-2*	*008-3-3-3*	*008-3-3-4*	*008-3-3-5*
Oxides (wt.%)					
P_2O_5	0.016	0.022	0.016	0.023	0.033
SiO_2	64.517	64.522	64.516	64.489	64.492
TiO_2	0.008	0.005	0.006	0.009	0.005
Al_2O_3	18.522	18.497	18.523	18.444	18.502
FeO	0.006	bdl	bdl	0.004	bdl
CaO	0.033	0.025	0.026	0.033	0.021
Na_2O	0.267	0.233	0.207	0.265	0.238
K_2O	15.755	15.888	15.739	15.809	15.787
Rb_2O	0.643	0.233	0.274	0.244	0.236
Cs_2O	0.209	0.032	0.037	0.042	0.033
Total	99.976	99.457	99.344	99.362	99.347
Ions on the basis of 8 O					
P	0.001	0.001	0.001	0.001	0.001
Si	2.993	2.996	2.998	2.998	2.997
Ti	0.000	0.000	0.000	0.000	0.000
Sum	2.994	2.997	2.998	2.999	2.998
Al	1.013	1.012	1.014	1.010	1.013
Fe	0.000	bdl	bdl	0.000	bdl
Ca	0.002	0.001	0.001	0.002	0.001
Na	0.024	0.021	0.019	0.024	0.021
K	0.933	0.941	0.933	0.937	0.936
Rb	0.019	0.007	0.008	0.007	0.007
Cs	0.004	0.001	0.001	0.001	0.001
Sum	0.982	0.971	0.962	0.971	0.966

Table A.10 Electron microprobe analyses of potassium feldspar from outer-intermediate zone samples of the Dumper Dew pegmatite.

Outer-Intermediate Zone Samples					
	001-1-1-1	*001-1-1-2*	*001-1-1-3*	*001-1-1-4*	*001-1-1-5*
Oxides (wt.%)					
P_2O_5	0.012	0.004	0.011	0.005	0.022
SiO_2	64.311	64.222	64.378	64.295	64.344
TiO_2	0.005	0.008	0.005	0.007	0.000
Al_2O_3	18.994	19.004	19.033	18.967	18.955
FeO	0.008	0.006	0.006	0.007	0.007
CaO	0.005	0.000	0.000	0.006	0.008
Na_2O	0.566	0.455	0.511	0.489	0.455
K_2O	15.444	15.431	15.478	15.366	14.650
Rb_2O	0.344	0.412	0.376	0.400	0.676
Cs_2O	0.078	0.080	0.075	0.094	0.087
Total	99.767	99.622	99.873	99.636	99.204
Ions on the basis of 8 O					
P	0.000	0.000	0.000	0.000	0.001
Si	2.978	2.978	2.978	2.980	2.988
Ti	0.000	0.000	0.000	0.000	0.000
Sum	2.978	2.979	2.979	2.981	2.989
Al	1.037	1.039	1.038	1.036	1.037
Fe	0.000	0.000	0.000	0.000	0.000
Ca	0.000	0.000	0.000	0.000	0.000
Na	0.051	0.041	0.046	0.044	0.041
K	0.912	0.913	0.913	0.909	0.868
Rb	0.010	0.012	0.011	0.012	0.020
Cs	0.002	0.002	0.001	0.002	0.002
Sum	0.975	0.968	0.972	0.967	0.931

Table A.10 Continued

	001-1-1-6
Oxides (wt.%)	
P_2O_5	bdl
SiO_2	64.455
TiO_2	0.008
Al_2O_3	18.934
FeO	0.000
CaO	0.000
Na_2O	0.323
K_2O	14.655
Rb_2O	0.711
Cs_2O	0.096
Total	99.182
Ions on the basis of 8 O	
P	bdl
Si	2.993
Ti	0.000
Sum	2.993
Al	1.036
Fe	0.000
Ca	0.000
Na	0.029
K	0.868
Rb	0.021
Cs	0.002
Sum	0.920

Table A.11 Electron microprobe analyses of muscovite from outer-intermediate zone samples of the Dumper Dew pegmatite.

	Outer-Intermediate Zone Samples				
	001-1-3-1	*001-1-3-2*	*001-1-3-3*	*001-1-3-4*	*001-1-3-5*
Oxide (wt.%)					
SiO_2	45.400	45.442	45.388	45.422	45.420
TiO_2	0.093	0.078	0.074	0.080	0.076
Al_2O_3	35.589	35.634	35.558	35.608	35.664
FeO	2.555	2.655	2.650	2.457	2.550
MnO	bdl	bdl	bdl	bdl	bdl
MgO	0.078	0.095	0.067	0.095	0.085
CaO	0.045	0.030	0.035	0.033	0.037
Na_2O	0.342	0.333	0.356	0.323	0.412
K_2O	10.003	9.877	9.897	9.955	9.887
Rb_2O	0.654	0.645	0.609	0.622	0.598
Cs_2O	0.096	0.107	0.088	0.098	0.092
H_2O	3.632	3.586	3.626	3.585	3.582
F	1.888	2.005	1.894	1.993	2.012
Subtotal	100.375	100.487	100.242	100.271	100.415
-O=F	0.795	0.844	0.798	0.839	0.847
Total	99.580	99.642	99.444	99.432	99.568
Ions on the basis of 12 (O,OH,F)					
Si	3.007	3.004	3.008	3.007	3.002
Ti	0.005	0.004	0.004	0.004	0.004
Sum	3.012	3.008	3.012	3.011	3.006
Al	2.778	2.776	2.778	2.778	2.779
Fe	0.142	0.147	0.147	0.136	0.141
Mn	bdl	bdl	bdl	bdl	bdl
Mg	0.008	0.009	0.007	0.009	0.008
Ca	0.002	0.002	0.003	0.002	0.003
Na	0.044	0.043	0.046	0.041	0.053
K	0.845	0.833	0.837	0.841	0.834
Rb	0.028	0.027	0.026	0.026	0.025
Cs	0.003	0.003	0.002	0.003	0.003
Sum	1.072	1.064	1.067	1.059	1.067
OH	1.605	1.581	1.603	1.583	1.579
F	0.395	0.419	0.397	0.417	0.421

Table A.12 Electron microprobe analyses of muscovite from inner-intermediate zone samples of the Dumper Dew pegmatite.

	Inner-Intermediate Zone Samples				
	002-1-13-1	*002-1-13-2*	*002-1-13-3*	*002-1-13-4*	*002-1-13-5*
Oxide (wt.%)					
SiO_2	45.432	45.367	45.400	45.387	45.374
TiO_2	0.067	0.077	0.078	0.082	0.079
Al_2O_3	36.444	36.520	36.506	36.434	36.477
FeO	2.899	2.912	2.963	2.994	3.034
MnO	0.032	0.029	0.031	0.034	0.027
MgO	0.095	0.114	0.096	0.097	0.104
CaO	0.033	0.043	0.036	0.032	0.034
Na_2O	0.111	0.145	0.109	0.132	0.150
K_2O	9.445	9.456	9.432	9.374	9.450
Rb_2O	0.621	0.604	0.599	0.632	0.604
Cs_2O	0.078	0.060	0.056	0.067	0.073
H_2O	3.567	3.474	3.475	3.491	3.498
F	2.120	2.343	2.340	2.295	2.287
Subtotal	100.944	101.144	101.121	101.051	101.191
-O=F	0.893	0.987	0.985	0.966	0.963
Total	100.051	100.157	100.136	100.085	100.228
Ions on the basis of 12 (O,OH,F)					
Si	2.980	2.967	2.970	2.972	2.969
Ti	0.003	0.004	0.004	0.004	0.004
Sum	2.983	2.971	2.973	2.976	2.973
Al	2.817	2.815	2.814	2.812	2.813
Fe	0.159	0.159	0.162	0.164	0.166
Mn	0.002	0.002	0.002	0.002	0.001
Mg	0.009	0.011	0.009	0.009	0.010
Ca	0.003	0.002	0.002	0.008	0.006
Na	0.014	0.018	0.014	0.017	0.019
K	0.790	0.789	0.787	0.783	0.789
Rb	0.026	0.025	0.025	0.027	0.025
Cs	0.002	0.002	0.002	0.002	0.002
Sum	1.005	1.010	1.003	1.006	1.015
OH	1.560	1.515	1.516	1.525	1.527
F	0.440	0.485	0.484	0.475	0.473

Table A.13 Electron microprobe analyses of muscovite from inner-intermediate zone samples of the Dumper Dew pegmatite.

	Inner-Intermediate Zone Samples				
	002-4-13-1	*002-4-13-2*	*002-4-13-3*	*002-4-13-4*	*002-4-13-5*
Oxide (wt.%)					
SiO_2	45.452	45.442	45.398	45.520	45.449
TiO_2	0.083	0.032	0.024	0.022	0.029
Al_2O_3	36.755	36.565	36.740	36.777	36.672
FeO	3.009	2.233	2.145	2.226	2.185
MnO	0.009	0.013	0.009	0.020	0.021
MgO	0.110	0.089	0.070	0.090	0.077
CaO	0.033	0.043	0.054	0.056	0.032
Na_2O	0.222	0.232	0.240	0.222	0.210
K_2O	9.320	9.345	9.223	9.322	9.198
Rb_2O	0.865	0.834	0.798	0.789	0.822
Cs_2O	0.044	0.056	0.037	0.054	0.056
H_2O	3.668	3.655	3.623	3.654	3.637
F	1.934	1.897	1.974	1.930	1.940
Subtotal	101.504	100.436	100.335	100.682	100.328
-O=F	0.814	0.799	0.831	0.813	0.817
Total	100.690	99.637	99.503	99.869	99.511
Ions on the basis of 12 (O,OH,F)					
Si	2.972	2.991	2.986	2.987	2.990
Ti	0.004	0.002	0.001	0.001	0.001
Sum	2.976	2.993	2.987	2.988	2.992
Al	2.832	2.837	2.848	2.844	2.844
Fe	0.165	0.123	0.118	0.122	0.120
Mn	0.000	0.001	0.001	0.001	0.001
Mg	0.011	0.009	0.007	0.009	0.008
Ca	0.004	0.004	0.002		
Na	0.028	0.030	0.031	0.028	0.027
K	0.777	0.785	0.774	0.780	0.772
Rb	0.036	0.035	0.034	0.033	0.035
Cs	0.001	0.002	0.001	0.002	0.002
Sum	1.021	0.987	0.968	0.979	0.966
OH	1.600	1.605	1.589	1.599	1.596
F	0.400	0.395	0.411	0.401	0.404

Table A.14 Electron microprobe analyses of muscovite from wall zone above a quartz lens of the Dumper Dew pegmatite.

	Wall Zone Samples				
	003-2-13-1	*003-2-13-2*	*003-2-13-3*	*003-2-13-4*	*003-2-13-5*
Oxide (wt.%)					
SiO_2	45.343	45.279	45.342	45.222	45.320
TiO_2	0.055	0.060	0.044	0.057	0.062
Al_2O_3	35.578	35.650	35.556	35.712	35.560
FeO	2.455	2.223	2.312	2.330	2.340
MnO	0.009	0.007	0.009	0.013	0.022
MgO	0.032	0.034	0.027	0.025	0.030
CaO	0.109	0.087	0.094	0.095	0.112
Na_2O	0.277	0.000	0.000	0.000	0.000
K_2O	9.676	9.677	9.650	9.733	9.455
Rb_2O	0.733	0.000	0.000	0.000	0.000
Cs_2O	0.116	0.000	0.000	0.000	0.000
H_2O	3.510	3.310	3.336	3.410	3.400
F	2.140	2.560	2.500	2.334	2.345
Subtotal	100.033	98.887	98.870	98.931	98.646
-O=F	0.901	1.078	1.053	0.983	0.987
Total	99.132	97.809	97.817	97.948	97.659
Ions on the basis of 12 (O,OH,F)					
Si	3.005	3.002	3.008	3.003	3.013
Ti	0.003	0.003	0.002	0.003	0.003
Sum	3.008	3.005	3.010	3.006	3.016
Al	2.779	2.786	2.780	2.795	2.786
Fe	0.136	0.123	0.128	0.129	0.130
Mn	0.001	0.000	0.001	0.001	0.001
Mg	0.003	0.003	0.003	0.002	0.003
Ca	0.007	0.007	0.008	0.003	0.003
Na	0.036	0.000	0.000	0.000	0.000
K	0.818	0.819	0.817	0.824	0.802
Rb	0.031	0.000	0.000	0.000	0.000
Cs	0.003	0.000	0.000	0.000	0.000
Sum	1.036	0.952	0.955	0.964	0.944
OH	1.551	1.463	1.475	1.510	1.507
F	0.449	0.537	0.525	0.490	0.493

Table A.15 Electron microprobe analyses of muscovite from wall zone samples of the Dumper Dew pegmatite.

	Wall Zone Samples				
	008-3-4-1	*008-3-4-2*	*008-3-4-3*	*008-3-4-4*	*008-3-4-5*
Oxide (wt.%)					
SiO_2	45.700	45.678	45.698	45.709	45.677
TiO_2	0.055	0.045	0.048	0.044	0.048
Al_2O_3	36.508	36.478	36.500	36.498	36.512
FeO	2.655	2.567	2.674	2.650	2.733
MnO	0.009	bdl	bdl	0.007	bdl
MgO	0.022	0.027	0.033	0.021	0.025
CaO	0.036	0.040	0.044	0.032	0.044
Na_2O	0.217	0.220	0.269	0.234	0.309
K_2O	9.477	9.566	9.489	9.433	9.500
Rb_2O	0.344	0.355	0.312	0.349	0.367
Cs_2O	0.022	0.031	0.022	0.027	0.025
H_2O	3.470	3.429	3.395	3.412	3.439
F	2.366	2.456	2.544	2.499	2.448
Subtotal	100.881	100.892	101.028	100.915	101.127
-O=F	0.996	1.034	1.071	1.052	1.031
Total	99.885	99.857	99.957	99.863	100.096
Ions on the basis of 12 (O,OH,F)					
Si	2.984	2.983	2.978	2.982	2.978
Ti	0.003	0.002	0.002	0.002	0.002
Sum	2.987	2.985	2.981	2.984	2.981
Al	2.810	2.807	2.804	2.806	2.806
Fe	0.145	0.140	0.146	0.145	0.149
Mn	0.000	bdl	bdl	0.000	bdl
Mg	0.002	0.003	0.003	0.002	0.002
Ca	0.003	0.002	0.003	0.002	0.002
Na	0.027	0.028	0.034	0.030	0.039
K	0.790	0.797	0.789	0.785	0.790
Rb	0.014	0.015	0.013	0.015	0.015
Cs	0.001	0.001	0.001	0.001	0.001
Sum	0.982	0.986	0.989	0.979	1.000
OH	1.511	1.493	1.476	1.484	1.495
F	0.489	0.507	0.524	0.516	0.505

Table A.16 Electron microprobe analyses of muscovite from replacement unit samples of the Dumper Dew pegmatite.

	Replacement Unit Samples				
	010-3-7-1	*010-3-7-2*	*010-3-7-3*	*010-3-7-4*	*010-3-7-5*
Oxide (wt.%)					
SiO_2	45.698	45.659	45.633	45.653	45.659
TiO_2	0.033	0.042	0.020	0.026	0.023
Al_2O_3	36.567	36.588	36.620	36.655	36.600
FeO	2.564	2.454	2.444	2.412	2.334
MnO	bdl	bdl	bdl	bdl	bdl
MgO	bdl	0.009	bdl	0.023	0.020
CaO	0.028	0.022	0.031	0.026	0.033
Na_2O	0.223	0.312	0.256	0.266	0.231
K_2O	9.444	9.512	9.458	9.450	9.422
Rb_2O	0.312	0.656	0.633	0.650	0.675
Cs_2O	0.038	0.043	0.044	0.047	0.042
H_2O	3.335	3.341	3.292	3.340	3.334
F	2.677	2.672	2.776	2.673	2.673
Subtotal	100.919	101.310	101.207	101.221	101.046
-O=F	1.127	1.125	1.169	1.126	1.126
Total	99.792	100.184	100.038	100.095	99.921
Ions on the basis of 12 (O,OH,F)					
Si	2.977	2.972	2.970	2.972	2.976
Ti	0.002	0.002	0.001	0.001	0.001
Sum	2.979	2.974	2.971	2.973	2.977
Al	2.808	2.807	2.809	2.812	2.812
Fe	0.140	0.134	0.133	0.131	0.127
Mn	bdl	bdl	bdl	bdl	bdl
Mg	bdl	0.001	bdl	0.002	0.002
Ca	0.002	0.002	0.002	0.000	0.002
Na	0.028	0.039	0.032	0.034	0.029
K	0.785	0.790	0.785	0.785	0.783
Rb	0.013	0.027	0.026	0.027	0.028
Cs	0.001	0.001	0.001	0.001	0.001
Sum	0.969	0.994	0.981	0.982	0.974
OH	1.448	1.450	1.429	1.450	1.449
F	0.552	0.550	0.571	0.550	0.551

Table A.17 Electron microprobe analyses of muscovite from core margin zone samples of the Tiger Bill pegmatite.

	Tiger Bill Core Margin Zone Samples				
	TB-3-13-1	*TB-3-13-2*	*TB-3-13-3*	*TB-3-13-4*	*TB-3-13-5*
Oxide (wt.%)					
SiO_2	45.487	45.500	45.478	45.452	45.445
TiO_2	0.077	0.090	0.084	0.083	0.083
Al_2O_3	35.888	35.909	35.899	35.879	35.897
FeO	2.676	2.875	2.898	3.009	3.067
MnO	0.015	0.009	0.013	0.011	0.016
MgO	0.765	0.767	0.699	0.735	0.774
CaO	0.000	0.034	0.023	0.041	0.033
Na_2O	0.228	0.234	0.321	0.308	0.323
K_2O	10.121	10.112	10.094	10.085	10.104
Rb_2O	0.031	0.027	0.031	0.026	0.034
Cs_2O	bdl	bdl	bdl	bdl	bdl
H_2O	3.858	3.823	3.731	3.782	3.807
F	1.454	1.554	1.765	1.648	1.600
Subtotal	100.600	100.934	101.036	101.059	101.183
-O=F	0.612	0.654	0.743	0.694	0.674
Total	99.988	100.280	100.292	100.365	100.509
Ions on the basis of 12 (O,OH,F)					
Si	2.998	2.991	2.985	2.986	2.984
Ti	0.004	0.004	0.004	0.004	0.004
Sum	3.002	2.995	2.989	2.990	2.988
Al	2.788	2.782	2.777	2.778	2.778
Fe	0.147	0.158	0.159	0.165	0.168
Mn	0.001	0.001	0.001	0.001	0.001
Mg	0.075	0.075	0.068	0.072	0.076
Ca	0.002	0.003	0.002	0.002	0.002
Na	0.029	0.030	0.041	0.039	0.041
K	0.851	0.848	0.845	0.845	0.846
Rb	0.001	0.001	0.001	0.001	0.001
Cs	bdl	bdl	bdl	bdl	bdl
Sum	1.105	1.115	1.117	1.126	1.136
OH	1.697	1.677	1.634	1.658	1.668
F	0.303	0.323	0.366	0.342	0.332

Table A.18 Electron microprobe analyses of garnet from inner-intermediate zone samples of the Dumper Dew pegmatite.

	Inner-Intermediate Zone Samples				
	002-1-14-1	002-1-14-2	002-1-14-3	002-1-14-5	002-1-14-5
Oxides (wt.%)					
SiO_2	36.432	36.479	36.448	36.509	36.487
TiO_2	0.005	0.004	bdl	bdl	0.005
Al_2O_3	20.558	20.612	20.522	20.527	20.444
Fe_2O_3	0.102	0.068	0.162	0.205	0.286
FeO	22.636	22.828	22.810	22.588	22.507
MnO	19.567	19.388	19.412	19.634	19.588
MgO	0.116	0.098	0.096	0.121	0.089
CaO	0.766	0.856	0.764	0.770	0.787
Total	100.182	100.333	100.214	100.354	100.193
Ions on the basis of 12 O					
Si	2.998	2.997	2.999	2.999	3.002
Ti	0.000	0.000	bdl	bdl	0.000
Sum	2.998	2.997	2.999	2.999	3.003
Al	1.994	1.996	1.990	1.988	1.983
Fe^{3+}	0.006	0.004	0.010	0.013	0.018
Sum	2.000	2.000	2.000	2.000	2.000
Fe^{2+}	1.558	1.569	1.570	1.552	1.549
Mn	1.364	1.349	1.353	1.366	1.365
Mg	0.014	0.012	0.012	0.015	0.011
Ca	0.068	0.075	0.067	0.068	0.069
Sum	3.003	3.005	3.002	3.001	2.994

Table A.19 Electron microprobe analyses of garnet from inner-intermediate zone samples of the Dumper Dew pegmatite.

	Inner-Intermediate Zone Samples				
	002-1-15-1	002-1-15-2	002-1-15-3	002-1-15-4	002-1-15-5
Oxides (wt.%)					
SiO_2	36.467	36.511	36.543	36.488	36.456
TiO_2	bdl	bdl	0.004	0.006	0.006
Al_2O_3	20.521	20.565	20.559	20.600	20.563
Fe_2O_3	0.188	0.133	0.130	0.073	0.103
FeO	22.594	22.641	22.683	22.732	22.716
MnO	19.596	19.489	19.312	19.433	19.426
MgO	0.140	0.137	0.134	0.129	0.128
CaO	0.765	0.784	0.790	0.789	0.779
Total	100.272	100.260	100.155	100.250	100.177
Ions on the basis of 12 O					
Si	2.998	3.001	3.004	2.999	2.999
Ti	bdl	bdl	0.000	0.000	0.000
Sum	2.998	3.001	3.005	3.000	2.999
Al	1.989	1.992	1.992	1.996	1.994
Fe^{3+}	0.012	0.008	0.008	0.005	0.006
Sum	2.000	2.000	2.000	2.000	2.000
Fe^{2+}	1.554	1.556	1.560	1.563	1.563
Mn	1.365	1.357	1.345	1.353	1.354
Mg	0.017	0.017	0.016	0.016	0.016
Ca	0.067	0.069	0.070	0.069	0.069
Sum	3.003	2.999	2.990	3.001	3.001

Table A.20 Electron microprobe analyses of garnet from wall zone samples of the Dumper Dew pegmatite.

	Wall Zone Samples				
	008-3-2-1	008-3-2-2	008-3-2-3	008-3-2-4	008-3-2-5
Oxides (wt.%)					
SiO_2	36.399	36.455	36.451	36.511	36.422
TiO_2	0.007	bdl	0.005	bdl	bdl
Al_2O_3	20.489	20.530	20.514	20.522	20.620
Fe_2O_3	0.198	0.137	0.202	0.198	0.021
FeO	21.711	21.665	21.827	21.827	21.924
MnO	20.545	20.433	20.428	20.374	20.399
MgO	0.000	0.000	0.000	0.000	0.000
CaO	0.888	0.933	0.930	0.897	0.906
Total	100.238	100.153	100.357	100.329	100.292
Ions on the basis of 12 O					
Si	2.997	3.001	2.997	3.001	2.996
Ti	0.000	bdl	0.000	bdl	bdl
Sum	2.997	3.001	2.997	3.001	2.996
Al	1.988	1.992	1.988	1.988	1.999
Fe^{3+}	0.012	0.008	0.012	0.012	0.001
Sum	2.000	2.000	2.000	2.000	2.000
Fe^{2+}	1.495	1.491	1.501	1.500	1.508
Mn	1.433	1.425	1.423	1.418	1.421
Mg	0.000	0.000	0.000	0.000	0.000
Ca	0.078	0.082	0.082	0.079	0.080
Sum	3.006	2.998	3.005	2.998	3.009

Table A.21 Electron microprobe analyses of garnet from replacement unit samples of the Dumper Dew pegmatite.

	Replacement Unit Samples				
	010-3-11-1	010-3-11-2	010-3-11-3	010-3-11-4	010-3-11-5
Oxides (wt.%)					
SiO_2	36.456	36.545	36.549	36.412	36.512
TiO_2	0.008	bdl	bdl	0.006	0.008
Al_2O_3	20.589	20.600	20.563	20.558	20.622
Fe_2O_3	0.506	0.526	0.566	0.542	0.571
FeO	20.420	20.530	20.264	20.467	20.584
MnO	23.411	23.338	23.443	23.412	23.540
MgO	bdl	bdl	bdl	bdl	bdl
CaO	0.967	0.899	0.956	0.970	0.996
Total	102.357	102.438	102.341	102.366	102.833
Ions on the basis of 12 O					
Si	2.959	2.963	2.965	2.957	2.953
Ti	0.000	bdl	bdl	0.000	0.000
Sum	2.960	2.963	2.965	2.957	2.954
Al	1.970	1.969	1.966	1.968	1.966
Fe^{3+}	0.031	0.032	0.035	0.033	0.035
Sum	2.001	2.001	2.001	2.001	2.001
Fe^{2+}	1.386	1.392	1.375	1.390	1.392
Mn	1.610	1.603	1.611	1.610	1.613
Mg	bdl	bdl	bdl	bdl	bdl
Ca	0.084	0.078	0.083	0.084	0.086
Sum	3.080	3.073	3.069	3.085	3.091

Table A.22 Electron microprobe analyses of garnet from core margin zone samples of the Tiger Bill pegmatite.

	Tiger Bill Core Margin Zone Samples				
	TB-3-14-1	TB-3-14-2	TB-3-14-3	TB-3-14-4	TB-3-14-5
Oxides (wt.%)					
SiO_2	36.433	36.465	36.500	36.487	36.577
TiO_2	0.012	0.016	0.011	0.021	0.009
Al_2O_3	20.566	20.665	20.563	20.555	20.488
Fe_2O_3	0.412	0.313	0.415	0.399	0.551
FeO	23.726	23.829	23.713	23.646	23.468
MnO	19.879	19.922	19.659	19.700	19.889
MgO	0.098	0.078	0.066	0.087	0.091
CaO	0.677	0.709	0.775	0.688	0.655
Total	101.803	101.998	101.702	101.583	101.728
Ions on the basis of 12 O					
Si	2.969	2.966	2.975	2.976	2.979
Ti	0.001	0.001	0.001	0.001	0.001
Sum	2.970	2.967	2.975	2.977	2.980
Al	1.975	1.981	1.975	1.976	1.967
Fe^{3+}	0.025	0.019	0.025	0.025	0.034
Sum	2.000	2.000	2.000	2.000	2.001
Fe^{2+}	1.617	1.621	1.616	1.613	1.599
Mn	1.372	1.373	1.357	1.361	1.372
Mg	0.012	0.009	0.008	0.011	0.011
Ca	0.059	0.062	0.068	0.060	0.057
Sum	3.060	3.065	3.049	3.045	3.039

Table A.23 Electron microprobe analyses of apatite from inner-intermediate zone samples of the Dumper Dew pegmatite.

	Purple Apatite from the Inner Intermediate Zone				
Oxides (wt.%)					
P_2O_5	42.159	42.211	42.221	42.256	42.322
SiO_2	0.065	0.077	0.053	bdl	bdl
Al_2O_3	bdl	bdl	0.022	bdl	bdl
SrO	bdl	0.009	0.021	0.009	bdl
FeO	0.122	0.094	0.092	0.088	0.112
MnO	1.223	1.432	1.194	1.222	1.093
MgO	bdl	bdl	bdl	bdl	bdl
CaO	54.223	54.198	54.322	54.219	54.228
F	3.587	3.611	3.559	3.546	3.622
Subtotal	101.379	101.632	101.484	101.340	101.377
-O=F	1.510	1.521	1.499	1.493	1.525
Total	99.869	100.111	99.985	99.847	99.852
Ions on the basis of 13 (O,OH,F)					
P	2.995	2.994	2.996	3.000	3.000
Si	0.005	0.006	0.004	bdl	bdl
Sum	3.000	3.000	3.000	3.000	3.000
Al	bdl	bdl	0.002	bdl	bdl
Sr	bdl	0.000	0.001	0.000	bdl
Fe	0.009	0.007	0.006	0.006	0.008
Mn	0.087	0.102	0.085	0.087	0.078
Mg	bdl	bdl	bdl	bdl	bdl
Ca	4.874	4.865	4.878	4.872	4.865
Sum	4.970	4.973	4.972	4.965	4.950
F	0.952	0.957	0.943	0.940	0.959

Table A.24 Electron microprobe analyses of apatite from inner-intermediate zone samples of the Dumper Dew pegmatite.

	Purple Apatite from the Inner Intermediate Zone				
Oxides (wt.%)					
P_2O_5	42.178	42.223	42.265	42.165	42.198
SiO_2	bdl	bdl	bdl	bdl	bdl
Al_2O_3	bdl	bdl	bdl	bdl	bdl
SrO	0.007	0.014	0.011	0.008	0.013
FeO	0.212	0.194	0.197	0.204	0.220
MnO	1.232	1.226	1.298	1.225	1.227
MgO	bdl	bdl	bdl	bdl	bdl
CaO	53.976	54.002	53.988	53.943	53.955
F	3.598	3.589	3.600	3.587	3.599
Subtotal	101.203	101.248	101.359	101.132	101.212
-O=F	1.515	1.511	1.516	1.510	1.515
Total	99.688	99.737	99.843	99.622	99.697
Ions on the basis of 13 (O,OH,F)					
P	3.000	3.000	3.000	3.000	3.000
Si	bdl	bdl	bdl	bdl	bdl
Sum	3.000	3.000	3.000	3.000	3.000
Al	bdl	bdl	bdl	bdl	bdl
Sr	0.000	0.001	0.001	0.000	0.001
Fe	0.015	0.014	0.014	0.014	0.015
Mn	0.088	0.087	0.092	0.087	0.087
Mg	bdl	bdl	bdl	bdl	bdl
Ca	4.859	4.856	4.850	4.857	4.855
Sum	4.962	4.957	4.956	4.959	4.958
F	0.956	0.953	0.955	0.953	0.956

Table A.25 Electron microprobe analyses of apatite from inner-intermediate zone samples of the Dumper Dew pegmatite.

	Purple Apatite from the Inner Intermediate Zone				
Oxides (wt.%)					
P_2O_5	42.344	42.306	42.222	42.256	42.333
SiO_2	bdl	bdl	bdl	bdl	bdl
Al_2O_3	bdl	bdl	bdl	bdl	bdl
SrO	0.023	0.013	0.032	0.033	0.034
FeO	0.080	0.056	0.063	0.055	0.050
MnO	0.676	0.557	0.456	0.612	0.588
MgO	bdl	bdl	bdl	bdl	bdl
CaO	54.556	54.656	54.734	54.567	54.643
F	3.566	3.454	3.444	3.378	3.299
Subtotal	101.245	101.042	100.951	100.901	100.947
-O=F	1.502	1.454	1.450	1.422	1.389
Total	99.743	99.588	99.501	99.479	99.558
Ions on the basis of 13 (O,OH,F)					
P	3.000	3.000	3.000	3.000	3.000
Si	bdl	bdl	bdl	bdl	bdl
Sum	3.000	3.000	3.000	3.000	3.000
Al	bdl	bdl	bdl	bdl	bdl
Sr	0.001	0.001	0.002	0.002	0.002
Fe	0.006	0.004	0.004	0.004	0.004
Mn	0.048	0.040	0.032	0.043	0.042
Mg	bdl	bdl	bdl	bdl	bdl
Ca	4.892	4.905	4.922	4.903	4.901
Sum	4.946	4.949	4.960	4.952	4.948
F	0.944	0.915	0.914	0.896	0.873

Table A.26 Electron microprobe analyses of apatite from inner-intermediate zone samples of the Dumper Dew pegmatite.

	Purple Apatite from the Inner Intermediate Zone				
Oxides (wt.%)					
P_2O_5	42.400	42.444	42.520	42.489	42.656
SiO_2	0.034	0.043	0.055	0.042	0.055
Al_2O_3	bdl	bdl	bdl	0.034	bdl
SrO	0.023	0.043	0.012	0.000	0.000
FeO	0.120	0.090	0.115	0.128	0.098
MnO	0.989	0.999	1.005	0.967	0.955
MgO	0.009	0.012	0.007	0.006	0.011
CaO	54.567	54.767	54.788	54.789	54.767
F	3.367	3.334	3.367	3.255	3.300
Subtotal	101.509	101.732	101.869	101.710	101.842
-O=F	1.418	1.404	1.418	1.371	1.390
Total	100.091	100.328	100.451	100.339	100.452
Ions on the basis of 13 (O,OH,F)					
P	2.997	2.996	2.995	2.997	2.995
Si	0.003	0.004	0.005	0.003	0.005
Sum	3.000	3.000	3.000	3.000	3.000
Al	bdl	bdl	bdl	bdl	bdl
Sr	0.001	0.002	0.001	0.000	0.000
Fe	0.008	0.006	0.008	0.009	0.007
Mn	0.070	0.071	0.071	0.068	0.067
Mg	0.001	0.001	0.001	0.001	0.001
Ca	4.882	4.893	4.885	4.890	4.867
Sum	4.962	4.974	4.965	4.971	4.943
F	0.889	0.879	0.886	0.858	0.866

Table A.27 Electron microprobe analyses of apatite from replacement unit samples of the Dumper Dew pegmatite.

	Purple Apatite from the Replacement Unit				
Oxides (wt.%)					
P_2O_5	42.232	42.345	42.226	42.198	42.222
SiO_2	0.025	0.320	0.043	0.033	0.054
Al_2O_3	bdl	bdl	bdl	bdl	bdl
SrO	0.322	0.223	0.095	0.075	0.023
FeO	0.064	0.058	0.052	0.064	0.056
MnO	0.569	0.601	0.597	0.578	0.603
MgO	bdl	bdl	bdl	bdl	bdl
CaO	54.766	54.875	54.777	54.734	54.677
F	3.220	3.445	3.342	3.311	3.244
Subtotal	101.198	101.867	101.132	100.993	100.879
-O=F	1.356	1.451	1.407	1.394	1.366
Total	99.842	100.416	99.725	99.599	99.513
Ions on the basis of 13 (O,OH,F)					
P	2.998	2.973	2.996	2.997	2.995
Si	0.002	0.027	0.004	0.003	0.005
Sum	3.000	3.000	3.000	3.000	3.000
Al	bdl	bdl	bdl	bdl	bdl
Sr	0.016	0.011	0.005	0.004	0.001
Fe	0.004	0.004	0.004	0.004	0.004
Mn	0.040	0.042	0.042	0.041	0.043
Mg	bdl	bdl	bdl	bdl	bdl
Ca	4.920	4.877	4.919	4.920	4.909
Sum	4.981	4.934	4.970	4.969	4.957
F	0.854	0.904	0.886	0.879	0.860

Table A.28 Electron microprobe analyses of apatite from replacement unit samples of the Dumper Dew pegmatite.

	Purple Apatite from the Replacement Unit				
Oxides (wt.%)					
P_2O_5	42.245	42.214	42.224	42.446	42.194
SiO_2	0.034	0.055	0.041	0.033	0.036
Al_2O_3	bdl	bdl	bdl	0.022	bdl
SrO	0.006	0.009	0.056	0.006	bdl
FeO	0.060	0.063	0.058	0.062	0.055
MnO	0.723	0.711	0.695	0.745	0.650
MgO	0.008	0.008	bdl	bdl	bdl
CaO	54.722	54.760	54.657	54.733	54.678
F	3.133	3.215	3.116	3.256	3.300
Subtotal	100.931	101.035	100.847	101.303	100.913
-O=F	1.319	1.354	1.312	1.371	1.390
Total	99.612	99.681	99.535	99.932	99.523
Ions on the basis of 13 (O,OH,F)					
P	2.997	2.995	2.997	2.997	2.997
Si	0.003	0.005	0.003	0.003	0.003
Sum	3.000	3.000	3.000	3.000	3.000
Al	bdl	bdl	bdl	0.002	bdl
Sr	0.000	0.000	0.003	0.000	bdl
Fe	0.004	0.004	0.004	0.004	0.004
Mn	0.051	0.050	0.049	0.053	0.046
Mg	0.001	0.001	bdl	bdl	bdl
Ca	4.914	4.918	4.909	4.891	4.915
Sum	4.970	4.974	4.965	4.951	4.965
F	0.830	0.852	0.826	0.859	0.876

Table A.29 Electron microprobe analyses of apatite from replacement unit samples of the Dumper Dew pegmatite.

	Purple Apatite from the Replacement Unit				
Oxides (wt.%)					
P_2O_5	42.300	42.246	42.224	42.341	42.225
SiO_2	0.023	0.023	0.045	0.025	bdl
Al_2O_3	0.022	0.013	0.009	bdl	bdl
SrO	0.008	bdl	bdl	0.056	0.077
FeO	0.055	0.065	0.055	0.053	0.054
MnO	0.678	0.723	0.599	0.734	0.700
MgO	bdl	bdl	0.011	0.013	0.009
CaO	54.987	54.960	55.222	55.009	54.955
F	3.222	3.213	3.114	3.234	3.233
Subtotal	101.295	101.243	101.279	101.465	101.253
-O=F	1.357	1.353	1.311	1.362	1.361
Total	99.938	99.890	99.968	100.103	99.892
Ions on the basis of 13 (O,OH,F)					
P	2.998	2.998	2.996	2.998	3.000
Si	0.002	0.002	0.004	0.002	0.000
Sum	3.000	3.000	3.000	3.000	3.000
Al	0.002	0.001	0.001	0.000	0.000
Sr	0.000	bdl	bdl	0.003	0.004
Fe	0.004	0.005	0.004	0.004	0.004
Mn	0.048	0.051	0.043	0.052	0.050
Mg	bdl	bdl	0.001	0.002	0.001
Ca	4.932	4.936	4.959	4.929	4.942
Sum	4.987	4.994	5.008	4.989	5.000
F	0.853	0.852	0.825	0.855	0.858

Table A.30 Electron microprobe analyses of apatite from replacement unit samples of the Dumper Dew pegmatite.

	Purple Apatite from the Replacement Unit				
Oxides (wt.%)					
P_2O_5	42.211	42.196	42.195	42.005	42.120
SiO_2	0.023	0.018	0.020	0.017	0.022
Al_2O_3	bdl	bdl	bdl	bdl	0.024
SrO	0.034	0.022	0.026	0.033	0.004
FeO	0.123	0.132	0.114	0.145	0.178
MnO	0.522	0.517	0.544	0.512	0.506
MgO	bdl	0.008	0.012	bdl	bdl
CaO	54.556	54.673	54.567	54.566	54.634
F	3.122	3.223	3.267	3.322	3.233
Subtotal	100.591	100.789	100.745	100.600	100.721
-O=F	1.315	1.357	1.376	1.399	1.361
Total	99.276	99.432	99.369	99.201	99.360
Ions on the basis of 13 (O,OH,F)					
P	2.998	2.998	2.998	2.999	2.998
Si	0.002	0.002	0.002	0.001	0.002
Sum	3.000	3.000	3.000	3.000	3.000
Al	bdl	bdl	bdl	bdl	0.002
Sr	0.002	0.001	0.001	0.002	0.000
Fe	0.009	0.009	0.008	0.010	0.013
Mn	0.037	0.037	0.039	0.037	0.036
Mg	bdl	0.001	0.002	bdl	bdl
Ca	4.904	4.917	4.907	4.930	4.922
Sum	4.951	4.965	4.957	4.978	4.973
F	0.828	0.856	0.867	0.886	0.860

Table A.31 Electron microprobe analyses of apatite from replacement unit samples of the Dumper Dew pegmatite.

	Purple Apatite from the Replacement Unit				
Oxides (wt.%)					
P_2O_5	42.322	42.256	42.324	42.123	42.332
SiO_2	0.007	0.032	0.025	0.023	0.033
Al_2O_3	bdl	0.033	bdl	bdl	bdl
SrO	0.034	0.020	0.012	0.009	0.034
FeO	0.033	0.023	0.028	0.027	0.019
MnO	0.544	0.787	0.778	0.785	0.760
MgO	0.022	bdl	0.006	0.012	0.000
CaO	54.443	54.566	54.650	54.653	54.634
F	3.325	3.210	3.134	3.256	3.214
Subtotal	100.730	100.927	100.957	100.888	101.026
-O=F	1.400	1.352	1.320	1.371	1.353
Total	99.330	99.575	99.637	99.517	99.673
Ions on the basis of 13 (O,OH,F)					
P	2.999	2.997	2.998	2.998	2.997
Si	0.001	0.003	0.002	0.002	0.003
Sum	3.000	3.000	3.000	3.000	3.000
Al	bdl	0.003	bdl	bdl	bdl
Sr	0.002	0.001	0.001	0.000	0.002
Fe	0.002	0.002	0.002	0.002	0.001
Mn	0.039	0.056	0.055	0.056	0.054
Mg	0.003	bdl	0.001	0.002	0.000
Ca	4.883	4.899	4.899	4.923	4.896
Sum	4.929	4.960	4.958	4.983	4.953
F	0.880	0.851	0.829	0.866	0.850

Table A.32 Electron microprobe analyses of apatite from replacement unit samples of the Dumper Dew pegmatite.

	Purple Apatite from the Replacement Unit				
Oxides (wt.%)					
P_2O_5	42.233	42.210	42.233	42.430	42.317
SiO_2	0.123	0.132	0.105	0.111	0.105
Al_2O_3	bdl	bdl	0.034	bdl	0.064
SrO	0.027	0.043	0.045	0.021	0.024
FeO	0.121	0.100	0.132	0.120	0.133
MnO	0.887	0.890	0.934	0.887	0.834
MgO	0.007	bdl	0.005	bdl	bdl
CaO	54.723	54.777	54.689	54.766	54.578
F	3.332	3.317	3.267	3.322	3.276
Subtotal	101.453	101.469	101.444	101.657	101.331
-O=F	1.403	1.397	1.376	1.399	1.379
Total	100.050	100.072	100.068	100.258	99.952
Ions on the basis of 13 (O,OH,F)					
P	2.990	2.989	2.991	2.991	2.991
Si	0.010	0.011	0.009	0.009	0.009
Sum	3.000	3.000	3.000	3.000	3.000
Al	bdl	bdl	0.003	bdl	0.006
Sr	0.001	0.002	0.002	0.001	0.001
Fe	0.008	0.007	0.009	0.008	0.009
Mn	0.063	0.063	0.066	0.063	0.059
Mg	0.001	bdl	0.001	bdl	bdl
Ca	4.903	4.909	4.902	4.886	4.883
Sum	4.976	4.981	4.984	4.958	4.958
F	0.881	0.877	0.864	0.875	0.865

Table A.33 Electron microprobe analyses of apatite from replacement unit samples of the Dumper Dew pegmatite.

	Purple Apatite from the Replacement Unit				
Oxides (wt.%)					
P_2O_5	42.400	42.343	42.288	42.300	42.233
SiO_2	0.089	0.056	0.077	0.098	0.045
Al_2O_3	0.008	0.022	0.009	bdl	0.056
SrO	bdl	bdl	bdl	0.006	0.005
FeO	0.023	0.022	0.021	0.019	0.017
MnO	0.656	0.566	0.721	0.566	0.533
MgO	bdl	bdl	0.006	bdl	bdl
CaO	54.780	54.888	54.788	54.589	54.788
F	3.210	3.210	3.122	3.211	3.265
Subtotal	101.166	101.107	101.032	100.789	100.942
-O=F	1.352	1.352	1.315	1.352	1.375
Total	99.814	99.755	99.717	99.437	99.567
Ions on the basis of 13 (O,OH,F)					
P	2.993	2.995	2.994	2.992	2.996
Si	0.007	0.005	0.006	0.008	0.004
Sum	3.000	3.000	3.000	3.000	3.000
Al	0.001	0.002	0.001	bdl	0.006
Sr	bdl	bdl	bdl	0.000	bdl
Fe	0.002	0.002	0.001	0.001	0.001
Mn	0.046	0.040	0.051	0.040	0.038
Mg	bdl	bdl	0.001	bdl	bdl
Ca	4.893	4.914	4.909	4.887	4.919
Sum	4.942	4.958	4.963	4.928	4.964
F	0.846	0.848	0.826	0.848	0.865

Table A.34 Electron microprobe analyses of apatite from inner-intermediate zone samples of the Dumper Dew pegmatite.

	Green Apatite from the Inner Intermediate Zone				
Oxides (wt.%)					
P_2O_5	41.893	42.009	42.100	41.984	42.110
SiO_2	0.330	0.067	0.055	0.043	0.040
Al_2O_3	bdl	bdl	0.034	0.032	bdl
SrO	0.067	0.078	0.034	bdl	0.008
FeO	0.087	0.076	0.112	0.098	0.078
MnO	5.560	5.344	5.455	5.333	5.450
MgO	0.034	0.029	0.032	0.027	0.031
CaO	50.656	50.007	50.012	50.233	50.344
F	3.223	3.045	3.144	3.323	3.323
Subtotal	101.850	100.655	100.978	101.073	101.384
-O=F	1.357	1.282	1.324	1.399	1.399
Total	100.493	99.373	99.654	99.674	99.985
Ions on the basis of 13 (O,OH,F)					
P	2.972	2.994	2.995	2.996	2.997
Si	0.028	0.006	0.005	0.004	0.003
Sum	3.000	3.000	3.000	3.000	3.000
Al	bdl	bdl	0.003	0.003	bdl
Sr	0.003	0.004	0.002	bdl	0.000
Fe	0.006	0.005	0.008	0.007	0.005
Mn	0.395	0.381	0.388	0.381	0.388
Mg	0.004	0.004	0.004	0.003	0.004
Ca	4.549	4.511	4.503	4.537	4.534
Sum	4.957	4.905	4.909	4.932	4.932
F	0.854	0.811	0.836	0.886	0.883

Table A.35 Electron microprobe analyses of apatite from inner-intermediate zone samples of the Dumper Dew pegmatite.

	Green Apatite from the Inner Intermediate Zone				
Oxides (wt.%)					
P_2O_5	41.786	41.689	41.673	41.745	41.750
SiO_2	0.121	0.097	0.145	0.154	0.165
Al_2O_3	bdl	bdl	0.056	0.023	bdl
SrO	0.210	0.434	0.312	0.094	0.005
FeO	0.211	0.326	0.267	0.300	0.321
MnO	6.112	6.232	6.310	6.097	6.233
MgO	0.033	0.076	0.018	0.000	0.009
CaO	49.786	49.785	49.700	49.679	49.842
F	3.222	3.167	3.340	3.256	3.222
Subtotal	101.481	101.806	101.821	101.348	101.547
-O=F	1.357	1.334	1.406	1.371	1.357
Total	100.124	100.472	100.415	99.977	100.190
Ions on the basis of 13 (O,OH,F)					
P	2.990	2.992	2.988	2.987	2.986
Si	0.010	0.008	0.012	0.013	0.014
Sum	3.000	3.000	3.000	3.000	3.000
Al	bdl	bdl	0.006	0.002	bdl
Sr	0.010	0.021	0.015	0.005	0.000
Fe	0.015	0.023	0.019	0.021	0.023
Mn	0.438	0.447	0.453	0.436	0.446
Mg	0.004	0.010	0.002	0.000	0.001
Ca	4.508	4.522	4.510	4.499	4.512
Sum	4.975	5.023	5.004	4.963	4.982
F	0.861	0.849	0.895	0.870	0.861

Table A.36 Electron microprobe analyses of apatite from inner-intermediate zone samples of the Dumper Dew pegmatite.

	Green Apatite from the Inner Intermediate Zone				
Oxides (wt.%)					
P_2O_5	41.877	42.433	42.095	42.045	42.005
SiO_2	0.230	0.267	0.312	0.222	0.134
Al_2O_3	bdl	bdl	bdl	bdl	bdl
SrO	0.067	0.095	0.089	0.087	0.077
FeO	0.087	0.098	0.123	0.112	0.094
MnO	5.622	5.688	5.876	5.900	5.768
MgO	0.009	bdl	0.011	0.011	0.014
CaO	49.555	49.788	49.744	49.800	49.877
F	3.244	3.322	3.210	3.345	3.334
Subtotal	100.691	101.691	101.460	101.522	101.303
-O=F	1.366	1.399	1.352	1.409	1.404
Total	99.325	100.292	100.108	100.113	99.899
Ions on the basis of 13 (O,OH,F)					
P	2.981	2.978	2.974	2.981	2.989
Si	0.019	0.022	0.026	0.019	0.011
Sum	3.000	3.000	3.000	3.000	3.000
Al	bdl	bdl	bdl	bdl	bdl
Sr	0.003	0.005	0.004	0.004	0.004
Fe	0.006	0.007	0.009	0.008	0.007
Mn	0.400	0.399	0.415	0.419	0.411
Mg	0.001	bdl	0.001	0.001	0.002
Ca	4.464	4.422	4.448	4.469	4.491
Sum	4.875	4.833	4.877	4.901	4.914
F	0.863	0.871	0.847	0.886	0.886

Table A.37 Electron microprobe analyses of apatite from inner-intermediate zone samples of the Dumper Dew pegmatite.

	Green Apatite from the Inner Intermediate Zone				
Oxides (wt.%)					
P_2O_5	42.045	42.056	42.095	42.654	42.776
SiO_2	0.022	0.014	0.019	0.014	0.022
Al_2O_3	bdl	bdl	bdl	bdl	bdl
SrO	0.134	0.167	0.214	0.145	0.122
FeO	0.121	0.134	0.122	0.145	0.120
MnO	5.893	5.987	5.986	5.934	5.893
MgO	0.043	0.056	0.047	0.047	0.053
CaO	49.778	49.940	49.875	49.777	49.894
F	3.244	3.322	3.210	3.345	3.334
Subtotal	98.036	98.354	98.358	98.716	98.880
-O=F	1.366	1.399	1.352	1.409	1.404
Total	99.325	100.292	100.108	100.113	99.899
Ions on the basis of 13 (O,OH,F)					
P	2.998	2.999	2.998	2.999	2.998
Si	0.002	0.001	0.002	0.001	0.002
Sum	3.000	3.000	3.000	3.000	3.000
Al	bdl	bdl	bdl	bdl	bdl
Sr	0.007	0.008	0.010	0.007	0.006
Fe	0.009	0.009	0.009	0.010	0.008
Mn	0.420	0.427	0.427	0.417	0.413
Mg	0.005	0.007	0.006	0.006	0.007
Ca	4.492	4.507	4.496	4.429	4.426
Sum	4.933	4.959	4.948	4.869	4.860
F	0.863	0.871	0.847	0.886	0.886

Table A.38 Electron microprobe analyses of tourmaline from inner-intermediate zone samples of the Dumper Dew pegmatite.

	Inner-Intermediate Zone Samples				
	002-1-10-1	*002-1-10-2*	*002-1-10-3*	*002-1-10-4*	*002-1-10-5*
Oxides (wt.%)					
SiO_2	36.665	36.589	36.683	36.673	36.597
TiO_2	0.565	0.558	0.545	0.564	0.588
B_2O_3 (calc.)	10.612	10.618	10.637	10.650	10.623
Al_2O_3	33.412	33.656	33.709	33.775	33.634
FeO	12.433	12.533	12.423	12.447	12.700
MnO	0.287	0.255	0.267	0.273	0.243
MgO	1.455	1.388	1.376	1.416	1.376
CaO	0.044	0.066	0.059	0.063	0.055
Li_2O (calc.)	0.581	0.549	0.579	0.563	0.531
Na_2O	2.388	2.289	2.349	2.338	2.280
K_2O	0.027	0.032	0.025	0.031	0.027
H_2O (calc.)	3.039	3.063	3.086	3.035	3.031
F	1.312	1.267	1.232	1.348	1.337
Subtotal	102.821	102.863	102.971	103.176	103.023
-O=F	0.552	0.533	0.519	0.568	0.563
Total	102.268	102.330	102.452	102.608	102.460
Ions on the basis of 31 (O, OH, F)					
Si	6.004	5.988	5.993	5.984	5.987
Al	0.000	0.012	0.007	0.016	0.013
Tet. Sum	6.004	6.000	6.000	6.000	6.000
B	3.000	3.000	3.000	3.000	3.000
Al (Z)	6.000	6.000	6.000	6.000	6.000
Al	0.449	0.481	0.484	0.480	0.472
Ti	0.070	0.069	0.067	0.069	0.072
Fe^{2+}	1.703	1.715	1.697	1.699	1.737
Mn	0.040	0.035	0.037	0.038	0.034
Mg	0.355	0.339	0.335	0.344	0.335
Li	0.383	0.362	0.381	0.370	0.349
Y sum	2.999	3.000	3.001	3.000	3.000
Ca	0.008	0.012	0.010	0.011	0.010
Na	0.758	0.726	0.744	0.740	0.723
K	0.006	0.007	0.005	0.006	0.006
Vacancy	0.228	0.255	0.240	0.243	0.262
X sum	1.000	1.000	1.000	1.000	1.000
F	0.679	0.656	0.637	0.696	0.692
OH	3.320	3.344	3.363	3.304	3.308

Table A.39 Electron microprobe analyses of tourmaline from inner-intermediate zone samples of the Dumper Dew pegmatite.

	Inner-Intermediate Zone Samples				
	002-1-11-1	*002-1-11-2*	*002-1-11-3*	*002-1-11-4*	*002-1-11-5*
Oxides (wt.%)					
SiO_2	36.687	36.711	36.656	36.721	36.673
TiO_2	0.512	0.478	0.489	0.534	0.528
B_2O_3 (calc.)	10.637	10.632	10.633	10.651	10.644
Al_2O_3	33.778	33.762	33.773	33.764	33.720
FeO	12.566	12.506	12.544	12.563	12.457
MnO	0.322	0.420	0.393	0.388	0.394
MgO	1.221	1.154	1.327	1.258	1.300
CaO	0.057	0.057	0.072	0.067	0.078
Li_2O (calc.)	0.580	0.588	0.535	0.574	0.591
Na_2O	2.334	2.322	2.256	2.344	2.412
K_2O	0.022	0.031	0.020	0.026	0.025
H_2O (calc.)	3.090	3.116	3.073	3.047	3.122
F	1.223	1.165	1.256	1.323	1.160
Subtotal	103.030	102.941	103.027	103.261	103.104
-O=F	0.515	0.491	0.529	0.557	0.488
Total	102.515	102.450	102.498	102.704	102.616
Ions on the basis of 31 (O, OH, F)					
Si	5.993	6.001	5.991	5.991	5.987
Al	0.007	0.000	0.009	0.009	0.013
Tet. Sum	6.000	6.001	6.000	6.000	6.000
B	3.000	3.000	3.000	3.000	3.000
Al (Z)	6.000	6.000	6.000	6.000	6.000
Al	0.498	0.505	0.497	0.484	0.476
Ti	0.063	0.059	0.060	0.066	0.065
Fe^{2+}	1.717	1.710	1.715	1.714	1.701
Mn	0.045	0.058	0.054	0.054	0.054
Mg	0.297	0.281	0.323	0.306	0.316
Li	0.381	0.386	0.351	0.377	0.388
Y sum	3.001	2.999	3.000	3.001	3.000
Ca	0.010	0.010	0.013	0.012	0.014
Na	0.739	0.736	0.715	0.742	0.764
K	0.005	0.006	0.004	0.005	0.005
Vacancy	0.246	0.248	0.268	0.241	0.218
X sum	1.000	1.000	1.000	1.000	1.000
F	0.632	0.602	0.649	0.683	0.599
OH	3.368	3.397	3.350	3.317	3.400

Table A.40 Electron microprobe analyses of tourmaline from inner-intermediate zone samples of the Dumper Dew pegmatite.

	Inner-Intermediate Zone Samples				
	002-2-4-1	*002-2-4-2*	*002-2-4-3*	*002-2-4-4*	*002-2-4-5*
Oxides (wt.%)					
SiO_2	36.620	36.578	36.622	36.653	36.695
TiO_2	0.384	0.344	0.376	0.431	0.378
B_2O_3 (calc.)	10.596	10.617	10.636	10.629	10.941
Al_2O_3	33.324	33.443	33.496	33.421	33.433
FeO	12.788	12.877	12.888	12.846	12.873
MnO	0.334	0.455	0.426	0.444	0.465
MgO	1.433	1.445	1.478	1.338	1.342
CaO	0.034	0.036	0.039	0.040	0.037
Li_2O (calc.)	0.544	0.516	0.516	0.564	1.215
Na_2O	2.455	2.556	2.563	2.592	2.523
K_2O	0.028	0.028	0.024	0.022	0.025
H_2O (calc.)	3.076	3.057	3.089	3.134	3.144
F	1.223	1.277	1.223	1.125	1.330
Subtotal	102.838	103.229	103.376	103.239	104.401
-O=F	0.515	0.538	0.515	0.474	0.560
Total	102.323	102.691	102.861	102.766	103.841
Ions on the basis of 31 (O, OH, F)					
Si	6.006	5.987	5.984	5.992	5.829
Al	0.000	0.013	0.016	0.008	0.171
Tet. Sum	6.006	6.000	6.000	6.000	6.000
B	3.000	3.000	3.000	3.000	3.000
Al (Z)	6.000	6.000	6.000	6.000	6.000
Al	0.442	0.439	0.434	0.433	0.088
Ti	0.047	0.042	0.046	0.053	0.045
Fe^{2+}	1.754	1.763	1.761	1.756	1.710
Mn	0.046	0.063	0.059	0.061	0.063
Mg	0.350	0.352	0.360	0.326	0.318
Li	0.359	0.340	0.339	0.371	0.776
Y sum	2.999	3.000	2.999	3.000	3.000
Ca	0.006	0.006	0.007	0.007	0.006
Na	0.781	0.811	0.812	0.822	0.777
K	0.006	0.006	0.005	0.005	0.005
Vacancy	0.207	0.177	0.176	0.167	0.212
X sum	1.000	1.000	1.000	1.000	1.000
F	0.634	0.661	0.632	0.582	0.668
OH	3.365	3.338	3.367	3.418	3.331

Table A.41 Electron microprobe analyses of tourmaline from outer-intermediate zone samples of the Dumper Dew pegmatite.

	Outer-Intermediate Zone Samples				
	010-3-9-1	*010-3-9-2*	*010-3-9-3*	*010-3-9-4*	*010-3-9-5*
Oxides (wt.%)					
SiO_2	35.543	35.577	35.623	35.612	35.540
TiO_2	0.250	0.310	0.256	0.287	0.322
B_2O_3 (calc.)	10.510	10.535	10.531	10.532	10.536
Al_2O_3	34.555	34.655	34.596	34.632	34.588
FeO	11.004	10.966	10.934	10.998	11.033
MnO	0.156	0.177	0.154	0.178	0.189
MgO	1.865	1.899	1.834	1.830	1.922
CaO	0.034	0.030	0.041	0.033	0.037
Li_2O (calc.)	0.533	0.530	0.572	0.543	0.535
Na_2O	2.455	2.458	2.532	2.456	2.540
K_2O	0.033	0.028	0.036	0.033	0.026
H_2O (calc.)	3.048	3.013	2.999	2.981	3.001
F	1.221	1.312	1.340	1.378	1.340
Subtotal	101.206	101.490	101.447	101.493	101.609
-O=F	0.514	0.552	0.564	0.580	0.564
Total	100.692	100.938	100.883	100.913	101.044
Ions on the basis of 31 (O, OH, F)					
Si	5.877	5.868	5.878	5.876	5.861
Al	0.123	0.132	0.122	0.124	0.139
Tet. Sum	6.000	6.000	6.000	6.000	6.000
B	3.000	3.000	3.000	3.000	3.000
Al (Z)	6.000	6.000	6.000	6.000	6.000
Al	0.611	0.606	0.607	0.611	0.585
Ti	0.031	0.038	0.032	0.036	0.040
Fe^{2+}	1.522	1.513	1.509	1.518	1.522
Mn	0.022	0.025	0.022	0.025	0.026
Mg	0.460	0.467	0.451	0.450	0.472
Li	0.354	0.351	0.379	0.361	0.355
Y sum	3.000	3.000	3.000	3.000	3.000
Ca	0.006	0.005	0.007	0.006	0.007
Na	0.787	0.786	0.810	0.786	0.812
K	0.007	0.006	0.008	0.007	0.005
Vacancy	0.200	0.203	0.175	0.202	0.176
X sum	1.000	1.000	1.000	1.000	1.000
F	0.638	0.684	0.699	0.719	0.699
OH	3.362	3.316	3.301	3.281	3.301

Table A.42 Electron microprobe analyses of exocontact tourmaline samples collected from around the Dumper Dew.

	Exocontact Tourmaline				
	022-3-12-1	*022-3-12-2*	*022-3-12-3*	*022-3-12-4*	*022-3-12-5*
Oxides (wt.%)					
SiO_2	36.432	36.488	36.522	36.487	36.533
TiO_2	0.320	0.368	0.385	0.344	0.323
B_2O_3 (calc.)	10.697	10.718	10.724	10.718	10.719
Al_2O_3	34.233	34.156	34.205	34.211	34.154
FeO	11.887	11.900	11.893	11.934	11.798
MnO	0.095	0.101	0.094	0.095	0.104
MgO	2.455	2.644	2.573	2.555	2.675
CaO	0.056	0.040	0.052	0.044	0.046
Li_2O (calc.)	0.406	0.377	0.393	0.394	0.386
Na_2O	2.456	2.477	2.456	2.493	2.484
K_2O	0.022	0.033	0.031	0.041	0.035
H_2O (calc.)	3.060	3.056	3.087	3.067	3.071
F	1.332	1.355	1.295	1.332	1.324
Subtotal	103.450	103.713	103.710	103.716	103.652
-O=F	0.561	0.571	0.545	0.561	0.557
Total	102.890	103.142	103.165	103.155	103.095
Ions on the basis of 31 (O, OH, F)					
Si	5.918	5.916	5.918	5.915	5.922
Al	0.082	0.084	0.082	0.085	0.078
Tet. Sum	6.000	6.000	6.000	6.000	6.000
B	3.000	3.000	3.000	3.000	3.000
Al (Z)	6.000	6.000	6.000	6.000	6.000
Al	0.473	0.443	0.451	0.452	0.448
Ti	0.039	0.045	0.047	0.042	0.039
Fe^{2+}	1.615	1.614	1.612	1.618	1.600
Mn	0.013	0.014	0.013	0.013	0.014
Mg	0.594	0.639	0.621	0.617	0.646
Li	0.265	0.246	0.256	0.257	0.252
Y sum	3.000	3.000	3.000	3.000	3.000
Ca	0.010	0.007	0.009	0.008	0.008
Na	0.774	0.779	0.772	0.784	0.781
K	0.005	0.007	0.006	0.008	0.007
Vacancy	0.212	0.208	0.213	0.200	0.204
X sum	1.000	1.000	1.000	1.000	1.000
F	0.684	0.695	0.664	0.683	0.679
OH	3.316	3.305	3.336	3.317	3.321

Table A.43 Electron microprobe analyses of tourmaline from core margin zone samples of the Tiger Bill pegmatite.

	Tiger Bill Core Margin Zone Samples				
	TB-4-2-1	*TB-4-2-2*	*TB-4-2-3*	*TB-4-2-4*	*TB-4-2-5*
Oxides (wt.%)					
SiO_2	36.604	36.584	36.599	36.523	36.478
TiO_2	0.330	0.270	0.290	0.310	0.260
B_2O_3 (calc.)	10.701	10.688	10.680	10.696	10.806
Al_2O_3	34.438	34.378	34.367	34.533	35.488
FeO	11.322	11.378	11.400	11.365	11.406
MnO	0.135	0.126	0.122	0.132	0.128
MgO	1.998	2.005	1.899	1.967	2.054
CaO	0.045	0.056	0.035	0.043	0.045
Li_2O (calc.)	0.588	0.582	0.595	0.576	0.515
Na_2O	2.556	2.566	2.549	2.548	2.555
K_2O	0.022	0.017	0.022	0.018	0.020
H_2O (calc.)	3.128	3.097	3.101	3.122	3.153
F	1.190	1.245	1.232	1.199	1.216
Subtotal	103.057	102.992	102.891	103.032	104.124
-O=F	0.501	0.524	0.519	0.505	0.512
Total	102.556	102.468	102.372	102.527	103.612
Ions on the basis of 31 (O, OH, F)					
Si	5.944	5.948	5.955	5.934	5.865
Al	0.056	0.052	0.045	0.066	0.135
Tet. Sum	6.000	6.000	6.000	6.000	6.000
B	3.000	3.000	3.000	3.000	2.999
Al (Z)	6.000	6.000	6.000	6.000	6.000
Al	0.536	0.536	0.546	0.547	0.591
Ti	0.040	0.033	0.035	0.038	0.031
Fe^{2+}	1.538	1.547	1.551	1.544	1.534
Mn	0.019	0.017	0.017	0.018	0.017
Mg	0.484	0.486	0.460	0.476	0.492
Li	0.384	0.380	0.389	0.376	0.333
Y sum	3.000	3.000	2.999	3.000	3.000
Ca	0.008	0.010	0.006	0.007	0.008
Na	0.805	0.809	0.804	0.803	0.797
K	0.005	0.004	0.005	0.004	0.004
Vacancy	0.183	0.178	0.185	0.186	0.192
X sum	1.000	1.000	1.000	1.000	1.000
F	0.611	0.640	0.634	0.616	0.618
OH	3.389	3.359	3.365	3.384	3.382

Table A.44 Electron microprobe analyses of exocontact tourmaline samples collected from the Dumper Dew pegmatite.

Exocontact Tourmaline					
Oxides (wt.%)					
SiO_2	36.567	35.652	35.554	35.621	35.555
TiO_2	0.023	0.017	0.013	0.017	0.021
B_2O_3 (calc.)	10.725	10.605	10.595	10.600	10.557
Al_2O_3	34.544	34.650	34.700	34.655	34.559
FeO	12.233	12.343	12.423	12.634	12.480
MnO	0.078	0.088	0.076	0.068	0.072
MgO	2.223	2.330	2.265	2.099	1.998
CaO	0.045	0.050	0.045	0.050	0.045
Li_2O (calc.)	0.415	0.291	0.291	0.316	0.337
Na_2O	2.544	2.498	2.523	2.554	2.488
K_2O	0.031	0.023	0.022	0.015	0.011
H_2O (calc.)	3.090	3.043	3.024	3.021	3.036
F	1.288	1.300	1.333	1.344	1.280
Subtotal	103.807	102.891	102.865	102.994	102.440
-O=F	0.542	0.547	0.561	0.566	0.539
Total	103.264	102.343	102.304	102.428	101.901
Ions on the basis of 31 (O, OH, F)					
Si	5.924	5.841	5.831	5.839	5.852
Al	0.076	0.159	0.169	0.161	0.148
Tet. Sum	6.000	6.000	6.000	6.000	6.000
B	3.000	2.999	2.999	2.999	3.000
Al (Z)	6.000	6.000	6.000	6.000	6.000
Al	0.521	0.533	0.538	0.535	0.556
Ti	0.003	0.002	0.002	0.002	0.003
Fe^{2+}	1.658	1.691	1.704	1.732	1.718
Mn	0.011	0.012	0.011	0.009	0.010
Mg	0.537	0.569	0.554	0.513	0.490
Li	0.271	0.192	0.192	0.208	0.223
Y sum	3.000	3.000	3.000	3.000	3.000
Ca	0.008	0.009	0.008	0.009	0.008
Na	0.799	0.794	0.802	0.812	0.794
K	0.006	0.005	0.005	0.003	0.002
Vacancy	0.187	0.193	0.185	0.176	0.196
X sum	1.000	1.000	1.000	1.000	1.000
F	0.660	0.674	0.691	0.697	0.666
OH	3.340	3.326	3.309	3.303	3.334

Table A.45 Electron microprobe analyses of beryl from outer-intermediate zone samples of the Dumper Dew pegmatite.

	Outer-Intermediate Zone Samples				
	001-1-4-1	*001-1-4-2*	*001-1-4-3*	*001-1-4-4*	*001-1-4-5*
Oxides (wt.%)					
SiO_2	66.877	66.789	66.844	66.851	66.798
Al_2O_3	18.672	18.755	18.643	18.708	18.800
FeO	0.110	0.160	0.190	0.220	0.160
Cs_2O	0.085	0.078	0.073	0.080	0.067
Rb_2O	0.080	0.110	0.233	0.178	0.213
MnO	0.022	0.011	0.013	0.015	0.007
MgO	bdl	bdl	bdl	bdl	bdl
CaO	bdl	0.008	bdl	bdl	bdl
Na_2O	0.776	0.800	0.778	0.794	0.804
K_2O	0.000	0.022	bdl	0.019	bdl
BeO	13.959	13.964	13.958	13.972	13.973
Total	100.581	100.697	100.732	100.837	100.822
Ions the basis of 18 (O)					
Si	5.983	5.973	5.980	5.975	5.970
Al	1.969	1.977	1.966	1.971	1.980
Fe	0.008	0.012	0.014	0.016	0.012
Cs	0.003	0.003	0.003	0.003	0.003
Rb	0.005	0.006	0.013	0.010	0.012
Mn	0.002	0.001	0.001	0.001	0.001
Mg	bdl	bdl	bdl	bdl	bdl
Ca	bdl	0.001	bdl	bdl	bdl
Na	0.135	0.139	0.135	0.138	0.139
K	0.000	0.003	bdl	0.002	bdl
Sum	0.152	0.164	0.167	0.170	0.167
Be	3.000	3.000	3.000	3.000	3.000

Table A.46 Electron microprobe analyses of beryl cores from outer-intermediate zone samples of the Dumper Dew pegmatite.

	Outer-Intermediate Zone Samples *Core of Beryl Crystal*				
	001-6-5-1	*001-6-5-2*	*001-6-5-3*	*001-6-5-4*	*001-6-5-5*
Oxides (wt.%)					
SiO_2	66.433	66.456	66.336	66.453	66.450
Al_2O_3	18.344	18.448	18.398	18.412	18.453
FeO	0.054	0.076	0.065	0.074	0.088
Cs_2O	0.788	0.800	0.976	0.877	0.898
Rb_2O	0.212	0.178	0.221	0.198	0.218
MnO	0.009	0.013	0.010	0.009	0.021
MgO	bdl	bdl	bdl	bdl	bdl
CaO	0.006	bdl	bdl	0.007	bdl
Na_2O	1.210	1.223	1.230	1.320	1.223
K_2O	0.233	0.254	0.223	0.156	0.233
BeO	13.896	13.918	13.893	13.918	13.921
Total	101.185	101.366	101.352	101.433	101.505
Ions the basis of 18 (O)					
Si	5.970	5.963	5.963	5.963	5.961
Al	1.943	1.951	1.949	1.947	1.951
Fe	0.004	0.006	0.005	0.006	0.007
Cs	0.031	0.037	0.034	0.034	0.034
Rb	0.012	0.010	0.013	0.011	0.013
Mn	0.001	0.001	0.001	0.001	0.002
Mg	bdl	bdl	bdl	bdl	bdl
Ca	0.001	bdl	bdl	0.001	bdl
Na	0.211	0.213	0.214	0.230	0.213
K	0.027	0.029	0.026	0.018	0.027
Sum	0.286	0.296	0.292	0.300	0.294
Be	3.000	3.000	3.000	3.000	3.000

Table A.47 Electron microprobe analyses of beryl rims from outer-intermediate zone samples of the Dumper Dew pegmatite.

	Outer-Intermediate Zone Samples *Rim of Beryl Crystal*				
	001-6-6-1	*001-6-6-2*	*001-6-6-3*	*001-6-6-4*	*001-6-6-5*
Oxides (wt.%)					
SiO_2	66.385	66.422	66.442	66.450	66.462
Al_2O_3	18.448	18.512	18.465	18.510	18.465
FeO	0.120	0.112	0.095	0.104	0.105
Cs_2O	0.877	0.956	0.987	0.889	0.976
Rb_2O	0.243	0.233	0.230	0.223	0.213
MnO	0.012	0.018	0.021	0.014	0.011
MgO	0.006	bdl	bdl	bdl	bdl
CaO	bdl	bdl	bdl	bdl	bdl
Na_2O	1.210	1.233	1.123	1.233	1.233
K_2O	0.334	0.326	0.288	0.312	0.305
BeO	13.916	13.933	13.919	13.936	13.931
Total	101.551	101.745	101.578	101.683	101.701
Ions the basis of 18 (O)					
Si	5.957	5.953	5.961	5.954	5.958
Al	1.951	1.955	1.952	1.955	1.951
Fe	0.009	0.008	0.007	0.008	0.008
Cs	0.037	0.038	0.034	0.037	0.001
Rb	0.014	0.013	0.013	0.013	0.012
Mn	0.001	0.001	0.002	0.001	0.001
Mg	0.001	bdl	bdl	bdl	bdl
Ca	bdl	bdl	bdl	bdl	bdl
Na	0.211	0.214	0.195	0.214	0.214
K	0.038	0.037	0.033	0.036	0.035
Sum	0.310	0.312	0.284	0.309	0.271
Be	3.000	3.000	3.000	3.000	3.000

Table A.48 Electron microprobe analyses of beryl from inner-intermediate zone samples of the Dumper Dew pegmatite.

	Inner-Intermediate Zone Samples				
	002-1-16-1	*002-1-16-2*	*002-1-16-3*	*002-1-16-4*	*002-1-16-5*
Oxides (wt.%)					
SiO_2	66.853	66.845	66.787	66.779	66.800
Al_2O_3	18.689	18.706	18.699	18.704	18.677
FeO	0.054	0.044	0.047	0.052	0.047
Cs_2O	0.088	0.096	0.086	0.090	0.097
Rb_2O	0.095	0.111	0.095	0.078	0.087
MnO	0.008	0.006	0.006	bdl	0.007
MgO	bdl	bdl	bdl	bdl	bdl
CaO	bdl	bdl	bdl	bdl	bdl
Na_2O	0.676	0.766	0.723	0.689	0.687
K_2O	0.034	0.040	0.037	0.043	0.034
BeO	13.947	13.955	13.941	13.937	13.937
Total	100.444	100.569	100.421	100.372	100.373
Ions the basis of 18 (O)					
Si	5.986	5.982	5.983	5.984	5.986
Al	1.972	1.973	1.974	1.975	1.972
Fe	0.004	0.003	0.004	0.004	0.004
Cs	0.004	0.003	0.003	0.004	0.002
Rb	0.005	0.006	0.005	0.004	0.005
Mn	0.001	0.000	0.000	bdl	0.001
Mg	bdl	bdl	bdl	bdl	bdl
Ca	bdl	bdl	bdl	bdl	bdl
Na	0.117	0.133	0.126	0.120	0.119
K	0.004	0.005	0.004	0.005	0.004
Sum	0.135	0.151	0.143	0.137	0.135
Be	3.000	3.000	3.000	3.000	3.000

Table A.49 Electron microprobe analyses of beryl from inner-intermediate zone samples of the Dumper Dew pegmatite.

	Inner-Intermediate Zone Samples				
	002-2-6-1	*002-2-6-2*	*002-2-6-3*	*002-2-6-4*	*002-2-6-5*
Oxides (wt.%)					
SiO_2	66.692	66.688	66.709	66.634	66.632
Al_2O_3	18.532	18.555	18.499	18.574	18.544
FeO	0.033	0.038	0.036	0.029	0.038
Cs_2O	0.064	0.059	0.056	0.062	0.059
Rb_2O	0.032	0.025	0.034	0.033	0.042
MnO	bdl	bdl	bdl	0.007	bdl
MgO	bdl	bdl	bdl	bdl	bdl
CaO	bdl	bdl	bdl	0.022	bdl
Na_2O	0.783	0.764	0.775	0.709	0.743
K_2O	0.045	0.065	0.049	0.054	0.050
BeO	13.902	13.904	13.900	13.895	13.891
Total	100.083	100.098	100.058	100.019	99.999
Ions the basis of 18 (O)					
Si	5.991	5.989	5.993	5.989	5.990
Al	1.962	1.964	1.959	1.967	1.965
Fe	0.002	0.003	0.003	0.002	0.003
Cs	0.002	0.002	0.002	0.002	0.003
Rb	0.002	0.001	0.002	0.002	0.002
Mn	bdl	bdl	bdl	0.001	bdl
Mg	bdl	bdl	bdl	bdl	bdl
Ca	bdl	bdl	bdl	0.002	bdl
Na	0.136	0.133	0.135	0.124	0.130
K	0.005	0.007	0.006	0.006	0.006
Sum	0.148	0.147	0.148	0.139	0.143
Be	3.000	3.000	3.000	3.000	3.000

Table A.50 Electron microprobe analyses of beryl from inner-intermediate zone samples of the Dumper Dew pegmatite.

	Inner-Intermediate Zone Samples				
	002-2-9-1	*002-2-9-2*	*002-2-9-3*	*002-2-9-4*	*002-2-9-5*
Oxides (wt.%)					
SiO_2	66.562	66.578	66.512	66.523	66.543
Al_2O_3	18.542	18.452	18.564	18.499	18.784
FeO	0.023	0.033	0.020	0.027	0.025
Cs_2O	0.075	0.080	0.073	0.074	0.072
Rb_2O	0.037	0.031	0.032	0.036	0.036
MnO	bdl	bdl	bdl	bdl	bdl
MgO	bdl	bdl	bdl	bdl	bdl
CaO	0.017	0.021	0.017	0.018	0.016
Na_2O	0.722	0.670	0.698	0.700	0.689
K_2O	0.045	0.033	0.023	0.032	0.024
BeO	13.878	13.864	13.870	13.863	13.907
Total	99.901	99.762	99.809	99.772	100.096
Ions the basis of 18 (O)					
Si	5.989	5.997	5.989	5.992	5.975
Al	1.966	1.959	1.970	1.964	1.988
Fe	0.002	0.002	0.002	0.002	0.002
Cs	0.003	0.003	0.003	0.003	0.004
Rb	0.002	0.002	0.002	0.002	0.002
Mn	bdl	bdl	bdl	bdl	bdl
Mg	bdl	bdl	bdl	bdl	bdl
Ca	0.002	0.002	0.002	0.002	0.002
Na	0.126	0.117	0.122	0.122	0.120
K	0.005	0.004	0.003	0.004	0.003
Sum	0.140	0.130	0.132	0.135	0.132
Be	3.000	3.000	3.000	3.000	3.000

Table A.51 Electron microprobe analyses of white beryl from inner-intermediate zone samples of the Dumper Dew pegmatite.

	Inner-Intermediate Zone Samples			
	Core		*Rim*	
	002-6-11-1	*002-6-11-2*	*002-6-12-1*	*002-6-12-2*
Oxides (wt.%)				
SiO_2	68.755	68.745	68.733	68.700
Al_2O_3	16.344	16.235	16.400	16.385
FeO	0.033	0.031	0.034	0.036
Cs_2O	bdl	bdl	bdl	bdl
Rb_2O	bdl	bdl	bdl	bdl
MnO	0.021	0.033	0.043	0.036
MgO	bdl	bdl	bdl	bdl
CaO	0.066	0.054	0.056	0.055
Na_2O	0.895	0.923	0.956	0.995
K_2O	0.045	0.040	0.038	0.043
BeO	13.939	13.923	13.949	13.946
Total	100.107	99.996	100.220	100.219
Ions the basis of 18 (O)				
Si	6.160	6.166	6.153	6.152
Al	1.726	1.716	1.730	1.729
Fe	0.002	0.002	0.003	0.003
Cs	bdl	bdl	bdl	0.001
Rb	bdl	bdl	bdl	bdl
Mn	0.002	0.003	0.003	0.003
Mg	bdl	bdl	bdl	bdl
Ca	0.006	0.005	0.005	0.005
Na	0.155	0.161	0.166	0.173
K	0.005	0.005	0.004	0.005
Sum	0.171	0.175	0.181	0.189
Be	3.000	3.000	3.000	3.000

Table A.52 Electron microprobe analyses of colorless beryl cores from inner-intermediate zone samples of the Dumper Dew pegmatite.

	Inner-Intermediate Zone Samples *Core of Colorless Beryl Crystal*				
	002-6-15-1	*002-6-15-2*	*002-6-15-3*	*002-6-15-4*	*002-6-15-5*
Oxides (wt.%)					
SiO_2	64.356	64.443	64.323	64.453	64.488
Al_2O_3	18.487	18.254	18.450	18.455	18.511
FeO	0.009	0.007	0.009	0.007	0.011
Cs_2O	0.210	0.223	0.230	0.243	0.222
Rb_2O	0.056	0.053	0.060	0.057	0.055
MnO	0.016	0.015	0.018	0.017	0.014
MgO	bdl	bdl	bdl	bdl	bdl
CaO	bdl	bdl	bdl	bdl	bdl
Na_2O	0.545	0.540	0.478	0.566	0.540
K_2O	0.040	0.560	0.145	0.174	0.133
BeO	13.490	16.441	13.479	13.510	13.520
Total	97.209	99.976	97.192	97.482	97.494
Ions the basis of 18 (O)					
Si	5.958	4.895	5.959	5.958	5.957
Al	2.017	1.634	2.015	2.010	2.015
Fe	0.001	0.000	0.001	0.001	0.001
Cs	0.007	0.009	0.010	0.009	0.013
Rb	0.003	0.003	0.004	0.003	0.003
Mn	0.001	0.001	0.001	0.001	0.001
Mg	bdl	bdl	bdl	bdl	bdl
Ca	bdl	bdl	bdl	bdl	bdl
Na	0.098	0.080	0.086	0.101	0.097
K	0.005	5.426	0.017	0.021	0.016
Sum	0.115	5.519	0.118	0.136	0.130
Be	3.000	3.000	3.000	3.000	3.000

Table A.53 Electron microprobe analyses of colorless beryl rims from inner-intermediate zone samples of the Dumper Dew pegmatite.

	Inner-Intermediate Zone Samples *Rim of Colorless Beryl Crystal*				
	002-6-16-1	*002-6-16-2*	*002-6-16-3*	*002-6-16-4*	*002-6-16-5*
Oxides (wt.%)					
SiO_2	64.455	64.398	64.385	64.384	64.377
Al_2O_3	18.344	18.455	18.488	18.405	18.418
FeO	bdl	0.008	0.009	0.011	0.007
Cs_2O	0.322	0.345	0.433	0.455	0.433
Rb_2O	0.065	0.075	0.089	0.093	0.095
MnO	0.012	0.012	0.013	0.015	0.011
MgO	bdl	bdl	bdl	bdl	bdl
CaO	bdl	bdl	bdl	bdl	bdl
Na_2O	0.654	0.634	0.655	0.634	0.600
K_2O	0.122	0.120	0.133	0.145	0.167
BeO	13.500	13.506	13.513	13.500	13.499
Total	97.474	97.553	97.718	97.642	97.607
Ions the basis of 18 (O)					
Si	5.962	5.954	5.950	5.956	5.956
Al	2.000	2.011	2.014	2.006	2.008
Fe	bdl	0.001	0.001	0.001	0.001
Cs	0.014	0.017	0.018	0.017	0.000
Rb	0.004	0.004	0.005	0.006	0.006
Mn	0.001	0.001	0.001	0.001	0.001
Mg	bdl	bdl	bdl	bdl	bdl
Ca	bdl	bdl	bdl	bdl	bdl
Na	0.117	0.114	0.117	0.114	0.108
K	0.014	0.014	0.016	0.017	0.020
Sum	0.150	0.151	0.158	0.155	0.135
Be	3.000	3.000	3.000	3.000	3.000

Table A.54 Electron microprobe analyses of green beryl cores from inner-intermediate zone samples of the Dumper Dew pegmatite.

	Inner-Intermediate Zone Samples *Core of Green Beryl Crystal*				
	002-6-17-1	*002-6-17-2*	*002-6-17-3*	*002-6-17-4*	*002-6-17-5*
Oxides (wt.%)					
SiO_2	64.345	64.487	64.500	64.487	64.448
Al_2O_3	18.556	18.600	18.566	18.601	18.523
FeO	0.289	0.311	0.309	0.322	0.298
Cs_2O	0.010	bdl	0.009	bdl	0.010
Rb_2O	bdl	0.010	bdl	bdl	bdl
MnO	0.021	0.022	0.023	0.027	0.023
MgO	0.008	bdl	bdl	bdl	bdl
CaO	bdl	bdl	bdl	bdl	bdl
Na_2O	0.233	0.240	0.245	0.220	0.211
K_2O	0.054	0.050	0.048	0.046	0.045
BeO	13.490	13.521	13.518	13.521	13.499
Total	97.014	97.241	97.218	97.233	97.057
Ions the basis of 18 (O)					
Si	5.956	5.956	5.959	5.956	5.962
Al	2.024	2.025	2.021	2.025	2.020
Fe	0.022	0.024	0.024	0.025	0.023
Cs	0.000	bdl	0.000	bdl	0.000
Rb	bdl	0.001	bdl	bdl	bdl
Mn	0.002	0.002	0.002	0.002	0.002
Mg	0.001	bdl	bdl	bdl	bdl
Ca	bdl	bdl	bdl	bdl	bdl
Na	0.042	0.043	0.044	0.039	0.038
K	0.006	0.006	0.006	0.005	0.005
Sum	0.073	0.076	0.075	0.072	0.068
Be	3.000	3.000	3.000	3.000	3.000

Table A.55 Electron microprobe analyses of green beryl rims from inner-intermediate zone samples of the Dumper Dew pegmatite.

	Inner-Intermediate Zone Samples *Rim of Green Beryl Crystal*				
	002-6-18-1	*002-6-18-2*	*002-6-18-3*	*002-6-18-4*	*002-6-18-5*
Oxides (wt.%)					
SiO_2	64.456	64.523	64.485	64.500	64.498
Al_2O_3	18.563	18.554	18.582	18.611	18.523
FeO	0.455	0.465	0.543	0.654	0.455
Cs_2O	0.009	0.010	bdl	bdl	0.009
Rb_2O	bdl	bdl	0.090	bdl	bdl
MnO	0.011	0.009	0.012	0.008	0.007
MgO	bdl	bdl	bdl	bdl	bdl
CaO	bdl	bdl	bdl	bdl	0.007
Na_2O	0.233	0.213	0.223	0.232	0.243
K_2O	0.040	0.043	0.042	0.038	0.038
BeO	13.518	13.527	13.533	13.546	13.520
Total	97.285	97.344	97.510	97.589	97.300
Ions the basis of 18 (O)					
Si	5.954	5.957	5.950	5.946	5.957
Al	2.021	2.019	2.021	2.022	2.016
Fe	0.035	0.036	0.042	0.050	0.035
Cs	0.000	0.000	bdl	bdl	0.007
Rb	bdl	bdl	0.005	bdl	bdl
Mn	0.001	0.001	0.001	0.001	0.001
Mg	bdl	bdl	bdl	bdl	bdl
Ca	bdl	bdl	bdl	bdl	bdl
Na	0.042	0.038	0.040	0.041	0.044
K	0.005	0.005	0.005	0.004	0.004
Sum	0.083	0.080	0.093	0.097	0.092
Be	3.000	3.000	3.000	3.000	3.000

Table A.56 Electron microprobe analyses of colorless beryl cores from inner-intermediate zone samples of the Dumper Dew pegmatite.

	Inner-Intermediate Zone Samples *Core of Colorless Beryl Crystal*				
	002-6-19-1	*002-6-19-2*	*002-6-19-3*	*002-6-19-4*	*002-6-19-5*
Oxides (wt.%)					
SiO_2	64.445	64.453	64.511	64.422	64.410
Al_2O_3	18.455	18.476	18.458	18.500	18.455
FeO	bdl	bdl	bdl	bdl	0.009
Cs_2O	0.189	0.213	0.223	0.198	0.210
Rb_2O	0.056	0.048	0.045	0.046	0.053
MnO	0.011	0.009	0.012	0.013	0.008
MgO	bdl	bdl	bdl	bdl	bdl
CaO	bdl	bdl	bdl	bdl	bdl
Na_2O	0.434	0.400	0.432	0.398	0.422
K_2O	0.054	0.050	0.054	0.056	0.049
BeO	13.490	13.492	13.502	13.490	13.484
Total	97.134	97.141	97.237	97.123	97.100
Ions the basis of 18 (O)					
Si	5.966	5.966	5.967	5.964	5.965
Al	2.013	2.016	2.012	2.018	2.014
Fe	bdl	bdl	bdl	bdl	0.001
Cs	0.008	0.009	0.008	0.008	0.013
Rb	0.003	0.003	0.003	0.003	0.003
Mn	0.001	0.001	0.001	0.001	0.001
Mg	bdl	bdl	bdl	bdl	bdl
Ca	bdl	bdl	bdl	bdl	bdl
Na	0.078	0.072	0.077	0.071	0.076
K	0.006	0.006	0.006	0.007	0.006
Sum	0.097	0.090	0.095	0.090	0.099
Be	3.000	3.000	3.000	3.000	3.000

Table A.57 Electron microprobe analyses of colorless beryl rims from inner-intermediate zone samples of the Dumper Dew pegmatite.

	Inner-Intermediate Zone Samples *Rim of Colorless Beryl Crystal*				
	002-6-20-1	*002-6-20-2*	*002-6-20-3*	*002-6-20-4*	*002-6-20-5*
Oxides (wt.%)					
SiO_2	64.412	64.398	64.387	64.483	64.403
Al_2O_3	18.372	18.409	18.430	18.387	18.411
FeO	bdl	bdl	bdl	0.008	bdl
Cs_2O	0.323	0.285	0.314	0.300	0.334
Rb_2O	0.064	0.074	0.077	0.078	0.084
MnO	bdl	bdl	bdl	0.009	0.009
MgO	bdl	bdl	bdl	bdl	bdl
CaO	bdl	bdl	bdl	bdl	bdl
Na_2O	0.455	0.523	0.544	0.487	0.500
K_2O	0.056	0.056	0.064	0.067	0.055
BeO	13.476	13.484	13.488	13.494	13.485
Total	97.158	97.229	97.304	97.313	97.281
Ions the basis of 18 (O)					
Si	5.969	5.964	5.961	5.967	5.964
Al	2.006	2.009	2.011	2.005	2.009
Fe	bdl	bdl	bdl	0.001	bdl
Cs	0.011	0.012	0.012	0.013	bdl
Rb	0.004	0.004	0.005	0.005	0.005
Mn	bdl	bdl	bdl	0.001	0.001
Mg	bdl	bdl	bdl	bdl	bdl
Ca	bdl	bdl	bdl	bdl	bdl
Na	0.082	0.094	0.098	0.087	0.090
K	0.007	0.007	0.008	0.008	0.006
Sum	0.103	0.117	0.122	0.114	0.102
Be	3.000	3.000	3.000	3.000	3.000

Table A.58 Electron microprobe analyses of beryl from outer-intermediate zone samples of the Dumper Dew pegmatite.

	Outer-Intermediate Zone Samples				
	010-3-10-1	*010-3-10-2*	*010-3-10-3*	*010-3-10-4*	*010-3-10-5*
Oxides (wt.%)					
SiO_2	66.654	66.598	66.599	66.545	66.452
Al_2O_3	18.599	18.534	18.555	18.645	18.555
FeO	0.021	0.017	0.020	0.016	0.022
Cs_2O	0.098	0.088	0.095	0.090	0.089
Rb_2O	0.033	0.037	0.034	0.038	0.040
MnO	bdl	bdl	bdl	bdl	bdl
MgO	bdl	bdl	bdl	bdl	bdl
CaO	bdl	0.008	0.007	bdl	bdl
Na_2O	0.698	0.709	0.712	0.683	0.723
K_2O	0.077	0.056	0.053	0.047	0.037
BeO	13.900	13.881	13.885	13.886	13.860
Total	100.080	99.928	99.960	99.950	99.778
Ions the basis of 18 (O)					
Si	5.988	5.991	5.990	5.985	5.987
Al	1.969	1.965	1.967	1.976	1.970
Fe	0.002	0.001	0.002	0.001	0.002
Cs	0.003	0.004	0.003	0.003	0.030
Rb	0.002	0.002	0.002	0.002	0.002
Mn	bdl	bdl	bdl	bdl	bdl
Mg	bdl	bdl	bdl	bdl	bdl
Ca	bdl	0.001	0.001	bdl	bdl
Na	0.122	0.124	0.124	0.119	0.126
K	0.009	0.006	0.006	0.005	0.004
Sum	0.137	0.138	0.138	0.131	0.165
Be	3.000	3.000	3.000	3.000	3.000

Table A.59 Electron microprobe analyses of golden beryl cores from outer-intermediate zone samples of the Dumper Dew pegmatite.

	Outer-Intermediate Zone Samples *Core of Golden Beryl Crystal*				
	009-6-13-1	*009-6-13-2*	*009-6-13-3*	*009-6-13-4*	*009-6-13-5*
Oxides (wt.%)					
SiO_2	64.567	64.540	64.623	64.630	64.488
Al_2O_3	18.440	18.520	18.435	18.555	18.455
FeO	0.213	0.255	0.232	0.255	0.264
Cs_2O	0.020	0.022	0.019	0.023	0.022
Rb_2O	0.013	0.012	0.014	0.014	0.012
MnO	0.023	0.021	0.024	0.024	0.023
MgO	bdl	0.009	bdl	0.020	bdl
CaO	0.009	bdl	bdl	bdl	bdl
Na_2O	0.432	0.434	0.445	0.483	0.600
K_2O	0.038	0.044	0.020	0.041	0.122
BeO	13.520	13.530	13.529	13.556	13.529
Total	97.275	97.387	97.341	97.601	97.515
Ions the basis of 18 (O)					
Si	5.964	5.957	5.965	5.954	5.952
Al	2.007	2.015	2.006	2.015	2.008
Fe	0.016	0.020	0.018	0.020	0.020
Cs	0.001	0.001	0.001	0.001	0.001
Rb	0.001	0.001	0.001	0.001	0.001
Mn	0.002	0.002	0.002	0.002	0.002
Mg	bdl	0.001	bdl	0.003	bdl
Ca	0.001	bdl	bdl	bdl	bdl
Na	0.077	0.078	0.080	0.086	0.107
K	0.004	0.005	0.002	0.005	0.014
Sum	0.103	0.107	0.104	0.117	0.146
Be	3.000	3.000	3.000	3.000	3.000

Table A.60 Electron microprobe analyses of golden beryl rims from outer-intermediate zone samples of the Dumper Dew pegmatite.

	Outer-Intermediate Zone Samples *Rim of Golden Beryl Crystal*				
	009-6-14-1	*009-6-14-2*	*009-6-14-3*	*009-6-14-4*	*009-6-14-5*
Oxides (wt.%)					
SiO_2	64.544	64.456	64.500	64.530	64.455
Al_2O_3	18.540	18.566	18.485	18.630	18.555
FeO	0.287	0.263	0.276	0.266	0.287
Cs_2O	0.023	0.025	0.022	0.024	0.026
Rb_2O	0.015	0.021	0.016	0.017	0.020
MnO	0.018	0.019	0.020	0.022	0.018
MgO	bdl	bdl	bdl	bdl	bdl
CaO	bdl	bdl	bdl	bdl	bdl
Na_2O	0.430	0.422	0.387	0.440	0.345
K_2O	0.045	0.076	0.066	0.064	0.054
BeO	13.535	13.524	13.516	13.546	13.516
Total	97.437	97.372	97.288	97.539	97.276
Ions the basis of 18 (O)					
Si	5.955	5.952	5.959	5.949	5.955
Al	2.016	2.021	2.013	2.024	2.021
Fe	0.022	0.020	0.021	0.021	0.022
Cs	0.001	0.001	0.001	0.001	0.008
Rb	0.001	0.001	0.001	0.001	0.001
Mn	0.001	0.001	0.002	0.002	0.001
Mg	bdl	bdl	bdl	bdl	bdl
Ca	bdl	bdl	bdl	bdl	bdl
Na	0.077	0.076	0.069	0.079	0.062
K	0.005	0.009	0.008	0.008	0.006
Sum	0.108	0.108	0.102	0.110	0.101
Be	3.000	3.000	3.000	3.000	3.000

Table A.61 Electron microprobe analyses of pink beryl cores from outer-intermediate zone samples of the Dumper Dew pegmatite.

	Outer-Intermediate Zone Samples *Core of Pink Beryl Crystal*				
	009-6-7-1	*009-6-7-2*	*009-6-7-3*	*009-6-7-4*	*009-6-7-5*
Oxides (wt.%)					
SiO_2	66.523	66.498	66.552	66.498	66.500
Al_2O_3	18.653	18.632	18.674	18.564	18.551
FeO	0.133	0.198	0.183	0.183	0.176
Cs_2O	0.032	0.021	0.024	0.026	0.031
Rb_2O	0.021	0.011	0.009	0.032	0.021
MnO	0.056	0.065	0.070	0.063	0.055
MgO	bdl	0.032	bdl	bdl	bdl
CaO	bdl	bdl	0.012	0.008	bdl
Na_2O	0.345	0.352	0.367	0.345	0.360
K_2O	0.300	0.326	0.323	0.309	0.305
BeO	13.880	13.884	13.897	13.869	13.865
Total	99.943	100.028	100.117	99.906	99.864
Ions the basis of 18 (O)					
Si	5.985	5.981	5.981	5.988	5.989
Al	1.978	1.975	1.978	1.970	1.969
Fe	0.010	0.015	0.014	0.014	0.013
Cs	0.001	0.001	0.001	0.001	0.001
Rb	0.001	0.001	0.001	0.002	0.001
Mn	0.004	0.005	0.005	0.005	0.004
Mg	bdl	0.004	bdl	bdl	bdl
Ca	bdl	bdl	0.001	0.001	bdl
Na	0.060	0.061	0.064	0.060	0.063
K	0.034	0.037	0.037	0.035	0.035
Sum	0.111	0.124	0.123	0.118	0.118
Be	3.000	3.000	3.000	3.000	3.000

Table A.62 Electron microprobe analyses of pink beryl rims from outer-intermediate zone samples of the Dumper Dew pegmatite.

	Outer-Intermediate Zone Samples *Rim of Pink Beryl Crystal*				
	009-6-8-1	*009-6-8-2*	*009-6-8-3*	*009-6-8-4*	*009-6-8-5*
Oxides (wt.%)					
SiO_2	66.384	66.542	66.565	66.557	66.623
Al_2O_3	18.623	18.672	18.575	18.667	18.623
FeO	0.110	0.256	0.145	0.154	0.113
Cs_2O	0.028	0.031	0.034	0.029	0.033
Rb_2O	0.023	0.017	0.018	0.020	0.020
MnO	0.073	0.067	0.073	0.065	0.077
MgO	bdl	bdl	bdl	bdl	bdl
CaO	bdl	bdl	bdl	bdl	bdl
Na_2O	0.430	0.342	0.316	0.331	0.312
K_2O	0.278	0.285	0.305	0.309	0.276
BeO	13.858	13.894	13.876	13.889	13.888
Total	99.807	100.106	99.914	100.021	99.965
Ions the basis of 18 (O)					
Si	5.982	5.981	5.991	5.984	5.991
Al	1.978	1.978	1.970	1.978	1.974
Fe	0.008	0.019	0.011	0.012	0.008
Cs	0.001	0.001	0.001	0.001	0.001
Rb	0.001	0.001	0.001	0.001	0.001
Mn	0.006	0.005	0.006	0.005	0.006
Mg	bdl	bdl	bdl	bdl	bdl
Ca	bdl	bdl	bdl	bdl	bdl
Na	0.075	0.060	0.055	0.058	0.054
K	0.032	0.033	0.035	0.035	0.032
Sum	0.123	0.119	0.109	0.112	0.103
Be	3.000	3.000	3.000	3.000	3.000

Table A.63 Electron microprobe analyses of colorless beryl cores from outer-intermediate zone samples of the Dumper Dew pegmatite.

	Outer-Intermediate Zone Samples *Core of Colorless Beryl Crystal*				
	009-6-9-1	*009-6-9-2*	*009-6-9-3*	*009-6-9-4*	*009-6-9-5*
Oxides (wt.%)					
SiO_2	64.456	64.656	64.623	64.534	64.554
Al_2O_3	18.553	18.612	18.599	18.633	18.622
FeO	0.021	0.032	0.028	0.026	0.029
Cs_2O	0.037	0.045	0.044	0.043	0.044
Rb_2O	0.025	0.033	0.036	0.033	0.028
MnO	0.044	0.046	0.049	0.044	0.050
MgO	bdl	bdl	bdl	bdl	bdl
CaO	bdl	bdl	bdl	bdl	bdl
Na_2O	0.344	0.333	0.324	0.389	0.344
K_2O	0.123	0.212	0.223	0.214	0.210
BeO	13.512	13.550	13.543	13.537	13.535
Total	97.185	97.519	97.469	97.453	97.416
Ions the basis of 18 (O)					
Si	5.957	5.959	5.959	5.953	5.956
Al	2.021	2.022	2.021	2.026	2.025
Fe	0.002	0.002	0.002	0.002	0.002
Cs	0.002	0.002	0.002	0.002	0.001
Rb	0.001	0.002	0.002	0.002	0.002
Mn	0.003	0.004	0.004	0.003	0.004
Mg	bdl	bdl	bdl	bdl	bdl
Ca	bdl	bdl	bdl	bdl	bdl
Na	0.062	0.060	0.058	0.070	0.062
K	0.015	0.025	0.026	0.025	0.025
Sum	0.084	0.094	0.094	0.104	0.095
Be	3.000	3.000	3.000	3.000	3.000

Table A.64 Electron microprobe analyses of colorless beryl rims from outer-intermediate zone samples of the Dumper Dew pegmatite.

	Outer-Intermediate Zone Samples *Rim of Colorless Beryl Crystal*				
	009-6-10-1	*009-6-10-2*	*009-6-10-3*	*009-6-10-4*	*009-6-10-5*
Oxides (wt.%)					
SiO_2	64.650	64.673	64.577	64.566	64.530
Al_2O_3	18.445	18.465	18.500	18.566	18.488
FeO	0.033	0.032	0.027	0.031	0.028
Cs_2O	0.033	0.034	0.033	0.029	0.027
Rb_2O	0.020	0.021	0.026	0.036	0.029
MnO	0.045	0.048	0.051	0.045	0.043
MgO	bdl	bdl	bdl	bdl	bdl
CaO	bdl	0.009	bdl	bdl	0.009
Na_2O	0.324	0.350	0.298	0.305	0.311
K_2O	0.320	0.310	0.230	0.220	0.033
BeO	13.530	13.538	13.518	13.526	14.302
Total	97.407	97.480	97.260	97.324	97.791
Ions the basis of 18 (O)					
Si	5.967	5.965	5.966	5.961	5.635
Al	2.006	2.007	2.014	2.020	1.903
Fe	0.003	0.002	0.002	0.002	0.002
Cs	0.001	0.001	0.001	0.001	0.000
Rb	0.001	0.001	0.002	0.002	0.002
Mn	0.004	0.004	0.004	0.004	0.003
Mg	bdl	bdl	bdl	bdl	bdl
Ca	bdl	0.001	bdl	bdl	0.001
Na	0.058	0.063	0.053	0.055	0.053
K	0.038	0.036	0.027	0.026	0.004
Sum	0.104	0.109	0.089	0.090	0.905
Be	3.000	3.000	3.000	3.000	3.000

Table A.65 Electron microprobe analyses of columbite-tantalite from outer-intermediate zone samples of the Dumper Dew pegmatite.

	Outer-Intermediate Zone Samples				
	001-6-4-1	001-6-4-2	001-6-4-3	001-6-4-4	001-6-4-5
Oxides (wt.%)					
FeO	16.956	16.877	16.789	16.867	16.655
MnO	3.121	3.309	3.387	3.200	3.445
TiO_2	0.244	0.187	0.221	0.217	0.197
Ta_2O_5	13.877	14.009	14.236	14.544	14.765
Nb_2O_5	66.563	66.312	66.350	65.967	65.776
SnO_2	0.322	0.278	0.266	0.310	0.278
Total	101.083	100.972	101.249	101.105	101.116
Ions the basis of 6 (O)					
Fe	0.833	0.831	0.825	0.831	0.821
Mn	0.155	0.165	0.169	0.160	0.172
Sum	0.989	0.996	0.993	0.991	0.993
Ti	0.011	0.008	0.010	0.010	0.009
Ta	0.222	0.224	0.227	0.233	0.237
Nb	1.768	1.765	1.762	1.757	1.754
Sn	0.008	0.007	0.006	0.007	0.007
Sum	2.008	2.004	2.006	2.007	2.006

Table A.66 Electron microprobe analyses of columbite-tantalite from inner-intermediate zone samples of the Dumper Dew pegmatite.

	Inner-Intermediate Zone Samples		
	002-2-6	002-2-7	002-2-8
Oxides (wt.%)			
FeO	1.987	2.219	2.200
MnO	17.344	17.233	17.430
TiO_2	0.023	0.033	0.034
Ta_2O_5	17.960	18.030	18.430
Nb_2O_5	62.155	62.166	62.210
SnO_2	0.210	0.233	0.234
Total	99.679	99.914	100.538
Ions the basis of 6 (O)			
Fe	0.101	0.112	0.111
Mn	0.890	0.883	0.889
Sum	0.991	0.995	0.999
Ti	0.001	0.002	0.002
Ta	0.296	0.297	0.302
Nb	1.703	1.700	1.693
Sn	0.005	0.006	0.006
Sum	2.005	2.003	2.002

Table A.67 Electron microprobe analyses of columbite-tantalite from replacement unit samples of the Dumper Dew pegmatite.

	Replacement Unit Samples		
	010-6-3-8	010-6-3-9	010-6-3-10
Oxides (wt.%)			
FeO	0.967	1.098	1.110
MnO	15.340	15.476	15.338
TiO_2	0.112	0.096	0.094
Ta_2O_5	69.220	69.170	69.455
Nb_2O_5	10.223	10.315	10.056
SnO_2	0.254	0.312	0.332
Total	96.116	96.467	96.385
Ions the basis of 6 (O)			
Fe	0.067	0.075	0.076
Mn	1.071	1.076	1.069
Sum	1.138	1.151	1.146
Ti	0.007	0.006	0.006
Ta	1.552	1.544	1.554
Nb	0.381	0.383	0.374
Sn	0.008	0.010	0.011
Sum	1.948	1.943	1.945

Table A.68 Electron microprobe analyses of cassiterite from inner-intermediate zone samples of the Dumper Dew pegmatite.

	Inner-Intermediate Zone Samples				
	002-2-1	*002-2-2*	*002-2-3*	*002-2-4*	*002-2-5*
Oxides (wt.%)					
SnO_2	99.334	99.344	99.225	99.232	99.200
Ta_2O_5	0.122	0.131	0.112	0.134	0.139
Total	99.456	99.475	99.337	99.366	99.339
Ions on the basis of 2 O					
Sn	0.998	0.998	0.998	0.998	0.998
Ta	0.001	0.001	0.001	0.001	0.001
X sum	0.999	0.999	0.999	0.999	0.999

Table A.69 Electron microprobe analyses of cassiterite from inner-intermediate zone samples of the Dumper Dew pegmatite.

	Inner-Intermediate Zone Samples				
	002-2-10-1	*002-2-10-2*	*002-2-10-3*	*002-2-10-4*	*002-2-10-5*
Oxides (wt.%)					
SnO_2	99.270	99.217	99.112	99.412	99.344
Ta_2O_5	0.145	0.155	0.123	0.176	0.167
Total	99.415	99.372	99.235	99.588	99.511
Ions on the basis of 2 O					
Sn	0.997	0.996	0.998	0.997	0.996
Ta	0.001	0.001	0.001	0.001	0.001
X sum	0.998	0.997	0.999	0.998	0.998

Table A.70 Electron microprobe analyses of cassiterite from inner-intermediate zone samples of the Dumper Dew pegmatite.

	Inner-Intermediate Zone Samples				
	002-2-11-1	*002-2-11-2*	*002-2-11-3*	*002-2-11-4*	*002-2-11-5*
Oxides (wt.%)					
SnO_2	99.107	99.211	99.321	99.444	99.409
Ta_2O_5	0.145	0.155	0.176	0.156	0.176
Total	99.252	99.366	99.497	99.600	99.585
Ions on the basis of 2 O					
Sn	0.989	0.997	0.997	0.997	0.997
Ta	0.001	0.001	0.001	0.001	0.001
X sum	0.990	0.998	0.998	0.998	0.998

Table A.71 Electron microprobe analyses of cassiterite from replacement unit samples of the Dumper Dew pegmatite.

	Replacement Unit Samples				
	010-6-2-1	*010-6-2-2*	*010-6-2-3*	*010-6-2-4*	*010-6-2-5*
Oxides (wt.%)					
SnO_2	99.344	99.523	99.451	99.398	99.400
Ta_2O_5	0.110	0.114	0.089	0.098	0.109
Total	99.454	99.637	99.540	99.496	99.509
Ions on the basis of 2 O					
Sn	0.998	0.998	0.998	0.998	0.998
Ta	0.001	0.001	0.001	0.001	0.001
X sum	0.999	0.999	0.999	0.999	0.999

Table A.72 Electron microprobe analyses of oxides from replacement unit samples of the Dumper Dew pegmatite.

	Replacement Unit Samples				
	010-3-5-1	*010-3-5-2*	*010-3-5-3*	*010-3-5-4*	*010-3-5-5*
Oxides (wt.%)					
FeO	83.677	82.956	83.009	83.325	83.117
MnO	6.344	6.448	6.098	6.112	6.095
CaO	0.056	0.129	0.094	0.152	0.159
Total	90.077	89.533	89.201	89.589	89.371
Ions on the basis of 3 O					
Fe	2.784	2.776	2.788	2.786	2.786
Mn	0.214	0.219	0.207	0.207	0.207
Ca	0.002	0.006	0.004	0.007	0.007
X sum	3.000	3.000	3.000	3.000	3.000

Table A.73 Electron microprobe analyses of oxides from inner-intermediate zone samples of the Dumper Dew pegmatite.

	Inner-Intermediate Zone Samples				
	002-4-10-1	*002-4-10-2*	*002-4-10-3*	*002-4-10-4*	*002-4-10-5*
Oxides (wt.%)					
FeO	3.233	4.233	3.095	3.233	3.233
MnO	80.460	79.677	80.766	79.460	79.460
CaO	0.020	0.034	0.110	0.020	0.009
Total	83.713	83.944	83.971	82.713	82.702
Ions on the basis of 3 O					
Fe	0.114	0.149	0.109	0.116	0.116
Mn	2.885	2.849	2.886	2.883	2.884
Ca	0.001	0.002	0.005	0.001	0.000
X sum	3.000	3.000	3.000	3.000	3.000

Table A.74 Electron microprobe analyses of oxides from inner-intermediate zone samples of the Dumper Dew pegmatite.

	Inner-Intermediate Zone Samples				
	002-4-5-1	*002-4-5-2*	*002-4-5-3*	*002-4-5-4*	*002-4-5-5*
Oxides (wt.%)					
FeO	78.760	79.078	79.340	80.005	78.453
MnO	6.530	5.343	5.121	4.233	6.766
CaO	0.033	0.045	0.050	0.033	0.056
Total	85.695	84.950	85.013	84.683	85.703
Ions on the basis of 3 O					
Fe	2.738	2.769	2.774	2.813	2.724
Mn	0.230	0.189	0.181	0.151	0.238
Ca	0.001	0.002	0.002	0.001	0.002
X sum	2.969	2.960	2.958	2.965	2.964

Table A.75 Electron microprobe analyses of oxides from inner-intermediate zone samples of the Dumper Dew pegmatite.

	Inner-Intermediate Zone Samples				
	002-4-8-1	*002-4-8-2*	*002-4-8-3*	*002-4-8-4*	*002-4-8-5*
Oxides (wt.%)					
FeO	83.090	82.567	82.562	83.115	83.009
MnO	3.988	3.567	3.834	3.777	3.454
CaO	0.099	0.100	0.089	0.062	0.094
Total	87.429	86.501	86.729	87.265	86.883
Ions on the basis of 3 O					
Fe	2.839	2.852	2.844	2.843	2.851
Mn	0.138	0.125	0.134	0.131	0.120
Ca	0.004	0.004	0.004	0.003	0.004
X sum	2.981	2.981	2.982	2.977	2.976

Table A.76 Electron microprobe analyses of oxides from inner-intermediate zone samples of the Dumper Dew pegmatite.

	Inner-Intermediate Zone Samples				
	002-4-11-1	*002-4-11-2*	*002-4-11-3*	*002-4-11-4*	*002-4-11-5*
Oxides (wt.%)					
FeO	2.566	2.555	2.780	2.456	2.430
MnO	80.322	80.111	80.212	80.143	80.078
CaO	0.006	0.000	0.013	0.008	0.014
Total	83.025	82.759	83.061	82.639	82.534
Ions on the basis of 3 O					
Fe	0.091	0.091	0.099	0.088	0.087
Mn	2.897	2.901	2.896	2.909	2.911
Ca	0.000	0.000	0.001	0.000	0.001
X sum	2.989	2.992	2.996	2.998	2.999

Table A.77 Electron microprobe analyses of heterosite from inner-intermediate zone samples of the Dumper Dew pegmatite.

Chemical composition	Inner-Intermediate Zone Samples				
	002-1-6-1	*002-1-6-2*	*002-1-6-3*	*002-1-6-4*	*002-1-6-5*
Oxides (wt.%)					
Fe_2O_3	28.566	28.888	28.677	28.334	29.1
Mn_2O_3	20.978	20.777	20.887	20.454	19.778
CaO	1.06	0.997	1.213	1.116	1.2
P_2O_5	46.766	46.676	46.589	46.722	46.623
Total	97.504	97.394	97.366	96.647	96.747
Ions on the basis of 3.5 O					
Fe^{3+}	0.543	0.55	0.547	0.539	0.555
Mn^{3+}	0.403	0.4	0.403	0.394	0.381
Ca	0.029	0.027	0.033	0.03	0.033
X sum	0.975	0.977	0.983	0.963	0.969
P	1.000	1.000	1.000	1.000	1.000

Table A.78 Electron microprobe analyses of heterosite from inner-intermediate zone samples of the Dumper Dew pegmatite.

Chemical composition	Inner-Intermediate Zone Samples				
	002-2-8-1	*002-2-8-2*	*002-2-8-3*	*002-2-8-4*	*002-2-8-5*
Oxides (wt.%)					
Fe_2O_3	26.787	26.856	26.777	26.564	26.6
Mn_2O_3	23.009	23.24	23.6	23.655	23.587
CaO	1.112	0.095	0.088	0.098	1.098
P_2O_5	46.345	46.52	46.446	46.333	46.655
Total	97.253	96.711	96.911	96.65	97.94
Ions on the basis of 3.5 O					
Fe^{3+}	0.514	0.513	0.512	0.51	0.507
Mn^{3+}	0.446	0.449	0.457	0.459	0.455
Ca	0.03	0.003	0.002	0.003	0.03
X sum	0.991	0.965	0.972	0.971	0.991
P	1.000	1.000	1.000	1.000	1.000

Direct Coupled Plasma Spectrometry Analyses

Table B.1 DCP analyses of potassium feldspar from outer-intermediate zone samples of the Dumper Dew pegmatite.

	Outer-Intermediate Zone Samples	
Elemental Abundances	*07-002*	*07-002 XIV*
ppm B	nd	125
ppm Li	nd	91
ppm Rb	4342	3753
ppm Tl	nd	22
ppm K	128514	122544
K/Rb	30	33
K/Tl		5571
K wt%	12.851	12.254
K_2O wt%	15.481	14.762

nd=not detected

Table B.2 DCP analyses of potassium feldspar from an inner-intermediate zone sample of the Dumper Dew pegmatite.

	Inner-Intermediate Zone Sample
Elemental Abundances	*07-001*
ppm B	nd
ppm Li	nd
ppm Rb	3717
ppm Tl	Nd
ppm K	142034
K/Rb	38
K wt%	14.203
K_2O wt%	17.109

nd=not detected

Table B.3 DCP analyses of potassium feldspar from wall zone samples of the Dumper Dew pegmatite.

Elemental Abundances	Wall Zone Samples		
	07-008 TS	*WP-008 TS*	*WP-008 BS*
ppm B	nd	179	67
ppm Li	nd	nd	nd
ppm Rb	1276	2310	2850
ppm Tl	nd	nd	nd
ppm K	133674	123025	121678
K/Rb	105	53	43
K wt%	13.367	12.303	12.168
K_2O wt%	16.102	14.820	14.657

nd=not detected

Table B.4 DCP analyses of potassium feldspar from a replacement unit sample of the Dumper Dew pegmatite.

Elemental Abundances	Replacement Unit Sample
	07-010 I
ppm B	nd
ppm Li	nd
ppm Rb	4088
ppm Tl	nd
ppm K	133860
K/Rb	33
K wt%	13.386
K_2O wt%	16.125

nd=not detected

Table B.5 DCP analyses of potassium feldspar from core margin zone samples of the Tiger Bill pegmatite.

Elemental Abundances	Tiger Bill Core Margin Zone Samples	
	TB IV	*TB V*
ppm B	175	160
ppm Li	nd	nd
ppm Rb	2347	2204
ppm Tl	nd	5
ppm K	124900	120165
K/Rb	53	55
K/Tl		25444
K wt%	12.490	12.016
K_2O wt%	15.046	14.475

nd=not detected

Table B.6 DCP analyses of muscovite from a core margin zone sample of the Tiger Bill pegmatite.

Elemental Abundances	Tiger Bill Core Margin Zone Sample
	TB I
ppm B	122
ppm Li	1709
ppm Rb	2521
ppm Tl	12
ppm K	82816
K/Rb	33
K/Tl	7060
K wt%	8.282
K_2O wt%	9.976

nd=not detected

Table B.7 DCP analyses of muscovite from an extraneous sample of an Uncle Tom Mountain pegmatite.

Elemental Abundances	Extraneous Pegmatite Outcrop Sample *07-016*
ppm B	nd
ppm Li	538
ppm Rb	783
ppm Tl	nd
ppm K	85268
K/Rb	109
K wt%	8.527
K_2O wt%	10.271

nd=not detected

Table B.8 DCP analyses of muscovite from replacement unit samples of the Dumper Dew pegmatite.

Elemental Abundances	Replacement Unit Samples *07-010*	*07-010*	*07-010 I*	*07-010 II*
ppm B	21	30	nd	303
ppm Li	2602	2569	2135	3500
ppm Rb	5047	4386	5723	5250
ppm Tl	nd	nd	nd	14
ppm K	79291	80729	84525	92050
K/Rb	16	18	15	18
K/Tl				6658
K wt%	7.929	8.073	8.453	9.205
K_2O wt%	9.551	9.725	10.182	11.088

nd=not detected

Table B.9 DCP analyses of muscovite from wall zone samples of the Dumper Dew pegmatite.

Elemental Abundances	Wall Zone Samples	
	07-008 TSI	*07-008 BS*
ppm B	nd	265
ppm Li	1234	1313
ppm Rb	1677	2881
ppm Tl	nd	nd
ppm K	75638	67369
K/Rb	45	23
K wt%	7.564	6.737
K_2O wt%	9.111	8.115

nd=not detected

Table B.10 DCP analyses of muscovite from wall zone samples above a quartz lens in the Dumper Dew pegmatite.

Elemental Abundances	Outer Portion of Quartz Lens Samples			
	07-003 QL	*07-003 QL*	*07-003 BQL*	*WP-003*
ppm B	nd	nd	nd	201
ppm Li	648	670	758	1007
ppm Rb	1057	1517	1132	1393
ppm Tl	nd	nd	nd	2
ppm K	81375	75600	92925	91471
K/Rb	77	50	82	66 43667
K wt%	8.138	7.560	9.293	9.147
K_2O wt%	9.802	9.107	11.194	11.019

nd=not detected

Table B.11 DCP analyses of muscovite from inner-intermediate zone samples of the Dumper Dew pegmatite.

Elemental Abundances	Inner-Intermediate Zone Samples			
	07-002 II	*07-002 XIII*	*07-002*	*07-002*
ppm B	310	309	42	34
ppm Li	2293	4248	2310	2331
ppm Rb	5110	4860	6213	5784
ppm Tl	nd	8	nd	nd
ppm K	88900	77622	91875	87982
K/Rb	17	16	15	15
K/Tl		9652		
K wt%	8.890	7.762	9.188	8.798
K_2O wt%	10.709	9.350	11.067	10.598

nd=not detected

Table B.12 DCP analyses of muscovite from an outer-intermediate zone sample of the Dumper Dew pegmatite.

Elemental Abundances	Outer-Intermediate Zone Sample
	07-001 I
ppm B	nd
ppm Li	584
ppm Rb	1063
ppm Tl	nd
ppm K	78557
K/Rb	74
K wt%	7.856
K_2O wt%	9.463

nd=not detected

Table B.13 DCP analyses of schorl from inner-intermediate zone samples of the Dumper Dew pegmatite.

Elemental Abundances	Inner-Intermediate Zone Samples	
	07-002 XV	*07-002*
ppm B	17046	17666
ppm Li	211	325
ppm Rb	nd	nd
ppm Tl	25	38
ppm K	1153	980
K/Tl	46	26
K wt%	0.115	0.098
K_2O wt%	0.139	0.118

nd=not detected

Table B.14 DCP analyses of schorl from the wall zone above a quartz lens in the Dumper Dew pegmatite.

Elemental Abundances	Outer Portion of Quartz Lens Sample
	07-004a
ppm B	23054
ppm Li	nd
ppm Rb	nd
ppm Tl	38
ppm K	1345
K/Tl	36
K wt%	0.134
K_2O wt%	0.162

nd=not detected

Table B.15 DCP analyses of schorl from a replacement unit sample of the Dumper Dew pegmatite.

Elemental Abundances	Replacement Unit Sample *WP-010*
ppm B	16959
ppm Li	197
ppm Rb	nd
ppm Tl	32
ppm K	1082
K/Tl	34
K wt%	0.108
K_2O wt%	0.130

nd=not detected

Table B.16 DCP analyses of schorl from a core margin zone sample of the Tiger Bill pegmatite.

Elemental Abundances	Tiger Bill Core Margin Zone Sample *TB III*
ppm B	14413
ppm Li	29
ppm Rb	nd
ppm Tl	23
ppm K	796
K/Tl	34
K wt%	0.080
K_2O wt%	0.096

nd=not detected

Table B.17 DCP analyses of spodumene from inner-intermediate zone samples of the Dumper Dew pegmatite.

Elemental Abundances	Inner-Intermediate Zone Samples		
	07-002 VI	*07-002 VII*	*07-002 IX*
ppm B	nd	nd	nd
ppm Li	13717	18513	16555
ppm Rb	61	nd	nd
ppm Tl	nd	nd	nd
ppm K	1625	1939	2013
K/Rb	27		
K wt%	0.163	0.194	0.201
K_2O wt%	0.196	0.234	0.242

nd=not detected

Table B.18 DCP analyses of country rock samples from the Dumper Dew pegmatite.

Elemental Abundances	Host Rock Samples Extracted Above Quartz Lens	
	07-003 AQL	*WP-003 AQL*
ppm B	nd	68
ppm Li	327	548
ppm Rb	58	nd
ppm Tl	33	51
ppm K	34300	28889
K/Rb	590	
K/Tl	1048	561
K wt%	3.430	2.889
K_2O wt%	4.132	3.480

nd=not detected

Table B.19 DCP analyses of country rock samples from the Dumper Dew pegmatite.

Elemental Abundances	Host Rock Samples				
	07-004-1	*07-004b*	*WP-004*	*WP-004-1*	*WP-004-2*
ppm B	nd	nd	182	194	201
ppm Li	327	14	124	74	148
ppm Rb	nd	nd	nd	nd	nd
ppm Tl	48	15	17	39	30
ppm K	26963	29297	23438	22061	33009
K/Tl	564	2000	1396	560	1099
K wt%	2.696	2.930	2.344	2.206	3.301
K_2O wt%	3.248	3.529	2.823	2.657	3.976

nd=not detected

Table B.20 DCP analyses of a country rock sample from the Dumper Dew pegmatite.

Elemental Abundances	Biotite Granite Sample
	07-005
ppm B	nd
ppm Li	108
ppm Rb	nd
ppm Tl	nd
ppm K	6011
K wt%	0.601
K_2O wt%	0.724

nd=not detected

Table B.21 DCP analyses of a country rock sample from the Dumper Dew pegmatite.

Elemental Abundances	Country Rock Sample Extracted Above Replacement Unit *WP-010 I*
ppm B	290
ppm Li	609
ppm Rb	280
ppm Tl	57
ppm K	9480
K/Rb	34
K/Tl	167
K wt%	0.948
K_2O wt%	1.142

nd=not detected

Table B.22 DCP analyses of a country rock sample from the Dumper Dew pegmatite.

Elemental Abundances	Extraneous Country Rock Sample *WP-022*
ppm B	129
ppm Li	1394
ppm Rb	nd
ppm Tl	271
ppm K	21831
K/Tl	81
K wt%	2.183
K_2O wt%	2.630

nd=not detected

Vita

Jonathan South was born in Amory, Mississippi in 1977. He was raised in the small town of Winfield, Alabama. Frequent hunting trips with his father while he was growing up lead to a love of nature and the outdoors. He attended the Winfield City School System where his fascination with the natural world flourished with each fossilized organism, mineral specimen and volcano he and his classmates studied. After graduating from Winfield High School in 1996, he attended Bevill State Community College in Fayette, Alabama. In 2003 he moved to Tuscaloosa and enrolled at the University of Alabama to study geology. He received a Bachelor of Science Degree in Geology from the University of Alabama in 2006. Wanting to further his knowledge of the geologic sciences and contribute scholastically to the science he enrolled at the University of New Orleans in 2007. In 2009, he obtained his Master's Degree in Earth and Environmental Science from the University of New Orleans.